



ABDUR RAHIM

“SiO₂/MPc/C ELECTRICALLY CONDUCTIVE CERAMIC MATERIAL (Pc: PHTHALOCYANINE, M = Mn(II), Co(II), Cu(II)) A NEW SUBSTRATE FOR THE PREPARATION OF ELECTROCHEMICAL SENSORS AND BIOSENSORS”

“MATERIAL CERÂMICO ELETRICAMENTE CONDUTOR SiO₂/MPc/C (Pc: FTALOCIANINA, M = Mn(II), Co(II), Cu(II)) UM NOVO SUBSTRATO PARA O PREPARO DE SENSORES E BIOSENSORES ELETROQUÍMICOS”

CAMPINAS
2013



UNIVERSIDADE ESTADUAL DE CAMPINAS

INSTITUTO DE QUÍMICA

ABDUR RAHIM

“ $\text{SiO}_2/\text{MPc}/\text{C}$ ELECTRICALLY CONDUCTIVE CERAMIC MATERIAL (Pc: PHTHALOCYANINE, $M = \text{Mn(II)}$, Co(II) , Cu(II)) A NEW SUBSTRATE FOR THE PREPARATION OF ELECTROCHEMICAL SENSORS AND BIOSENSORS”

ORIENTADOR: PROF. DR. YOSHITAKA GUSHIKEM

“MATERIAL CERÂMICO ELÉTRICAMENTE CONDUTOR $\text{SiO}_2/\text{MPc}/\text{C}$ (Pc: FTALOCIANINA, $M = \text{Mn(II)}$, Co(II) , Cu(II)) UM NOVO SUBSTRATO PARA O PREPARO DE SENSORES E BIOSENSORES ELETROQUÍMICOS”

Tese de Doutorado apresentada ao Instituto de Química da Universidade Estadual de Campinas para obtenção do título de Doutor em Ciências.

Doctorate thesis presented to the Institute of Chemistry of the University of Campinas to obtain the Ph.D. in Sciences.

ESTE EXEMPLAR CORRESPONDE À VERSÃO FINAL DA TESE DEFENDIDA POR ABDUR RAHIM E ORIENTADA PELO PROF.DR.YOSHITAKA GUSHIKEM

Assinatura do Orientador

CAMPINAS
2013

CATALOGING RECORD PREPARED BY SIMONE LUCAS - CRB8/8144 – LIBRARY,
INSTITUTE OF CHEMISTRY, UNIVERSITY OF CAMPINAS

R129s Rahim, Abdur (1980-).
 SiO₂/MPc/C e electrically conductive ceramic material
(Pc: phthalocyanine, M=Mn(II), Co(II), Cu(II)) a new
substrate for the preparation of electrochemical sensors
and biosensors / Abdur Rahim. – Campinas, SP: [s.n.],
2013.

Supervisor: Yoshitaka Gushikem.

Thesis (doctorate) - University of Campinas, Institute
of Chemistry.

1. Sol-gel. 2. Carbon ceramic materials. 3. Metal
phthalocyanine. 4. SiO₂/C. 5. Electrochemical sensors.
I. Gushikem, Yoshitaka. II. University of Campinas.
Institute of Chemistry. III. Title.

Information for Digital Library

Portuguese title: Material cerâmico eletricamente condutor SiO₂/MPc/C (Pc: ftalocianina, M=Mn(II), Co(II), Cu(II)) um novo substrato para o preparo de sensores e biosensores eletroquímicos

Portuguese keywords:

Sol-gel
Material de carbono ceramic
Ftalocianina de metal
SiO₂/C
Sensores eletroquímicos

Subject concentration: Inorganic Chemistry

Academic degree: PhD in Sciences

Thesis evaluation comission:

Yoshitaka Gushikem [Supervisor]
Emerson Schwingel Ribeiro
Eduardo Nicolau dos Santos
Lauro Tatsuo Kubota
Pedro Paulo Corbi

Date: 18/02/2013

Graduate Program: Chemistry

DEDICATION

*To my beloved parents and my late
grandparents*

ACKNOWLEDGMENT

All praises for Almighty *ALLAH* the most compassionate, the most beneficent and ever merciful, who gives me the power to do, the sight to observe and mind to think and judge. His presence and love have sustained me through the valleys, storms and winds of research and writing up this thesis.

I feel a deep sense of gratitude and indepthness to my dignified supervisor Professor Dr. *Yoshitaka Gushikem* for his kind supervision, useful suggestions, consistent encouragement, friendly behavior, for giving me the opportunity to work in his research group and dynamic supervision which enabled me to complete this task successfully.

I feel pride in extending my vehement sense of gratitude and sincere feelings of reverence and regards to our collaborator Prof. Dr. *Lauro Tatsuo Kubota*, for his co-operation, useful comments, encouragement, great support, sharing their knowledge and friendly behaviour throughout this course of study.

Heartfelt, thanks are also extended to my co-worker and friends, Leliz, Lucas, Sergio, Thiago, Camila, Natalia, Cleo, Adriana, Cintia, Ramon, Vaeudo, Mauricio, Anton, Syed, Adnan, Ali, Khalid, Haleem, Almas, Surayya, Ana and Fozia. I am special obliged to my friend Gabriel, who helped me, whenever, I need his assistance.

A lot of thanks to my friends; especially, Zulqarnain, Ziarat, Umer, Hamid, Farhad, Ibrahim and Joao who gave me company during my stay in Brazil and helped me whenever I needed it. I am also thankful to Izabel, Gabriela and Miguel of CPG for their great help during my stay at Unicamp.

The occasion needs special mention of my beloved parents, whose uninterrupted support in various aspects of my life and studies, kept me going with grace and honor under the shades of their prayers. I can never repay their unlimited love and precious prayers. Furthermore, I am highly obliged to my uncle *Abdul Aziz* (Pharmacist) and my brothers Engr. *Abdul Majid*, and Dr. *Abdul Qadeer*, whose inspiration, encouragement, guideline and good wishes has always accompanied me. At last *TWAS* and *CNPq* for the PhD scholarship.

To keep it all, I owe my gratitude to all who directly and indirectly extended help and support me in one way or the other, in the accomplishment of this task.

Abdur Rahim

Curriculum Vitae

Personal Data

Abdur Rahim

Pakistani, born in Karak, on 01/01/1980

Residential address: Village Nawaz Abad, P/O Latamber, Tehsil & District Karak, KPK, Pakistan.

E-mail: rahimkhan533@yahoo.com

Education

- ❖ B.Sc. (Chemistry, Biology), GPGC, Karak, University of Peshawar (2001).
- ❖ M.Sc. (Chemistry), Department of Chemistry, Gomal University, D.I.Khan, Pakistan (2003).

Title: Comparative analysis of antibiotic (Quinolone group) and their complexation”.
- ❖ M.Phil. (Chemistry), Institute of Chemical Sciences, University of Peshawar, Pakistan (2007).

Title: Styrene monomer recovery from waste polystyrene by catalytic degradation”.
- ❖ Ph.D (Inorganic Chemistry), Institute of Chemistry, Unicamp, SP, Brazil (2013).

Title: SiO₂/MPc/C electrically conductive ceramic material (Pc:phthalocyanine, M = Mn(II), Co(II), Cu(II)) a new substrate for the preparation of electrochemical sensors and biosensors”.

Scientific articles published and submitted

1. **A. Rahim**, L.S.S. Santos, S.B.A. Barros, L.T. Kubota, Y. Gushikem, “Dissolved O₂ sensor based on Cobalt (II) phthalocyanine immobilized in situ on electrically conducting carbon ceramic mesoporous SiO₂/C material”, *Sensors and Actuators B* 177 (2013) 231–238.
2. S.B.A. Barros, **A. Rahim**, A.A. Tanaka, R. Landers, Y. Gushikem, “In situ immobilization of nickel(II) phthalocyanine on mesoporous SiO₂/C carbon ceramic matrices prepared by the sol–gel method: use in the simultaneous voltammetric determination of ascorbic acid and dopamine”, *Electrochimica Acta*, 87 (2013) 140–147.
3. M.P. Dos. Santos, **A. Rahim**, N.Fattori., L.T.Kubota, Y.Gushikem. “Novel amperometric sensor based on mesoporous silica chemically modified with ensal copper complexes for selective and sensitive dopamine determination”, *Sensors and Actuators B* 171– 172 (2012) 712– 718.
4. **A. Rahim**, S.B.A.Barros, L.T. Arenas, Y. Gushikem, “In situ immobilization of cobalt phthalocyanine on the mesoporous carbon ceramic SiO₂/C prepared by the sol gel process. Evaluation as an electrochemical sensor for oxalic acid”, *Electrochimica Acta*, v. 56, p. 1256-1261, 2011.
5. **A. Rahim**, S.B.A. Barros, L.T. Kubota, Y. Gushikem, “SiO₂/C/CuPc as a biomimetic catalyst for dopamine monooxygenase in the development of an amperometric sensor”, *Electrochimica Acta*, v. 56, p. 10116-10121, 2011.
6. M.R. Jan, J. Shah, **A. Rahim**, “Styrene monomer recovery from waste polystyrene by catalytic degradation”, *American Laboratory*, v. 40, p. 12-14, 2008.
7. **A. Rahim**, L.S.S. Santos, S.B.A. Barros, L.T. Kubota, R. Landers, Y. Gushikem “Electrochemical detection of nitrite in meat and water samples using a mesoporous carbon ceramic SiO₂/C electrode modified with Manganese (II) phthalocyanine” *Hazardous materials*, 2013(Submitted).

8. O. Tkachenko, **A. Rahim**, A. Baraban, R. Sukhov, Y. Gushikem, Y. Kholin “Hybrid silica-organic material with immobilized amino groups: surface probing and use for electrochemical determination of nitrite ions”, Journal of Sol-Gel Science and Technology, 2013 (Submitted).

Summary published in conference proceedings

1. **A. Rahim**, L. T. Kubota, Y. Gushikem, “*In situ* immobilization of manganese phthalocyanine on the mesoporous carbon ceramic SiO₂/C prepared by the sol-gel process. Application as an electrochemical sensor for nitrite” International and Expo on Material Science and Engineering, Oct. 22-24, 2012 Chicago-Northshore, USA, 2012, P 43-43.

2. **A. Rahim**, L.S.S, Santos, S.B.A. Barros, L.T. Kubota, Y. Gushikem. “Mesoporous carbon ceramic SiO₂/C prepared by sol-gel method and modified with manganese phthalocyanine (MnPc) and used as an electrochemical sensor for the oxidation of Nitrite”. 6th International Workshop "Characterization of Porous Materials" (CPM-6), Delray Beach, Florida, USA 2012, P74, p.151-151.

3 **A. Rahim**, L.S.S, Santos, L.T. Kubota, Y. Gushikem, “SiO₂/C/CuPc como catalisador biomimético da dopamina monoxigenase no desenvolvimento de um sensor amperométrico”. In: 34^a Reunião Anual SBQ, 2011, Florianópolis.Santa Catarina: ELE-194, 2011.

4. **A. Rahim**, L.T Kubota, Y. Gushikem. “Mesoporous carbon ceramic SiO₂/C prepared by sol-gel method and modified with copper phthalocyanine used as an amperometric sensor for 4-aminophenol”. In: Sixteenth International Symposium on Silicon Chemistry, 2011, Ontario, Canada 2011, v. 1, p. 219-219.

5. **A. Rahim**, S.B.A. Barros. L.T. Arenas, Y.Gushikem, “*In situ* immobilization of cobalt phthalocyanine on the mesoporous carbon ceramic SiO₂/C prepared by the sol gel process: application as an oxalic acid sensor”. In: X Meeting SBPMat 2011, Gramadao, RS, 2011. p. 88-88.

6. **A. Rahim**, L.T. Arenes, L.S.S. Santos, Y.Gushikem, “Desenvolvimento de um sensor eletroquímico de oxigênio dissolvido em águas a partir da ftalocianina de

cobalto (II) sintetizada in-situ em matriz SiO₂/grafite”. In the 33^a Reunião Anual SBQ, Aguas de Lindoia, 2010.

7. **A. Rahim**, L.T. Arenes, Y. Gushikem, “In-situ synthesis of Cobalt phthalocyanine (CoPc) on SiO₂/C matrix and use as an electrochemical sensor for the oxidation of Nitrite”. In the 11th international chemistry conference and Exhibition in Africa The Role of chemistry in development of Africa held at Luxor, Egypt from Nov 20 to 23, 2010.

8. **A. Rahim**, L.T. Arenes. S.B.A. Barros, Y. Gushikem., “Synthesis of SiO₂/C-graphite mesoporous ceramic material and their electrochemical study”. In the 11th International conference on advanced materials. In the VIII Econtro da SBPMat, Rio de Janeiro, ICAM 2009.

9. **A. Rahim**, S.B.A. Barros, L.T. Arenes, Y. Gushikem, “Effect of HF in the preparation of carbon-ceramic materials by sol-gel process”. In the 11th International conference on advanced materials. In the VIII Econtro da SBPMat, Rio de Janeiro, ICAM 2009.

10. **A. Rahim**, J. Shah., M.R. Jan, “Catalytic Degradation of Polystyrene in to Styrene” In the 7th International and 17th National Chemistry Conference, D.I.Khan, Pakistan, Feb 26-28, 2007.

11. **A. Rahim**, J. Shah, M.R. Jan, “Styrene monomer recovery from waste polystyrene by thermal and catalytic degradation. In the 9th Symposium on Analytical and Environmental Chemistry, Bara Gali, Summer Campus, University of Peshawar, Pakistan, July 24-26, 2006.

Participation in Events.

1. X Meeting SBPMat, September, 2011, Gramado, RS, Brazil (Meeting).
2. III International Workshop on Organic Chemistry, 2011 (workshop).
3. XXII National Congress of Post Graduates ANPG, 2010 (Conference).
4. II International Workshop on Organic Chemistry, 2010 (workshop).

5. 1st Sao Carlos Advanced School on Materials Science and Engineering, SanCAS-MSE, March 25 to 31, 2012.

6. 7th School of Electrochemistry at Institute of Chemistry, University of Sao Paulo, Brazil, December 2 to 8, 2012.

Teaching & Research Associate

Teaching & Research Associate of discipline QG- 650, Inorganic and Organic Lab Synthesis, Institute of Chemistry, State University of Campinas, Second semester of 2012.

Resumo

Título: *Material Cerâmico Eletricamente Condutor SiO₂/MPc/C (Pc: ftalocianina, M= Mn(II), Co(II), Cu(II)) um novo substrato para o preparo de sensores e biosensores eletroquímicos*

Este trabalho descreve as sínteses, caracterizações e as aplicações dos materiais carbono cerâmicos mesoporosos identificados como: SiO₂/20wt%C ($S_{\text{BET}} = 160 \text{ m}^2\text{g}^{-1}$) e SiO₂/50wt%C ($S_{\text{BET}} = 170 \text{ m}^2\text{g}^{-1}$), em que C corresponde ao carbono grafite. Tais materiais foram preparados através do método sol-gel e empregados como matrizes para o desenvolvimento de sensores e biosensores eletroquímicos. Imagens obtidas através da microscopia eletrônica de varredura (MEV) acoplada com a espectroscopia de energia dispersiva (EDS) mostraram que, com relação as resoluções utilizadas, não foram detectadas segregação de fases. Os materiais que contem 20 e 50 wt% de C apresentaram condutividades elétricas de $9,2 \times 10^{-5} \text{ S cm}^{-1}$ e $0,49 \text{ S cm}^{-1}$, respectivamente. Esses materiais foram utilizados como matrizes para suportar ftalocianinas de: cobalto (CoPc), cobre (CuPc) e manganês (MnPc), as quais foram preparadas *in situ* ao longo de suas superfícies de forma que fosse assegurada dispersão homogênea dos complexos eletroativos nos poros das matrizes. As densidades superficiais da ftalocianina de cobalto em ambas as superfícies da matriz foram: $0,014 \text{ mol cm}^{-2}$ e $0,015 \text{ mol cm}^{-2}$, para os materiais contendo 20 e 50 % m/m de C, respectivamente. Foram empregados como eletrodos de trabalho pastilhas preparadas a partir dos eletrodos carbono cerâmicos, considerando-se os seguintes materiais: SiO₂/C/CoPc, SiO₂/C/CuPc e SiO₂/C/MnPc. A técnica de XPS foi usada para determinar as proporções de Mn/Si atômicos dos materiais MnPc modificados.

O material $\text{SiO}_2/\text{C}/\text{CoPc}$ foi testado como um sensor de ácido oxálico e de oxigênio, e os materiais $\text{SiO}_2/\text{C}/\text{CuPc}$ e $\text{SiO}_2/\text{C}/\text{MnPc}$ foram testados como sensores para a dopamina e nitrito, respectivamente. Esses materiais tem se mostrado como alternativas promissoras para o desenvolvimento de sensores eletroquímicos e de biosensores, atuando como substratos robustos e versáteis para a construção de novos eletrodos carbono cerâmicos.

Abstract

Title: *SiO₂/MPc/C electrically conductive ceramic material (Pc: phthalocyanine, M = Mn(II), Co(II), Cu(II)) a new substrate for the preparation of electrochemical sensors and biosensors*

This work describes the synthesis, characterization and applications of mesoporous carbon ceramic materials identified as: SiO₂/20wt%C ($S_{\text{BET}} = 160 \text{ m}^2\text{g}^{-1}$) and SiO₂/50wt%C ($S_{\text{BET}} = 170 \text{ m}^2\text{g}^{-1}$), where C represents the carbon graphite. These materials were prepared by the sol-gel method and used as support for the development of electrochemical sensors and biosensors. Images obtained by scanning electron microscopy (SEM) coupled with energy dispersive spectroscopy (EDS) showed that, within the magnification used, no phase segregation was detectable. The materials containing 20 and 50 wt% of C presented electric conductivities of 9.2×10^{-5} and 0.49 S cm^{-1} , respectively.

These materials were used as matrices to support manganese phthalocyanines (MnPc), cobalt phthalocyanines (CoPc), and copper phthalocyanines (CuPc), prepared *in situ* on their surfaces, to assure homogeneous dispersion of the electroactive complex in the pores of matrices. The surface densities of cobalt phthalocyanine on both matrix surfaces were: $0.014 \text{ mol cm}^{-2}$ and $0.015 \text{ mol cm}^{-2}$, for materials containing 20 and 50% wt% of C, respectively. The pressed disk carbon ceramic electrode: SiO₂/C/MnPc, SiO₂/C/CoPc, and SiO₂/C/CuPc were used as working electrode. XPS was used to determine the Mn/Si atomic ratios of the MnPc-modified materials.

The material SiO₂/C/CoPc was tested as a sensor for oxalic acid and oxygen and the materials SiO₂/C/CuPc and SiO₂/C/MnPc were tested as sensors for

dopamine and nitrite, respectively. These materials have shown to be promising alternative in the development of electrochemical sensors and biosensor, acting as a robust and versatile conducting substrate for the construction of new carbon ceramic electrodes.

Abbreviation List

TEOS	Tetraethyl orthosilicate
XPS	X-ray photoelectron spectroscopy
BE	Binding energy
S _{BET}	Specific surface area BET method
UV-Vis	Ultra violet visible
BRB	Britton Robinson Buffer
SCE	Saturated calomel electrode
SEM	Scanning electron microscopy
EDS	Energy dispersive spectroscopy
LOD	Limit of detection
nA	Nano ampere
MPc	Metal phthalocyanine
DA	Dopamine
AA	Ascorbic acid
RE	Resorcinol
CA	Catechol
T	Temperature
t	Time

Index

Index of Tables	xxvii
Index of Figures	xxix
1. INTRODUCTION	1
1.1 Electrochemical sensors and biosensors using carbon ceramic materials SiO ₂ /C.....	1
1.2 Sol-gel process.....	5
1.3 Phthalocyanines.....	7
1.4 Oxalic acid, dopamine, Oxygen and nitrite.....	9
2. OBJECTIVES	11
3. EXPERIMENTAL PART	13
3.1 Reagents Used.....	13
3.2 Synthesis of SiO ₂ /C-grafite by sol-gel process.....	14
3.3 <i>In situ</i> synthesis of metallophthalocyanines (CoPc, CuPc and MnPc).....	15
3.4 Extraction of the in situ complex formed on SiO ₂ /C matrix.....	15
3.5 Characterization of the materials SiO ₂ /C/MPc.....	16
3.5.1 Determination of the specific surface area and pore distribution of the materials SiO ₂ / 50 wt % C and SiO ₂ /20 wt % C.....	16
3.5.2 Scanning electron microscopy (SEM).....	16

3.5.3 Electrical conductivities.....	16
3.5.4 Electronic Spectroscopy in UV-Vis Region.....	17
3.5.5 X-rays Photoelectron spectroscopy (XPS).....	17
3.6 Preparation of working electrodes.....	17
3.7 Electrochemical measurements of the SiO ₂ /C/MPcs materials.....	18
3.8 Assay of the nitrite content in food samples.....	19
4.0 RESULTS AND DISCUSSIONS.....	21
4.1 <i>In situ</i> immobilization of cobalt phthalocyanine on the mesoporous carbon ceramic SiO₂/C prepared by the sol-gel process. Evaluation as an electrochemical sensor for oxalic acid.....	21
4.1.1 Chemical analysis, surface areas, pore volume and diameter of the SiO ₂ /C.....	21
4.1.2 Scanning electron microscopy (SEM) coupled with Energy dispersive spectroscopy (EDS).....	22
4.1.3 Measurements of Electrical Conductivity.....	24
4.1.4 <i>In situ</i> generation of CoPc.....	25
4.1.5 Electronic Spectroscopy in UV-Vis Region.....	25
4.1.6 Electrochemical measurements and study of oxalic acid oxidation.....	26
4.2) Dissolved O₂ sensor based on Cobalt (II) phthalocyanine immobilized in situ on electrically conducting carbon ceramic mesoporous SiO₂/C material.....	34
4.2.1 <i>In situ</i> generation of CoPc.....	34

4.2.2 Scanning electron microscopy (SEM) coupled with Energy dispersive spectroscopy (EDS).....	35
4.2.3 Electrochemical characterization and sensor performance.....	36
4.2.4 Electrocatalytic reduction of oxygen on CoPc modified SiO ₂ /C electrode and influence of Phthalocyanine.....	38
4.2.5 Mechanistic studies of the oxygen reduction on SiO ₂ /C/CoPc.....	39
4.2.6 The sensor characteristics.....	45
4.2.7 Stability of CoPc on the SiO ₂ /C electrode.....	48
4.2.8 Application to the water sample and interference studies.....	49
4.3 SiO₂/C/CuPc as a biomimetic catalyst for dopamine monooxygenase in the development of an amperometric sensor.....	51
4.3.1 In situ generation of CuPc.....	51
4.3.2 Electronic Spectroscopy in UV-Vis Region.....	52
4.3.3 Electrochemical measurements and Electrode response.....	52
4.3.4 Influence of hydrogen peroxide.....	55
4.3.5 Influences of the applied potential, buffer and solutions pH.....	57
4.3.6 Sensor characteristics.....	59
4.3.7 Sensor application: interference and determination of dopamine in physiological solution.....	62
4.4 <i>Electrochemical detection of nitrite in meat and water samples using a mesoporous carbon ceramic SiO₂/C electrode modified with Manganese (II) phthalocyanine</i>.....	65
4.4.1 <i>In situ</i> synthesis of manganese phthalocyanine (MnPc).....	65

4.4.2 X-rays Photoelectron spectroscopy (XPS).....	66
4.4.3 Electrocatalytic oxidation of nitrite on MnPc modified SiO ₂ /C electrode and influence of Phthalocyanine.....	68
4.4.4 Influence of the solution pH value.....	69
4.4.5 Analytical characterization.....	70
4.4.6 Studies on the surface confined redox process behavior of MnPc.....	72
4.4.7 Stability of MnPc on the SiO ₂ /C electrode.....	73
4.4.8 Interferences.....	75
4.4.9 Determination of nitrite in water and sausage meat samples.....	75
5. Conclusions.....	78
6. References.....	81

INDEX OF TABLES

Table 3.1: Characteristics of the reagents utilized.....	13
Table 4.1: Comparison of the limit of detection for oxalic acid between the SiO ₂ /C/CoPc and other electrodes.....	33
Table 4.2: Quantitative Results of EDS spectrum.....	36
Table 4.3: Electrode response obtained with different electrode prepared in the same way, containing 6 mg L ⁻¹ of oxygen.....	48
Table 4.4: Determination of dissolved oxygen in pond and Tap water by the proposed sensor and DO meter (determinations in triplicate).....	49
Table 4.5: Interference effects on the detection of dissolved oxygen determination with proposed method in KOH/HCl pH 7 and oxygen concentration of 6 mg L ⁻¹ and interference species concentration=150 mg L ⁻¹	50
Table 4.6: Analytical parameters for dopamine detection with biomimetic sensors under optimized amperometric conditions.....	62
Table 4.7: Determination of dopamine in sample.....	64
Table 4.8: Peak intensities and atoms % for SiO ₂ /C/MnPc calculated from XPS data.....	68

Table 4.9: Determination of nitrite in water sample and sausage meat samples (n=3).....76

Table 4.10: Comparison of different nitrite sensors for the nitrite determination.....77

INDEX OF FIGURES

Figure 1.1: Structure of unmetallated phthalocyanine.....	8
Figure 1.2: Synthesis route of phthalocyanine.....	9
Figure 3.1: Fabrication of the SiO ₂ /C/MPc disk and the working electrode mounted after fixing the disk on the glass tube.....	18
Figure 4.1: N ₂ adsorption-desorption isotherms: (A) SiO ₂ /20wt%C and (B) SiO ₂ /50wt%C and pore size distribution curve respectively • adsorption ◦ desorption.....	22
Figure 4.2: SEM images for (A) SiO ₂ /20wt%C and (B) SiO ₂ /50wt%C.....	23
Figure 4.3: EDS images: silicon mapping: (A) SiO ₂ /20w%C and (B) SiO ₂ /50wt%C; Carbon mapping: (C) SiO ₂ /20w%C and (D) SiO ₂ /50wt%C.....	24
Figure 4.4: UV–Vis diffuse reflectance spectra of SiO ₂ /C/CoPc, expressed in Kubelka–Munk units.....	26
Figure 4.5: Cyclic voltammetry curves obtained for different concentration of oxalic acid (in mol L ⁻¹): a) 0.0, b) 3.98 x 10 ⁻⁵ , c) 7.94 x 10 ⁻⁵ , d) 1.19 x 10 ⁻⁴ , e) 1.57 x 10 ⁻⁴ , f) 1.96 x 10 ⁻⁴ , g) 2.34 x 10 ⁻⁴ , h) 2.72 x 10 ⁻⁴ , i) 3.1 x 10 ⁻⁴ , j) 3.47 x 10 ⁻⁴ , k) 3.84x 10 ⁻⁴). Potential scan rate: 20 mV s ⁻¹ ; supporting electrolyte: 1.0 mol L ⁻¹ KCl. (A) SiO ₂ /20wt%C/CoPc and (B) SiO ₂ /50wt%C/CoPc.....	28

Figure 4.6: Anodic peak current intensity plotted against number of oxidation-reduction. Conditions: oxalic acid: $7.5 \times 10^{-5} \text{ mol L}^{-1}$ in 1.0 mol L^{-1} KCl.....29

Figure 4.7: Dependence of the anodic peak current on the square root of scan rate, obtained for the $\text{SiO}_2/50\text{wt}\% \text{C}/\text{CoPc}$ electrode. Conditions: oxalic acid: $7.5 \times 10^{-5} \text{ mol L}^{-1}$ in 1.0 mol L^{-1} KCl.....30

Figure 4.8: Influence of pH on the peak potential for $\text{SiO}_2/50\text{wt}\% \text{C}/\text{CoPc}$ electrode. Measurements carried out in 1.0 mol L^{-1} KCl, scan rate of 20 mV s^{-1} and $[\text{H}_2\text{C}_2\text{O}_4] = 2.3 \times 10^{-4} \text{ mol L}^{-1}$ 31

Figure 4.9: Chronoamperograms for $\text{SiO}_2/50\text{wt}\% \text{C}/\text{CoPc}$ electrode in different concentrations of oxalic acid at fixed potential of 0.73 V ; Inset Figure plot of current intensity against oxalic acid concentration (measured at 50s).....32

Figure 4.10: SEM image (a) and EDS mapping of Co (b) for $\text{SiO}_2/\text{C}/\text{CoPc}$35

Figure 4.11: Cyclic voltammograms for: $\text{SiO}_2/\text{C}/\text{CoPc}$ electrode in the absence (a) and presence of O_2 (b) and voltammogram of SiO_2/C bare electrode in the presence of O_2 (c) in the concentration of $9.1 \text{ mg L}^{-1} \text{ O}_2$. Experimental conditions: $T = 298 \text{ K}$, scan rate $\nu = 10 \text{ mV s}^{-1}$; 1 mol L^{-1} KCl; $\text{pH} = 7$37

Figure 4.12: Cyclic voltammograms obtained for: $\text{SiO}_2/\text{C}/\text{CoPc}$ -in situ electrode (solid line), $\text{SiO}_2/\text{C}/\text{CoPc}$ -classically electrode (dotted line) and $\text{SiO}_2/\text{C}/\text{Co}$ electrode (dashed line), all in the presence of $8.2 \text{ mg L}^{-1} \text{ O}_2$. Experimental conditions: $T = 298 \text{ K}$, $\nu = 10 \text{ mV s}^{-1}$; 1 mol L^{-1} KCl, $\text{pH} = 7$39

Figure 4.13: (a) Cyclic voltammograms of the SiO₂/C/CoPc electrode at different scan rates (mV s⁻¹): from top to bottom: 5, 10, 20, 50, 75, 100, 150, 200. (b) Plot of cathodic peak current against square root of the scan rate ($v_{1/2}$). Experimental conditions: T = 298 K, [O₂] = 9.0 mg L⁻¹; 1 mol L⁻¹ KCl; pH = 7.....41

Figure 4.14: Differential pulse voltammetry measurement of SiO₂/C/CoPc electrode in the absence (a) and presence (b) of 9.0 mg L⁻¹ O₂. Experimental conditions: T = 298 K; 1 mol L⁻¹ KCl; pH = 7; $v = 10$ mV s⁻¹.....43

Figure 4.15: Values of cathodic peak current and reduction peak potential at a function of the solution pH obtained for the SiO₂/C/CoPc electrode. [O₂] = 9.0 mg L⁻¹; T = 298 K, and $v = 10$ mV s⁻¹.....45

Figure 3.16: (a) Amperometry response of the SiO₂/C/CoPc electrode in different oxygen concentrations (mg L⁻¹): from top to bottom: 0.0, 0.5, 1.4, 1.9, 2.8, 3.4, 4.4, 5.5, 6.6 (b) Plot of cathodic current (Δi_{cp}) vs [O₂] (measured at 50 s). Experimental conditions: T = 298 K, E_{appl} = -0.23 V; 1 mol L⁻¹ KCl; pH 7.....47

Figure 4.17: Diffuse reflectance spectrum of SiO₂/C/CuPc, expressed in Kubelka–Munk units.....52

Figure 4.18: Signals obtained with the proposed sensor using SiO₂/C/CuPc: (a) in absence and (b) presence of 100 $\mu\text{mol dm}^{-3}$ H₂O₂. Each step corresponds to the increment of 10 $\mu\text{mol dm}^{-3}$ dopamine. The inset figure shows the analytical curve. Applied potential -20 mV vs SCE in 0.08 mol dm⁻³ BRB at pH=6.0 containing 1 mol dm⁻³ KCl.....53

Figure 4.19: Proposed mechanism for the sensor SiO₂/C/CuPc response for dopamine.....55

Figure 4.20: Amperometric response for the biomimetic biosensor for dopamine. Each step corresponds to the increment of 10 μmol dm⁻³ dopamine and containing 100 μmol dm⁻³. The inset figure shows the analytical curve. Applied potential -20 mV vs SCE in 0.08 mol dm⁻³ BRB at pH=6.0 containing 1 mol dm⁻³ KCl.....57

Figure 4.21: Influence of the applied potential on the current density Δj. Measurements carried out in 0.08 mol dm⁻³ BRB at pH=6.0 containing 1 mol dm⁻³ KCl, and 10 μmol dm⁻³ of dopamine and 100 μmol dm⁻³ of H₂O₂.....58

Figure 4.22: Influence of the pH on the current density Δj. Measurements carried out in 0.08 mol dm⁻³ BRB containing 1 mol dm⁻³ KCl, and 10 μmol dm⁻³ of dopamine and 100 μmol dm⁻³ of H₂O₂.....59

Figure 4.23: A typical profile of the sensor response using the optimized conditions. Applied potential of -20 mV vs SCE, in 0.08 mol dm⁻³ BRB at pH= 6.0 containing 1 mol dm⁻³ KCl, and 100 μmol dm⁻³ of H₂O₂.....60

Figure 4.24: Current i vs. time for the addition of catechol (CA) resorcinol(RE) ascorbic acid (AA) and DA into the electrochemical cell in sequence at 75, 150, 175, 250 and 300 s. Concentrations in (μmol dm⁻³) of the analytes in the reaction cell: (a) [CA] = 10 , (b) [RE] = 10; (c) [AA] = 2; (d) [DA] = 10 (e) [CA] = 20 (f) [RE] = 20 (g) [AA] = 4 (h) [DA] = 20 and (i) [AA] = 5. Applied potential of -20

mV vs SCE, in 0.08 mol dm⁻³ BRB at pH= 6.0 containing 1 mol dm⁻³ KCl, and 100 μmol dm⁻³ H₂O₂.....63

Figure 4.25: UV–Vis diffuse reflectance spectra of SiO₂/C/MnPc, expressed in Kubelka–Munk units.....66

Figure 4.26: XPS spectrum for Manganese (a) and N (b).....67

Figure 4.27: Cyclic voltammograms obtained for: bare SiO₂/C electrode (a), SiO₂/C/Mn electrode (b) and SiO₂/C/MnPc electrode (c), all in the presence of 15.74 μmol L⁻¹ nitrite in 1 M KCl solution, 0.1 mol L⁻¹ phosphate buffer (pH 4), scan rate: 20 mV s⁻¹.....69

Figure 4.28: Dependence of the oxidation peak current on pH values in 12.63 μmol L⁻¹ nitrite in 1 M KCl solution, scan rate: 20 mV s⁻¹.....70

Figure. 4.29: (a) Cyclic voltammograms for SiO₂/C/MnPc electrode in different concentrations: (a) 0 (b) 0.79 (c) 1.59 (d) 3.19 (e) 4.65 (f) 6.36 (g) 7.93 (h) 9.51 (i) 11.07 (j) 12.63 (k)14.19 and (l)15.74 μmol L⁻¹ nitrite in 1 M KCl solution, 0.1 mol L⁻¹ phosphate buffer (pH 4), scan rate: 20 mV s⁻¹. Inset figure is a plot of peak current density against nitrite concentration.....71

Figure 4.30: Variation of the anodic peak current I_{pa} vs. the square root of the potential scan rate v^{1/2} for the SiO₂/C/MnPc electrode in 0.1 mol L⁻¹ phosphate

buffer solution (pH 4) containing $12.63 \mu\text{mol L}^{-1}$ nitrite. Scan rate 5–
 180mVs^{-1} 73

Figure 4.31: Relative response (%) at a function of the number of determinations.
Applied scan rate = 20mVs^{-1} , in 0.1mol L^{-1} phosphate buffer (pH 4.0), containing
 $12.63 \mu\text{mol L}^{-1}$ of nitrit.....74

1. INTRODUCTION

1.1 Electrochemical sensors and biosensors using carbon ceramic materials SiO₂/C.

Sensors are devices that register a physical, chemical or biological change and convert it into a measurable signal.¹ The sensor contains a recognition element that enables the selective response to a particular analyte or a group of analytes, thus minimizing interferences from other sample components. Another main component of a sensor is the transducer or the detector device that produces a signal. A signal processor collects, amplifies, and displays the signal.² The most important aspect of investigation of sensors is sensitivity, selectivity and stability. Sensors can be classified, according to the type of energy transfer, as thermal, electromagnetic, mechanical, and electrochemical. Among them the electrochemical sensors are very promising analytical methods because of their high degree of selectivity and sensitivity. They are more useful and easy to determine the concentrations of various analytes in samples such as fluids and dissolved solid materials. They are frequently used in clinical diagnostics, occupational safety, medical engineering, process measuring engineering and environmental analysis.³ Electrochemical biosensors are devices generally recognized a small robust portable and easy to use. These devices are used in determinations in aqueous solution or otherwise of significant chemical and biological compounds in low concentrations. Determining these substances occurs through redox reactions in the electrode interface/solution, which are then converted into electrical signals.³

Electrochemical sensor and Biosensors have gained ever-increasing attention due to their practical and potential applications in the areas of clinical analysis,^{4,5} food industry^{6,7} monitoring of waste industries⁸ and environmental monitoring.^{9,10} In the literature exist different types of electrochemical sensor and biosensor in the form electrodes, which are classified into conventional electrodes and chemically modified electrode (CME's).^{11,12}

The conventional electrodes are generally formed by a single material being the most common electrodes of gold (Au), platinum (Pt), carbon graphite (C) and glassy carbon (GC). These electrodes are characterized by a slow electron transfer kinetics, and by detecting analytes of interest in quite high potential¹³ in electrochemical analyses. In particular, the detection of substances to high potential is not desirable due to the possibility of oxidation or reduction of interfering in the same detection potential of the analyte of interest. Thus, in the 70s, the chemically modified electrodes (CMEs) appeared as an alternative for solving such cited problems, with generally low capacitive current and smaller oxidation or reduction potential of analytes.

The CMEs are characterized by modifying the surface of an electrode support or conventional electroactive species in order to change the electrochemical properties of the electrode interface / solution, resulting in a higher sensitivity and selectivity compared to conventional electrodes.¹⁴

The vast majority of modified electrodes are made by adsorption or covalent binding of various species on solid substrates, surface-assembled monolayer, homogeneous multilayer coatings (electroactive or semiconducting polymers or ion exchange resins) or even heterogeneous materials resulting from the dispersion of the modifier into a conductive composite matrix.¹¹ The goal is to block straight access to the electrode, inhibiting some processes and promoting

others. Normally the electroactive layer modifier is acting as electron transfer mediator between the solution and the electrode (substrate).

The electrodes modified with inorganic and organic materials form a subcategory of CMEs. Various inorganic matrices have been used as the modifying agent of conventional electrodes. They include metal oxides,^{15,16} metal phthalocyanines and porphyrins,¹⁷⁻²⁰ Prussian Blue films and related transition metal cyanides,^{21,22} phosphates and phosphonates,^{23,24} γ -alumina,²⁵ silica gel,^{26,27} fumed silica²⁸ or other oxides obtained by the sol-gel process,^{29,30} clays^{31,32} or layered double hydroxides,^{33,34} and zeolites.³⁵⁻³⁷

Single or mixed ceramic oxides have been used to prepare electrochemical sensors,³⁸ with a predominance of those based on carbon paste electrodes (CPEs).³⁹ These electrodes have been used to determine a great variety of analytes, such as dissolved oxygen in natural water,⁴⁰⁻⁴² hydrogen peroxide,⁴³ Pb(II),⁴⁴ phenolic compounds,⁴⁵ glucose,⁴⁶ NADH⁴⁷⁻⁴⁹ and oxalic acid.⁵⁰ Although CPEs have demonstrated good results in general, the mechanical resistance of these electrodes is low, limiting their use over a long period of time.

However, the major problem with such ceramics is the high electrical resistance, unwanted feature in electrochemical devices. To overcome this adversity, these materials have been used as carbon pastes. The carbon paste electrodes consist of a mechanical mixture of graphite powder and the material of interest with various nonconductive binders (Nujol, liquid paraffins, silicone oils). These electrodes are inexpensive, usually have low currents background (current capacitive) and easily renewable surfaces.⁵¹⁻⁵³

However, the reproducibility in the preparation of the pasts is difficult to achieve, and small changes in its composition significantly affect reactivity of the electrode.⁵³ A small increase in the amount of binder can sharply reduce the rate of

electron transfer, and the contributions from current background increase. Despite the popularity, the exact behavior of carbon paste electrodes is not well understood and involves problems such as permeation of the electroactive species in the liquid binder and tended to occur dissolution of liquid solutions containing organic solvents or components. These factors, coupled with the low reproducibility and stability of the electrodes limiting the use of pastes, for example, in chromatography analysis, in liquid flow analysis and other applications that routine electroanalytical spend a longer time during the measurements.

In 1994, O. Lev and coworker⁵⁴ synthesized a new carbon ceramic composites via sol-gel methods, known as carbon ceramic electrode (CCEs), which overcome the problems presented above. These electrodes basically consist of dispersing graphite in a ceramic matrix of silica or derived silica modified through sol-gel process. The electrodes may be prepared in different geometric shapes and configurations and include molding the gel in capillary tubes or thin film deposition on substrates.⁵⁴⁻⁵⁶ Since then, many studies have been performed on improving the electrodes and also the modification of ceramic matrices aimed the incorporation of electroactive species of electrochemical interest.^{30,57-59}

This type of materials present main characteristics such as rigidity, porosity, easy surface renewability, durability, and show good electrical conductivity due to good distribution of graphite particles in the silica matrix, being used as base material in the preparation of carbon ceramic electrodes (CCEs).^{54,56} Another important feature of CCEs are high sensitivity, when compared to the carbon past electrode, due to its porous structure to allow a large number of active sites participate in the electrochemical process.

Due to these characteristics, the carbon ceramic electrodes have been widely used in the construction of electrochemical sensors and biosensors.⁶⁰⁻⁶³

Several electron transfer mediators have been used to shuttle electrons between electrode surface and the oxygen. Electrodes modified with palladium,⁶⁴ bilirubin oxidase,⁶⁵ metallophthalocyanine,⁶⁶ cobalt(II) porphyrin complexes⁴⁰ have been used in the study of oxygen reduction.

Among them, the metallophthalocyanines and porphyrins have received considerable interest due to their singular properties, including high thermal stability and catalytic efficiency for a great number of molecules. These complexes belong to a class that makes possible to investigate details of the factors involved in the activation and reduction of molecular oxygen. Effects from axial and peripheral substitution in the macrocyclic ring, the nature of the metallic center and the conjugation degree of the ring can be cited as examples.⁶⁷

1.2 Sol-gel process

The sol-gel process is a highly versatile synthesis technique used to produce porous materials, highly homogeneous materials and hybrid thin films at relatively mild temperatures. Several factors have direct influence on the sol-gel process, as sort of precursor used, type of catalyst, temperature, nature of solvent used, pH, besides the amount of water employed etc. These factors directly contribute to the characteristics of materials made with regard to morphology and structural and consequently, with various properties and applications.⁶⁹ The sol-gel process is governed mainly by hydrolysis and condensation reactions of precursors. Several precursors can be used in this type of synthesis, among them, inorganic salts, carboxylates, acetylacetonates, transition metal alkoxides and silicon alkoxides. The silicon alkoxides are the most commonly used due to their high purity, ease of hydrolysis and present a slow kinetic reaction.⁷⁰ The reactions involved in the sol-gel process are divided into two steps and will be represented here using tetraalkoxisilanes as example: The first step is hydrolysis, which is the substitution of

the alkoxides groups with reactive hydroxy groups known as silanol groups. This change occurs in the presence of catalysts that may be acidic (HCl, HNO₃), or basic (NH₄OH, KOH). When the catalyst is acid, the hydrolysis reaction occurs in two steps: first occurs electrophilic attack of acid to alkoxide group (OR) followed by nucleophilic attack (SN₂) of oxygen in the water molecule in the central atom of the substrate, in this case silicon. The reactions catalyzed by acids are characterized by having slow hydrolysis forming materials with long chain, short branched and microporous structure, due to the fact that condensation reaction mainly occurs at the end of oligomers, which is characteristic slow hydrolysis reactions.

When HF used as acid catalyst, the F ions bind directly to the silicon atom followed by nucleophilic attack (SN₂) of oxygen contained in water molecule increasing the coordination number of intermediate species formed, from 4⁺ to 6⁺ yielding mesoporous materials.⁷⁰

When the catalyst is basic, the reaction occurs in a single step corresponding to nucleophilic attack (SN₂) of (-OH) group directly to the silicon atom with the formation of pentacoordinated intermediate.

The base-catalyzed reactions are characterized by the formation of highly dense materials with short branched chains polymer having meso or macroporous structure due to relatively rapid hydrolysis reaction and condensation occur in the middle of the oligomers formed. Therefore, the pH of the solution is a very important parameter in the formation of the structure of the final products.

The second step consists of condensation and polymerization reactions. These two reactions occur simultaneously giving rise to the polymeric network due to the

connection between the reactive silanol groups or alkoxides to form links M-O-M or M-⁺OH-M, with the possibility to eliminate water or alcohol molecules.

The reactions of hydrolysis, condensation and polymerization are closely related i.e. once the hydrolysis reaction is initiated the polymerization and condensation reactions start consecutively.

1.3 Phthalocyanines

Phthalocyanines(Pcs) were discovered in the 1930's and were used as blue and blue-green pigments and dyes.⁷¹ Over time, their properties have been developed, these include semi-conductivity in the 1940's⁷² and synthetic modifications in the 1970's. Amongst their numerous applications, they are now currently employed as photo-sensitizers in photodynamic therapy of cancer (PDT)⁷³, involved in linear⁷¹ and non-linear optics,⁷⁴ used as electro^{75,76} and biomimetic^{71,77} catalysts and as fluorescent agents.⁷⁸ They are also used as thin, light-absorbing films to coat compact discs (CDs).⁷⁹

Phthalocyanines are conjugated, aromatic, symmetrical, macrocyclic complexes with 18 π electron system.⁸⁰ They contain four isoindole groups which are linked by four nitrogen atoms. Unmetallated Pcs, Figure 1.1, are planar exhibiting D_{2h} symmetry, whereas, their metallated counterparts exhibit D_{4h} symmetry. They are similar to naturally occurring porphyrins, but have extended conjugation engendered by benzene rings, hence have improved chemical and thermal stability. Another set consisting of four benzene rings can be fused onto the Pc ring yielding naphthalocyanines, then subsequently anthralocyanines.

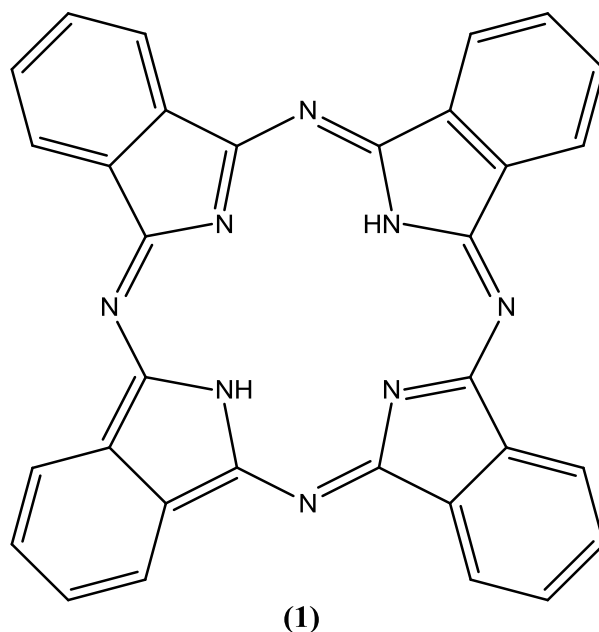


Figure 1.1: Structure of unmetallated phthalocyanine

Synthesis of phthalocyanines can be achieved using different routes depending on the type of phthalocyanines to be synthesized; metal free, symmetrical and asymmetrical metallophthalocyanines. Various precursors such as phthalonitrile, phthalic acid, phthalic acid anhydride, phthalimide, diiminoisoindoline and o-cyanobenzamide have been developed for this syntheses.^{81,82} Phthalonitrile, phthalic anhydride, phthalic acid and phthalimide, Figure 1.2, are the most used precursors for the synthesis of MPCs. The method using phthalonitrile are more used due to their relative simplicity.⁸³ This procedure can also be used when we want to get a metalated phthalocyanine.⁸⁴

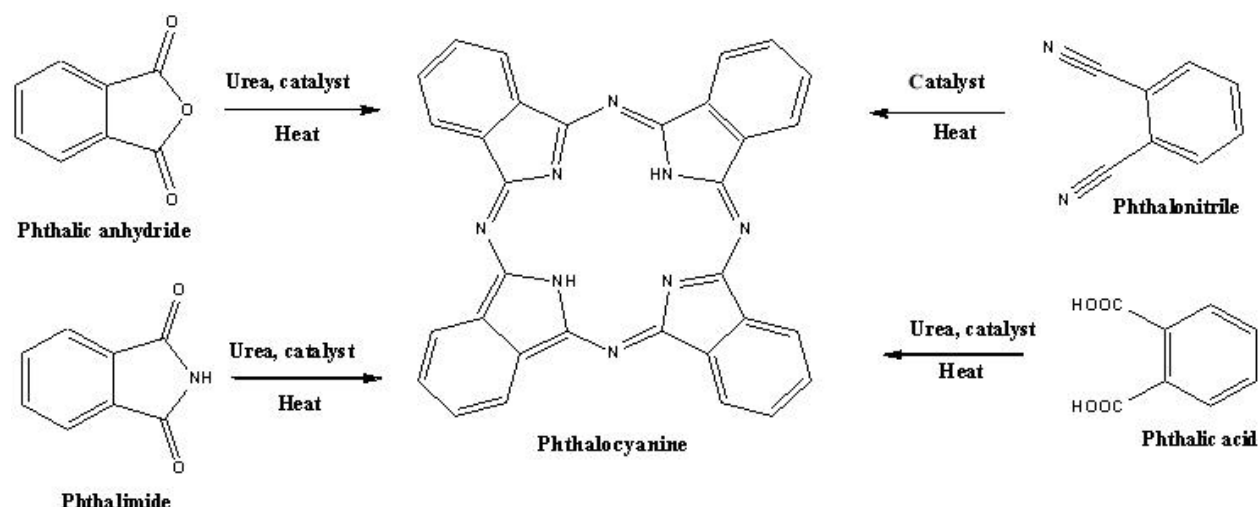


Figure 1.2: Synthesis route of phthalocyanine

The MPc complex ($M =$ transition metal) has high thermal stability.⁸⁵ When the central metal is electrochemically active, the phthalocyanine have received considerable interest due to their singular properties, including their high catalytic efficiency for a great number of molecules, presents optical properties, electronic and electrochemical changes related to the oxidation state of the central metal and contributions of π electrons of conjugated bonds.⁸⁶ As the Mn(II) Cu(II) and Co(II) are electroactive metals, the phthalocyanines containing these metals present electrochromic⁸⁷ and electrocatalytic⁸⁸ properties. For this reason these complexes are utilized in the electrocatalysis of trimethylamine,⁸⁹ oxalic acid,²⁰ dopamine,¹⁹ nitrite,⁹⁰ phenols,⁹¹ vitamine B1⁹² and molecular oxygen reduction.^{93,94}

1.4 Oxalic acid, dopamine, oxygen and nitrite

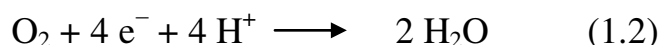
Oxalic acid naturally occurs in many plants (spinach, ginger, chocolate, etc) and combines with Ca, Fe, Na, Mg, or K to form less soluble salts known as oxalates.⁹⁵ High levels of these salts in the diet can lead to irritation of the digestive system, particularly of the stomach and kidneys. It is also known to contribute to

the formation of kidney stones. The urinary level of oxalic acid has long been recognized as an important indicator for the diagnosis of renal stone formation.^{96,97}

Dopamine (DA) is one of the most important catecholamines and belongs to the family of excitatory chemical neurotransmitter. It plays a very important role in the function of central nervous, cardiovascular, renal and hormonal systems, as well as a key role in the drug addiction. Abnormal levels of DA lead to brain disorders such as Parkinson and schizophrenia diseases.^{98,19}

The oxygen molecule (O_2) is of great importance in various fields of knowledge. It participates both in industrial process and biological systems. An important industrial application is in fuel cells,⁹⁹ since the oxygen reduction reaction takes place at the cathode of these cells. In biological aquatic systems, dissolved oxygen is essential for the maintenance of life. Therefore, the development of sensors capable of monitoring the amount of dissolved oxygen is so important.¹⁰⁰

The reduction of oxygen can occur by two different mechanisms, one using two electrons, with the formation of H_2O_2 , and another using four electrons, with the formation of water.^{101,102}



The most widely used method for determination of dissolved oxygen is using the Clark electrode,¹⁰³ (SKOOG), in this type of electrode oxygen reduction occurs on the surface of platinum through a mechanism involving four electrons.

Nitrite is ubiquitous within natural environment and food because it is commonly used as food preservative.¹⁰⁴ Nitrite ions can have detrimental effects via two mechanisms. They can combine with blood pigments producing methahemoglobin in which oxygen is no longer available to the tissues. In

addition, they may interact in the stomach with amines and amides forming highly carcinogenic N-nitrosamine compounds.¹⁰⁵ Because of its potential toxicity, its determination is important for public health and environmental security. Therefore, it is essential to develop a reliable and sensitive sensor to detect nitrite in food, drinking water and environmental samples.

2.OBJECTIVES

This work aims to synthesize and characterize the carbon ceramics materials (SiO_2/C) obtained by sol-gel process. The material was used as matrices to support metal phthalocyanine MPcs ($\text{M} = \text{Co}, \text{Cu}$ and Mn), prepared *in situ* on their surfaces, to assure homogeneous dispersion of the electroactive complex in the pores of the matrices. The material $\text{SiO}_2/\text{C}/\text{MPcs}$ were characterized by BET technique, scanning electron microscopy (SEM), energy dispersive spectroscopy (EDS), x-ray photoelectron spectroscopy (XPS) and diffuse reflectance spectroscopy.

Therefore, the prepared materials $\text{SiO}_2/\text{C}/\text{MPcs}$ were used in the construction of pressed disk electrodes as sensors. In order to study the electrocatalytic properties of oxalic acid, dopamine, oxygen reduction and nitrite, cyclic voltammetry, differential pulse voltammetry and amperometry techniques were used.

The material $\text{SiO}_2/\text{C}/\text{CoPc}$ was used as an electrochemical sensor for the oxidation of oxalic acid and oxygen reduction. The carbon ceramic materials $\text{SiO}_2/\text{C}/\text{CuPc}$ was used as a biomimetic catalyst for dopamine monooxygenase in the development of an amperometric biosensor. Pressed disk electrode of $\text{SiO}_2/\text{C}/\text{MnPc}$ was tested as electrochemical sensor for oxidation of nitrite.

3. Experimental part

3.1 Reagents Used

Table 3.1 shows the characteristics of the reagents used to perform this work.

Table 3.1: Characteristics of the reagents utilized

Reagents	Formula	Origin	Purity
Tetraethylorthosilicate (TEOS)	$\text{Si}(\text{C}_2\text{H}_5\text{O})_4$	Aldrich	98.0 %
Graphite	C	Aldrich	99.99 %
Hydrochloric Acid	HCl	Nuclear	37.0 %*
Phosphoric Acid	H_3PO_4	Synth	98.0 %
Hydrofluoric Acid	HF	Synth	40.0 %
Sodium Hydrogenphosphate	Na_2HPO_4	Aldrich	99.0 %
Potassium Dihydrogenphosphate	KH_2PO_4	Aldrich	99.0 %
Sodium Hydroxide	NaOH	Synth	97.0 %
Hydroquinone	$\text{C}_6\text{H}_8\text{O}_2$	Merck	99.0 %
Catechol	$\text{C}_6\text{H}_8\text{O}_2$	Merck	99.0 %
Resorcinol	$\text{C}_6\text{H}_8\text{O}_2$	Across Organics	98.0 %
Potassium Chloride	KCl	KCl Synth	99.0 %
Tris (hydroxymethyl) aminomethane	$\text{NH}_2\text{C}(\text{CH}_2\text{OH})_3$	Aldrich	99.99 %
Dopamine	$\text{C}_8\text{H}_{11}\text{NO}_2$	Sigma	99.0 %
Boric Acid	H_3BO_3	Merck	99.8 %
Acetic Acid	CH_3COOH	Nuclear	99.9 %
Physiological Solution	NaCl solution	Arboeto	-
Cobalt Acetate	$\text{Co}(\text{C}_2\text{H}_3\text{O}_2)_2$	Aldrich	99.0 %
Copper Acetate	$\text{Cu}(\text{C}_2\text{H}_3\text{O}_2)_2$	Aldrich	98.0 %
Manganese Acetate	$\text{Mn}(\text{C}_2\text{H}_3\text{O}_2)_2$	Across Organic	98.0 %
Phthalonitrile	$\text{C}_6\text{H}_4(\text{CN})_2$	Fluka	98.0 %
Oxalic Acid	$\text{C}_2\text{H}_2\text{O}_4$	Merck	99.5 %
Sodium Nitrite	NaNO_2	Synth	98.0 %

Hydrogen Peroxide	H ₂ O ₂	F.Maia	32.0 %*
Potassium Hydroxide	KOH	F.Maia	85.0 %
Magnesium Chloride	MgCl ₂	Merck	99.0 %
Calcium Chloride	CaCl ₂	Carlo Erba	96.0 %
Copper Nitrate	Cu(NO ₃) ₂	Ecibra	98.5 %
Ammonium Chloride	NH ₄ Cl	Vetec	99.0 %
Ferric Chloride	FeCl ₃	Ecibra	99.0 %
Potassium Nitrate	KNO ₃	Merck	97.0 %
Potassium Sulphate	K ₂ SO ₄	Carlo Erba	99.5 %
Sodium Chloride	NaCl	Carlo Erba	99.0 %

* Dissolved in water content

3.2 Synthesis of SiO₂/C-grafite by sol-gel process

The SiO₂/C matrix was prepared by the sol–gel processing method with two different SiO₂ and C proportions, according to the following:²⁰ 4 mL of deionized H₂O and 0.1mL of concentrated HNO₃ were added to 50 mL of a solution of tetraethylorthosilicate and absolute ethanol in the proportion 1:1 (v/v) of TEOS/ethanol. The resulting solution was heated to reflux temperature for 3 h under continuous magnetic stirring at the rate of 300rpm (solution A). Solution A was cooled to room temperature and then under continuous stirring 4.0 mL of deionized water and 20 wt% graphite, calculated from the expected SiO₂ weight were added. To this mixture 0.5 mL of HF was added and then sonicated until gelation of the material, which occurred about 30 min after addition of the HF. The resulting material was stored in the hood for a week at room temperature, just covered with filter paper, for solvent evaporation. In a similar experiment another material was prepared, using 50 wt% of graphite powder based on the expected SiO₂ weight. The resulting materials from these two preparations were ground in an agate mortar. The powder obtained was immersed in 50 mL of 2.0 mmolL⁻¹ HCl and stirred for 30 min, then filtered and washed with deionized water. Finally

the material was washed with absolute ethanol in a Soxhlet extractor for 3 h, and the solvent was eliminated under vacuum (10^{-3} Torr pressure) at 393 K. The materials obtained, nominally containing 20 wt% and 50 wt% graphite, will hereafter be designated as SiO₂/20 wt% C and SiO₂/50 wt% C, respectively.

3.3 *In situ* synthesis of metallophthalocyanines (CoPc, CuPc and MnPc)

Metallophthalocyanines (CoPc, CuPc and MnPc) were synthesized *in situ* on the SiO₂/20 wt% C and SiO₂/50 wt% C powder matrices as described.²⁰ In brief, 1.0 g of SiO₂/C was immersed in 10 mL of 0.01 mol L⁻¹ metal acetate M(OAc)₂ (M = Co, Cu and Mn) and the mixture was heated in a water bath at 343 K until complete evaporation of the solvent. The dry solid, now represented as SiO₂/C/M(II), was mixed with 0.22 g of phthalonitrile and heated in an ampoule at 493K for 3 h to form the MPc complex. Metal phthalocyanine not confined in the matrix pores and unreacted phthalonitrile were removed from the solid surface in a Soxhlet extractor with absolute ethanol. Then the solid was heated at 398K under vacuum to evaporate all the solvent.

3.4 Extraction of the *in situ* complex formed on SiO₂/C matrix

The amount of the *in situ* complex formed on SiO₂/C/CoPc was determined as described elsewhere²⁰ by immersing 10 mg of the SiO₂/C/CoPc in a solution of absolute ethanol, tetrahydrofuran (THF) and pyridine in the ratio of 50:35:15, respectively. The mixture was kept to rest for 15 h to fully extract the CoPc from the SiO₂/C surface. The final volume was adjusted to 25mL with ethanol and the concentration of CoPc in the solution phase was determined using a spectrophotometric method on a Shimadzu Multispec 1501 UV–Vis photodiode array spectrophotometer. The calibration curve was obtained by dissolving CoPc

(Aldrich) in a similar ratio of ethanol/THF/pyridine as used for extraction of CoPc of the matrix.

3.5 Characterization of the materials SiO₂/C/MPc

3.5.1 Determination of the specific surface area and pore distribution of the materials SiO₂/ 50 wt % C and SiO₂/20 wt % C.

The nitrogen adsorption–desorption isotherms of previously degassed material at 423K were determined at the liquid nitrogen boiling point on an Autosorb I Quantachrome instrument. The specific surface was determined from the BET (Brunauer, Emmett and Teller) multipoint method¹⁰⁶ and the pore size distribution was obtained using the BJH (Barret, Joyner, and Halenda) method.¹⁰⁷

3.5.2 Scanning electron microscopy (SEM).

Scanning electron micrograph (SEM) images were obtained using secondary back scattered electrons on a JEOL JSM 6360LV microscope operating at 20 kV, equipped with an energy dispersive (EDS) X-ray attachment from NORAN Instruments. The samples (~1mg) were fixed onto double-faced carbon tape (3M Electrical Division, Brazil) adhered to an aluminum support and coated with a gold layer using a Bal-Tec MD20 metallizing system.

3.5.3 Electrical conductivities

The electrical conductivities of the samples were obtained using the four point probe method on a National Instruments NI PXI-1033 equipment. Measurements were made for a disk of finely powdered SiO₂/C with 0.5cm diameter and approximately 0.01 cm thickness (w) pressed under a pressure of 4.5 ton. The conductivities (σ) were calculated by applying the equation:

$$\sigma = \frac{1}{RwF_2F_4}$$

where R is the electrical resistance, w is the thickness of the disk, and F_2 and F_4 are correction factors taken from the literature as 0.50 and 0.98, respectively.¹⁰⁸

3.5.4 Electronic Spectroscopy in UV-Vis Region

The electronic spectrum of MPc prepared in situ on the SiO_2/C matrix were obtained using the diffuse reflectance technique on a UV-Vis DRS CARY 5G UV/Vis spectrophotometer. Barium sulphate was used as the white reference sample. The Kubelka-Munk function was used for the analysis of diffuse reflectance spectrum obtained.

3.5.5 X-ray Photoelectron Spectroscopy (XPS)

The XPS spectra were obtained on a McPherson ESCA-36 spectrometer by using anode aluminum ($\text{Al K}\alpha = 1486.1 \text{ eV}$). The pressure was maintained at $2.63 \times 10^{-5} \text{ Pa}$ and calibration is performed based on the binding energy of the level in the silicon 2p 103.5 eV.¹⁰⁹ The analyses were performed at the Institute of Physics Gleb Wataghin, Unicamp.

3.6 Preparation of working electrodes

The working electrodes were prepared by pressing 25 mg of $\text{SiO}_2/\text{C}/\text{MPc}$ under a pressure of 4 ton, at normal atmospheric conditions. The resultant disks (diameter 0.5 cm, thickness $\sim 0.01 \text{ cm}$ and geometric area 0.20 cm^2) were immersed in pure fused paraffin at 343 K under vacuum (10^{-3} Torr), until all adsorbed gas in the matrix pores was completely eliminated. The resulting self-supported disk was polished with emery paper to remove the paraffin from the disk surface, and then glued with cyanoacrylate ester glue to the end of a glass tube (external area of 0.20

cm² and 15 cm length). A copper wire linked to the disk by graphite powder inserted inside the tube made the electrical contact.

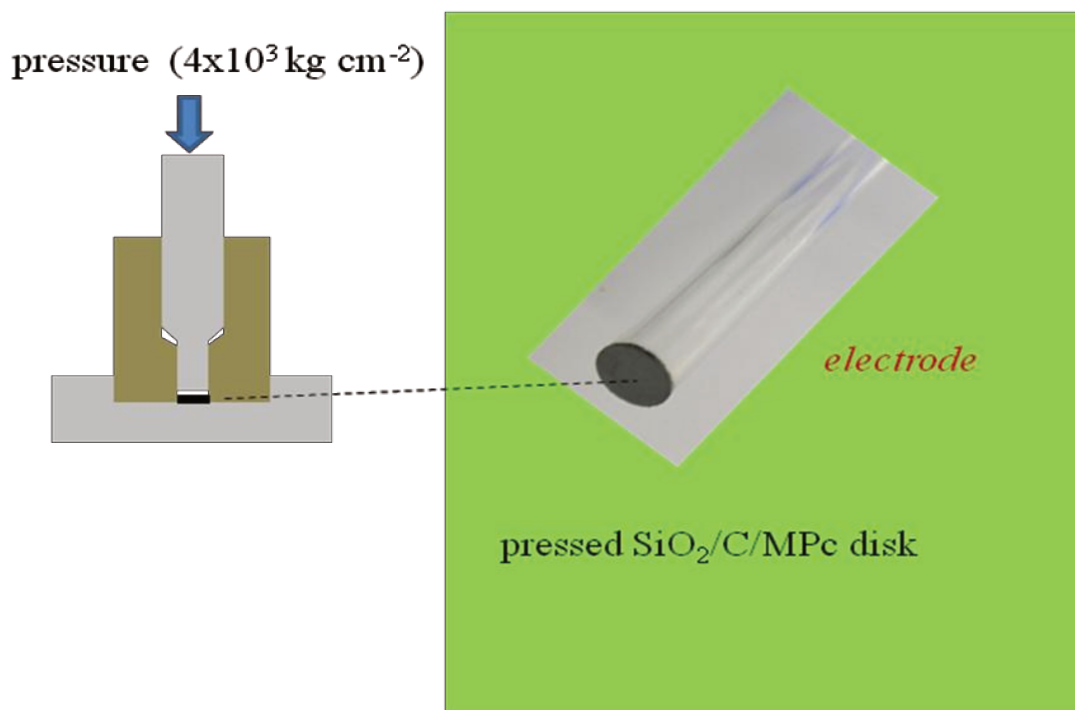


Figure 3.1: Fabrication of the SiO₂/C/MPc disk and the working electrode mounted after fixing the disk on the glass tube.

3.7 Electrochemical measurements of the SiO₂/C/MPc materials

The electrochemical measurements were performed by using a potentiostat / galvanostat Autolab PGSTAT-20, using an electrochemical cell consists of three electrodes, as follows: working electrode, auxiliary electrode (platinum wire) and reference electrode (saturated calomel electrode (SCE)).

Electrochemical analysis toward oxidation of oxalic acid was obtained in 25 mL of 1 mol L⁻¹ aqueous KCl under nitrogen atmosphere. In the investigation of electrochemical materials were employed cyclic voltammetry and chronoamperometry, all measurements were obtained at scan rate of 20 mV s⁻¹.

Electrochemical analysis of dopamine oxidation was obtained in 0.08 mol L⁻¹ Britton-Robinson buffer at pH 6.0, containing 1 mol dm⁻³ KCl. In the investigation of the material, the amperometry technique was used. All data were obtained at an applied potential of -20 mV.

The electrooxidation of nitrite was obtained in 0.1 mol L⁻¹ phosphate buffer containing, 1 mol L⁻¹ KCL at pH 4. All the electrochemical investigations were obtained by employing cyclic voltammetry at a scan rate of 20 mVs⁻¹.

The electrochemical reduction of oxygen was carried out in 25 mL of 1 mol L⁻¹ KCl at pH 7. In the electrochemical investigation of the materials were employed cyclic voltammetry, differential pulse voltammetry and chronoamperometry. All data were obtained at a scan rate of 10 mV s⁻¹.

3.8 Assay of the nitrite content in food samples

Samples of sausage were purchased at local stores. The pretreatment was performed as follows: first, 5 g of the sausage sample was crushed into mash and mixed with 12.5 ml saturated borax solution. Then, 300 mL of 70 °C water were added and the mixture was heated at boiling for 15 min. To precipitate the proteins, 5 mL of 20% zinc acetate was added. After being cooled to room temperature, the mixture was diluted to 500 ml with water and then filtered. The resulting sample solution was stored at 4°C in a refrigerator.¹¹⁰ The nitrite content in samples was determined according to the standard addition method. Standard nitrite solutions were added after measuring the sample solution. Thus, the concentration of nitrite in the real sample could be determined by cyclic voltammetry.



4.0 RESULTS AND DISCUSSIONS

4.1) *In-situ immobilization of cobalt phthalocyanine on the mesoporous carbon ceramic SiO₂/C prepared by the sol-gel process. Evaluation as an electrochemical sensor for oxalic acid.*

4.1.1 Chemical analysis, surface areas, pore volume and diameter of the SiO₂/C.

The amount of C used in the preparation of SiO₂/C, based on the number of moles of TEOS, corresponds to 20 and 50 wt% of graphite in the samples.

Figure 4.1(A) and 4.1(B) shows the adsorption-desorption nitrogen isotherms for samples possessing 20 and 50 wt% of graphite. Both samples exhibit isotherms with hysteresis, typical of mesoporous materials.^{111, 112}

The pore size distributions are shown in the inset Figure 4.1(A) and 4.1(B), respectively. The sample containing the lower amount of C, shows a mesopore distribution region with maximum at 19.4 nm diameter while the sample containing 50% of C shows a distribution curve with maximum around 15.8 nm diameter.

The surface area ($S_{\text{BET}}/ \text{m}^2\text{g}^{-1}$) and pore volume ($p_v/ \text{cm}^3\text{g}^{-1}$) obtained from the isotherms are: a) SiO₂/20wt%C, $S_{\text{BET}} = 160$, $p_v = 1.10$ and b) SiO₂/50wt%C, $S_{\text{BET}} = 170$, $p_v = 0.90$.

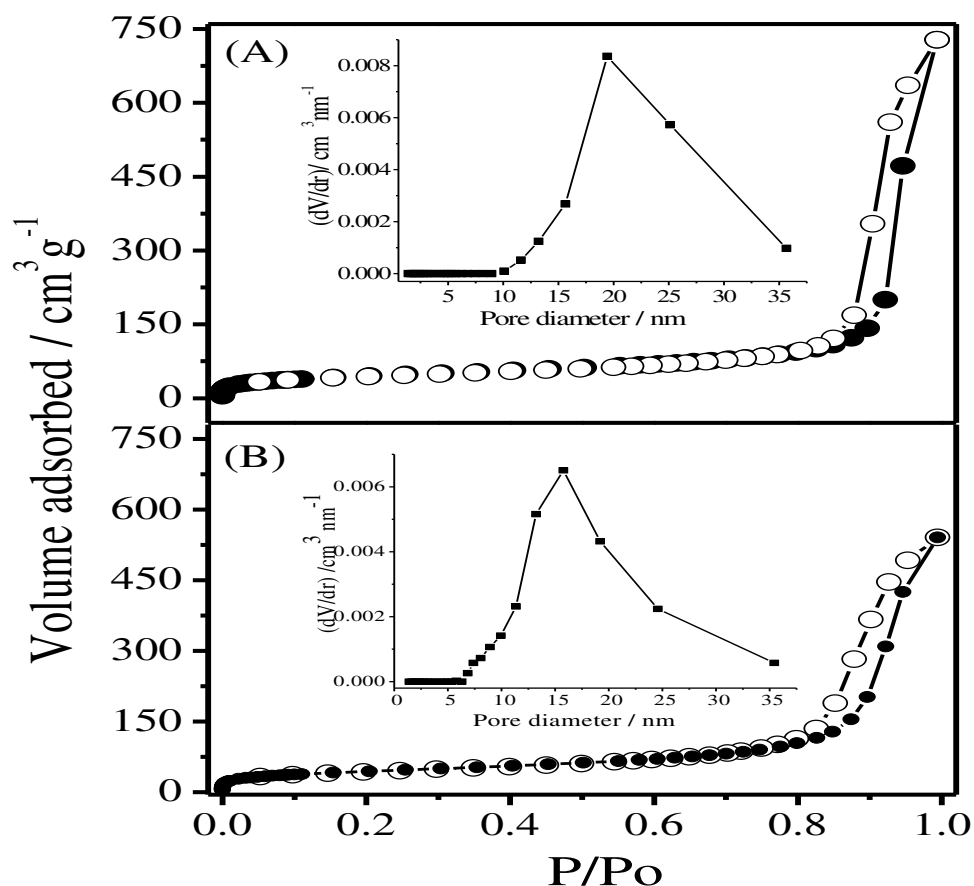


Figure 4.1. N₂ adsorption-desorption isotherms: (A) SiO₂/20wt%C and (B) SiO₂/50wt%C and pore size distribution curve respectively • adsorption ◦ desorption.

4.1.2 Scanning electron microscopy (SEM) coupled with energy dispersive spectroscopy (EDS).

Figure 4.2 shows the SEM images obtained for SiO₂/20wt%C (Figure 4.2(A)) and SiO₂/50wt%C (Figure 4.2(B)). It can be seen that samples possess

particles having granular form. There is a greater compactness of particles in the $\text{SiO}_2/20\text{wt}\% \text{C}$ sample.

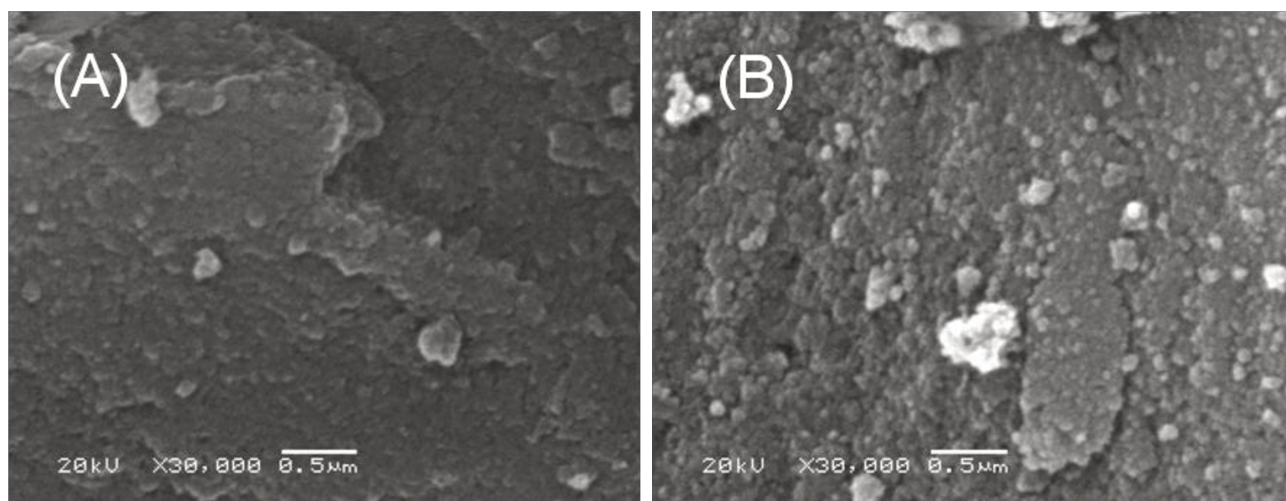


Figure 4.2. SEM images for (A) $\text{SiO}_2/20\text{wt}\% \text{C}$ and (B) $\text{SiO}_2/50\text{wt}\% \text{C}$.

Figure 4.3 shows the EDS mapping images for $\text{SiO}_2/20\text{wt}\% \text{C}$ and $\text{SiO}_2/50\text{wt}\% \text{C}$. Within the magnification used, there is no evidence that Si and C particles have segregated domains, indicating that the Si and C particles appear homogeneously dispersed in the matrix.

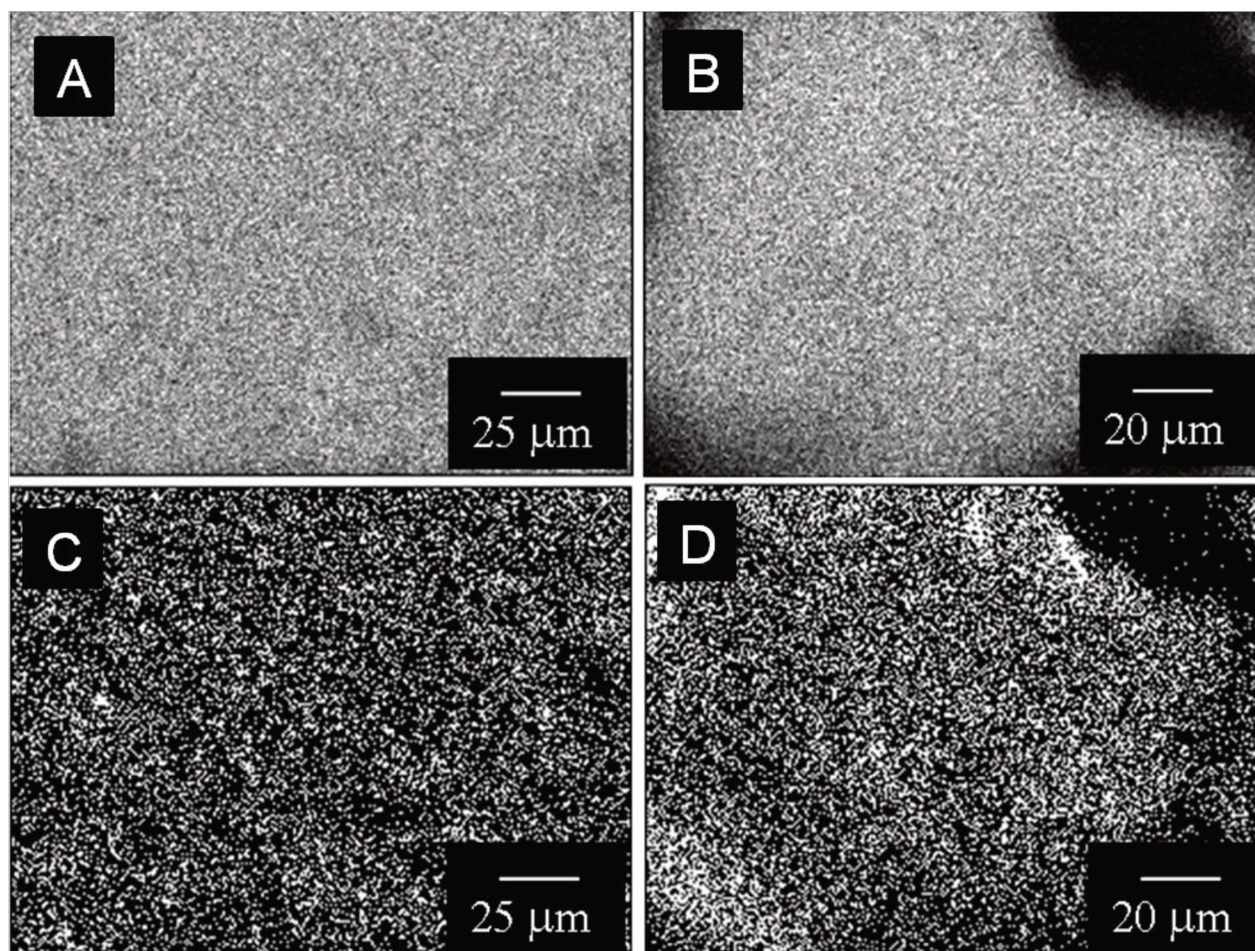


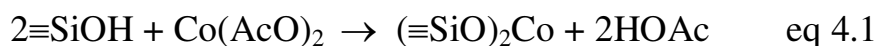
Figure 4.3: EDS images: silicon mapping: (A) SiO₂/20wt%C and (B) SiO₂/50wt%C; Carbon mapping: (C) SiO₂/20wt%C and (D) SiO₂/50wt%C.

4.1.3 Measurements of electrical conductivity

The conductivities obtained for SiO₂/20wt%C and SiO₂/50wt%C were (in S cm⁻¹) 0.25x10⁻⁵ and 0.4, respectively. The higher conductivity in the second sample is provided both by the larger amount and by the well dispersed and interconnected graphite particles in the silica network.

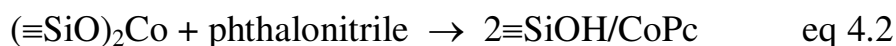
4.1.4 *In situ* generation of CoPc

The preparative procedures can be described by two reaction steps. In the first step, Co(II) is adsorbed on the silica surface by a reaction with formation of a Si-O-Co bond eq 4.1:



Where the Brønsted acid $\equiv\text{SiOH}$ represents the silanol groups present on the matrix surface.

In the second step the adsorbed Co(II) served as the template for phthalocyanine complex formation inside the silica pores. The adsorbed Co(II) on the matrix surface, in the presence of phthalonitrile at 473 K, forms CoPc through the reaction described by eq 4.2:



4.1.5 Electronic spectroscopy in UV-Vis region

Solid state diffuse reflectance spectrum of the material obtained, $\text{SiO}_2/\text{C}/\text{CoPc}$, showed two broad bands centered at 618 and 672 nm (Figure 4.4) that can be assigned as Q bands, for Co(II) under slightly distorted D_{4h} symmetry.¹¹³ The present spectrum when compared with those obtained using a similar procedure of confining pure CoPc on $\gamma\text{-Al}_2\text{O}_3$, SiO_2 or Zeolite-Y, is the same.^{114,115} The amount of CoPc generated on the matrices are: $\text{SiO}_2/20\text{wt}\%\text{C}/\text{CoPc} = 0.22 \text{ mmol g}^{-1}$ and $\text{SiO}_2/50\text{wt}\%\text{C}/\text{CoPc} = 0.26 \text{ mmol g}^{-1}$. The surface density of CoPc on the matrix surface, defined as $\delta = \text{Nf}/S_{\text{BET}}$ (in mol cm^{-2}), where Nf is the amount of complex species incorporated (in mol g^{-1}), are: $\delta = 1.6 \times 10^{-10}$ and $\delta = 1.5 \times 10^{-10} \text{ mol cm}^{-2}$ respectively, for material containing 20 and 50 wt% of C.

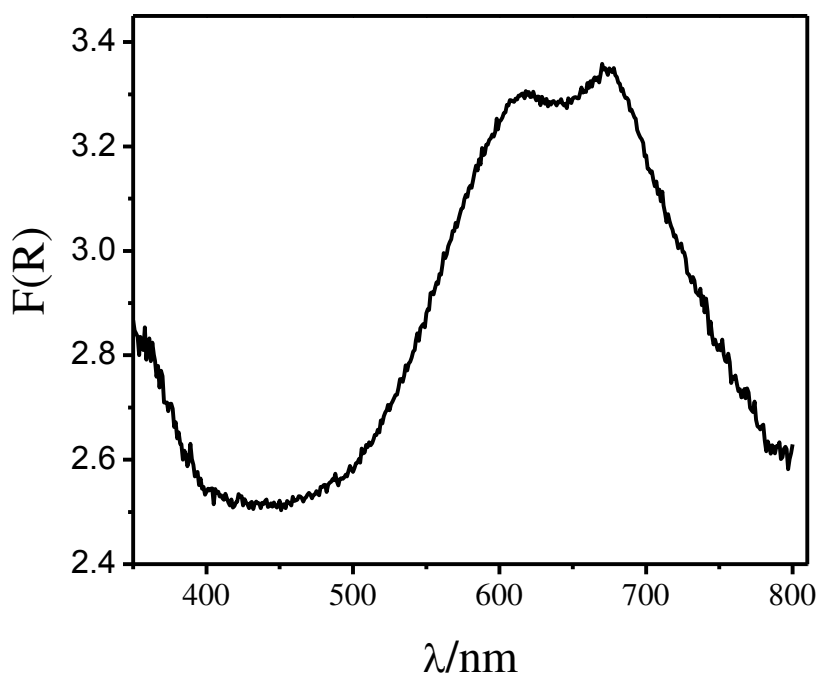


Figure 4.4: UV–Vis diffuse reflectance spectra of SiO₂/C/CoPc, expressed in Kubelka–Munk units.

4.1.6 Electrochemical measurements and study of oxalic acid oxidation

Pressed disks of SiO₂/C/CoPc having 20 and 50wt% C were used to fabricate the electrodes. To test the potential usefulness of the sensor, they were used to oxidize oxalic acid. This acid was chosen because it is well known that CoPc can electrocatalytic oxidation of this acid.¹¹⁶ Figure 4.5 shows cyclic voltammetry experiments of the oxidation of oxalic acid using both electrodes in 1.0 mol L⁻¹ KCl as supporting electrolyte at a scan rate of 20 mV s⁻¹. The acid concentrations changed between 0.0 – 3.84 × 10⁻⁴ mol L⁻¹. In Figure 4.5(A) and Figure 4.5(B), it is very clear the better performance of the electrode made with material containing 50 wt% of C, compared to that of material containing 20 wt%

C. The peak current intensities for oxalic acid oxidation are about ten times more intense for the former electrode. Oxidation peak potential is well defined and occurs at about 0.73 V while for electrode with less C it is not so well defined.

Plots of the anodic peak current intensity against the concentration of the acid $[\text{H}_2\text{C}_2\text{O}_4]$ (mol L^{-1}) for the $\text{SiO}_2/50\text{wt}\%\text{C}/\text{CoPc}$ electrode showed a linear correlation (inset Figure B) represented by the equation: $i_{pa}(\mu\text{A}) = 13.35 + 1.19 \times 10^6 [\text{H}_2\text{C}_2\text{O}_4](\text{mol L}^{-1})$, $r = 0.998$ and $n = 10$.

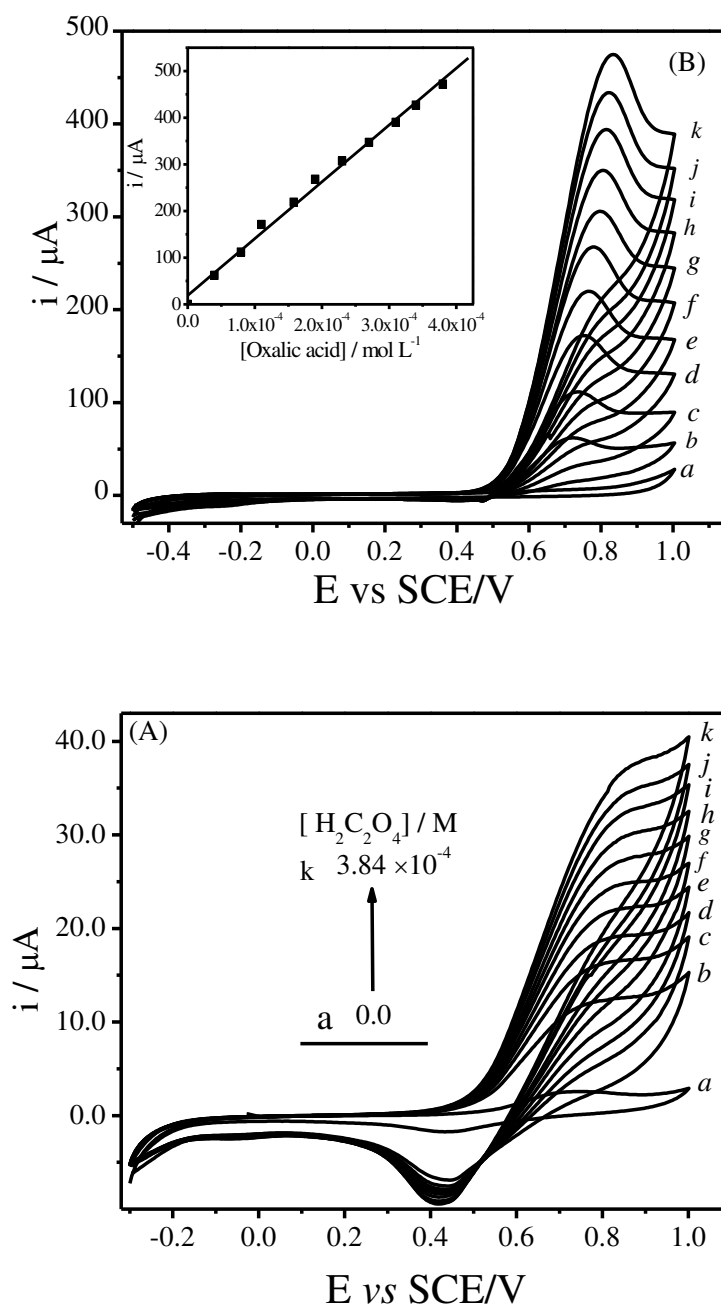


Figure 4.5: Cyclic voltammetry curves obtained for different concentration of oxalic acid (in mol L^{-1}): a) 0.0, b) 3.98×10^{-5} , c) 7.94×10^{-5} , d) 1.19×10^{-4} , e) 1.57×10^{-4} , f) 1.96×10^{-4} , g) 2.34×10^{-4} , h) 2.72×10^{-4} , i) 3.1×10^{-4} , j) 3.47×10^{-4} , k) 3.84×10^{-4}). Potential scan rate: 20 mV s^{-1} ; supporting electrolyte: 1.0 mol L^{-1} KCl. (A) SiO₂/20wt%C/CoPc and (B) SiO₂/50wt%C/CoPc.

The electrocatalytic process can be represented by the equations: ¹¹⁶



Since CoPc is generated in situ, the following experiment shows how strongly this complex is retained on the matrix surface. The stability of the SiO₂/C/CoPc electrode was checked by successively recording the cyclic voltammograms. After 100 cycles no significant changes of the anodic current intensity *i*_{pa} was observed in the voltammetric profile of the modified electrode (Figure 4.6). The *i*_{pa} intensity remained stable and the voltammograms were reproduced successively with relative standard deviation RSD of 0.12%, showing that CoPc electroactive species release to the solution phase is not detectable.

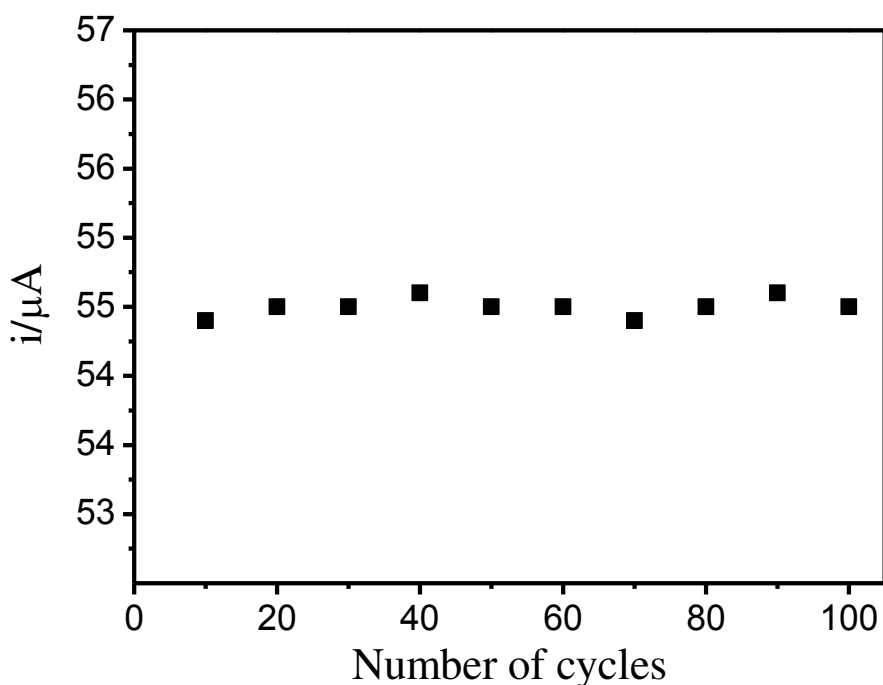


Figure 4.6: Anodic peak current intensity plotted against number of oxidation-reduction. Conditions: oxalic acid: $7.5 \times 10^{-5} \text{ mol L}^{-1}$ in 1.0 mol L^{-1} KCl.

A plot of the anodic peak current (i_{pa}) against the square root of scan rate ($v_{1/2}$) shows a linear relationship (Figure 4.7), with equation , $i_{pa} (\mu A) = 0.45 (\pm 3.04) + 24.03 (\pm 0.45) v_{1/2} (mVs^{-1})^{1/2}$ and $r = 0.998$, indicating that the oxidation process of oxalic acid is a diffusion controlled process.¹¹⁷ Since CoPc is strongly confined in the pores of the matrix surface, the analyte must diffuse into the surface-solution interface.

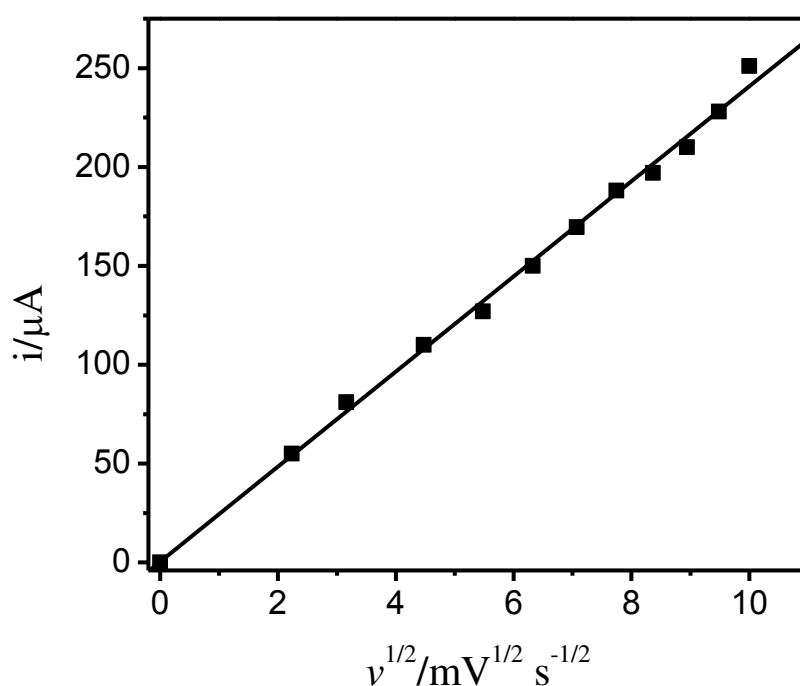


Figure. 4.7. Dependence of the anodic peak current on the square root of scan rate, obtained for the $SiO_2/50wt\%C/CoPc$ electrode. Conditions: oxalic acid: 7.5×10^{-5} mol L^{-1} in 1.0 mol L^{-1} KCl.

The oxalic acid oxidation process can depend on the solution pH, taking into account that the dissociation constants are $pK_1 = 1.27$ and $pK_2 = 4.26$.¹¹⁸. However, in the present case, the effect of pH on the electrooxidation response,

studied between pH 2 and pH 9 by cyclic voltammetry, was observed to have little effect. Concentration of the oxalic acid solution was fixed at $2.3 \times 10^{-4} \text{ mol L}^{-1}$ and the potential, E , between pH 5 and 9, remained practically invariable with RSD of 4.4% (Figure 4.8).

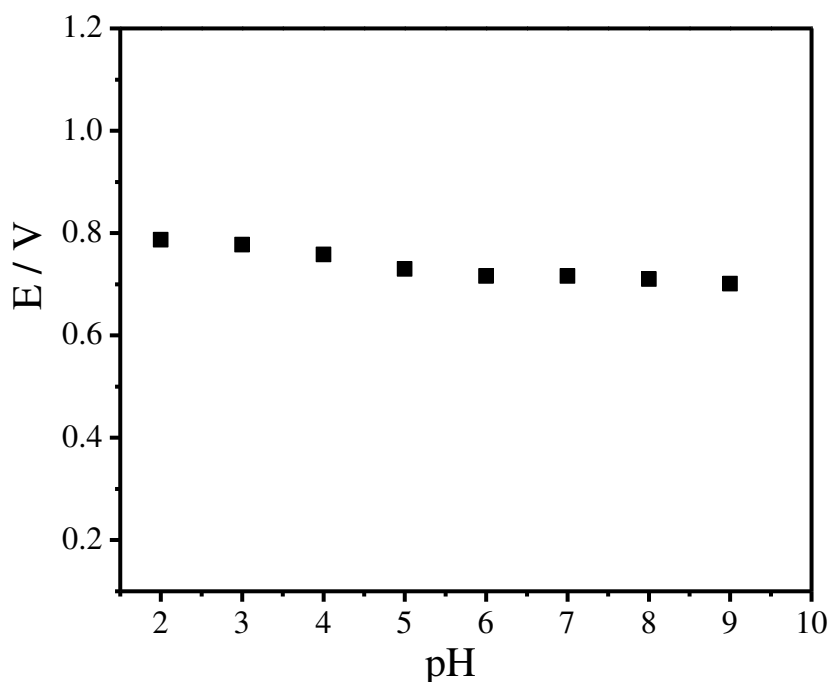


Figure 4.8: Influence of pH on the peak potential for $\text{SiO}_2/50\text{wt}\% \text{C}/\text{CoPc}$ electrode. Measurements carried out in $1.0 \text{ mol L}^{-1} \text{ KCl}$, scan rate of 20 mV s^{-1} and $[\text{H}_2\text{C}_2\text{O}_4] = 2.3 \times 10^{-4} \text{ mol L}^{-1}$.

In order to test the usefulness of the new electrode as an electrochemical oxalic acid sensor, the chronoamperometric technique was used. Figure 4.9 shows the chronoamperometric curves after successive addition of aliquots of oxalic acid solution at a fixed applied potential of 0.73 V , for 100 s . Inset Figure 4.9 shows the plot of current intensities against the concentration of oxalic acid, measured at 50 s .

It shows a linear relationship, in the concentration range between 4×10^{-5} and 4.6×10^{-4} mol L⁻¹ with a linear correlation represented by the equation: $i_{pa}(\mu\text{A}) = 0.18 (\pm 1.04) + 451.18 (\pm 3.84)[\text{H}_2\text{C}_2\text{O}_4](\text{mmol L}^{-1})$ ($n = 12$, $r = 0.999$). The limit of detection (3 standard deviation of the blank divided by the slope of calibration curve), $\text{LOD} = 0.58 \mu\text{mol L}^{-1}$, was found.

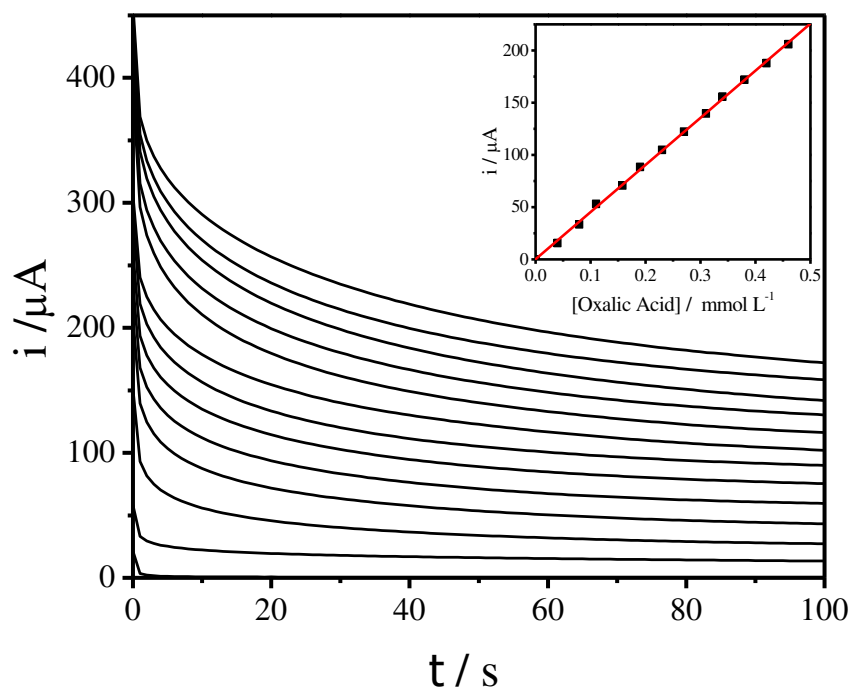


Figure 4.9: Chronoamperograms for $\text{SiO}_2/50\text{wt}\% \text{C}/\text{CoPc}$ electrode in different concentrations of oxalic acid at fixed potential of 0.73 V; Inset Figure plot of current intensity against oxalic acid concentration (measured at 50s).

Table 4.1 summarizes the results obtained to determine oxalic acid by electrochemical process using different types of electrodes^{84, 118-124}. It is clearly observed that a lower detection limit is obtained by using the pressed disk electrode $\text{SiO}_2/\text{C}/\text{CoPc}$, when compared to the other electrodes, especially when

comparing with SiO₂/CoPc-CPE where the LOD obtained was 1 x 10⁻³ mol L⁻¹. It is important to note that the surface density of CoPc in the CPE, electrode is $\delta = 0.44 \times 10^{-10}$ mol cm⁻², 3.4 times lower than that observed for SiO₂/50wt%C/CoPc (1.5 x 10⁻¹⁰ mol cm⁻²).¹²³

Table 4.1 Comparison of the limit of detection for oxalic acid between the SiO₂/C/CoPc and other electrodes.

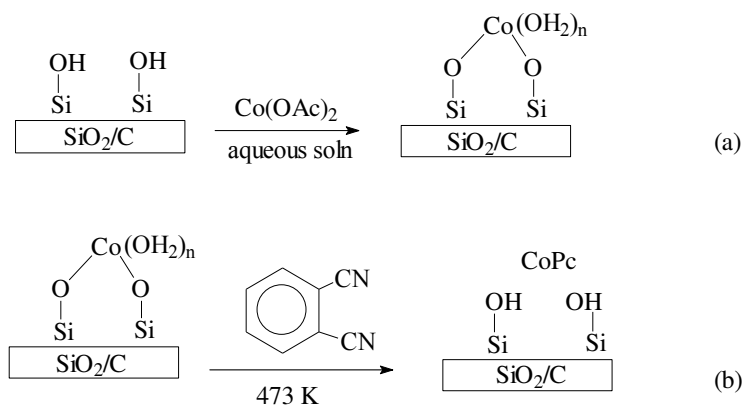
Electrode	Electroactive species	LOD	
		/ $\mu\text{mol L}^{-1}$	references
SiO ₂ /C/CoPc	CoPc	0.58	This work
glassy carbon	Rh phthalocyanin	1.0	[118]
glassy carbon	multiwall carbon nanotubes	12.0	[119]
pyrolytic graphite	-	0.70	[120]
Exfoliated graphite polystyrene composite	-	50.0	[121]
Boron-doped diamond/FIA ^a	-	0.0005	[122]
SiO ₂ /SnO ₂ /CoPc-CPME ^b	CoPc	30.0	[124]
SiO ₂ /SnO ₂ /C/SiPy/CoTsP ^c	CoTsPc	7.1	[84]
SiO ₂ /CoPc-CPME	CoPc prepared <i>in-situ</i>	1000	[123]

^aflow injection analysis; ^bcarbon paste modified electrode; ^ccobalt tetrasulphophthalocyanine

4.2) Dissolved O₂ sensor based on Cobalt (II) phthalocyanine immobilized in situ on electrically conducting carbon ceramic mesoporous SiO₂/C material

4.2.1 In situ generation of CoPc

The *in situ* synthesis of CoPc can be described by two reaction steps.²⁰ In the first step, cobalt acetate reacts with Bronsted acid –OH groups present on the silica surface, making the metal chemically adsorbed on the silica surface by a reaction with formation of a Si–O–Co bond (Scheme 1b). In the second step the adsorbed Co(II) served as the template for phthalocyanine complex formation inside the silica pores. The adsorbed Co(II) on the matrix surface, in the presence of phthalonitrile at 473 K, forms CoPc through the reaction described in Scheme 1:



Scheme 1. *In situ* generation of cobalt phthalocyanine (CoPc) inside the pores of SiO₂/C: Si-OH Bronsted acid sites in the pores of the matrix: a) adsorption of Co(II) on the surface through SiO-Co bond formation and b) generation of CoPc inside the pore.

The *in situ* reaction allows the adsorption of Co(II) on the surface of the matrix, since it is not possible to adsorb the metal ion throughout the bulk phase, as we concluded, when carrying out the electrochemical experiments.

4.2.2 Scanning electron microscopy (SEM) coupled with energy dispersive spectroscopy (EDS).

SEM and EDS images are shown in Figure 4.10. Within the magnification used we can observe that there are no segregated phases of SiO₂ and graphite particles (Figure. 4.10a) and the surface EDS image (Figure 4.10b) shows within the magnification used, cobalt are homogeneously dispersed throughout the matrix surface. Table 4.2 also shows the quantitative results obtained of the EDS spectrum and the amount of cobalt (in weight and atom %) are 1.73 and 0.54 respectively, this amount is sufficient for electrocatalysis.

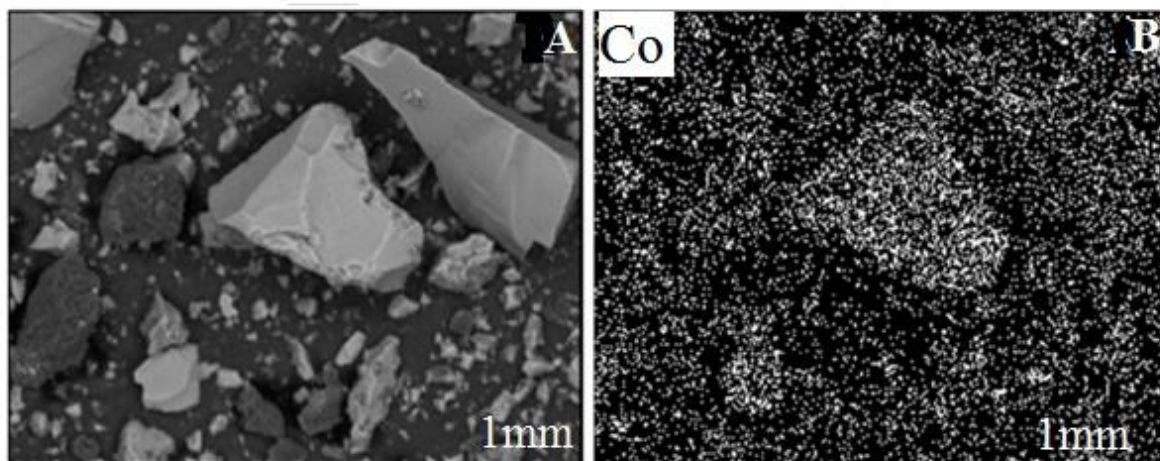


Figure 4.10: SEM image (a) and EDS mapping of Co (b) for SiO₂/C/CoPc.

Table 4.2: Quantitative Results of EDS spectrum

Element	Weight %	Atom %
C	13.75	21.20
O	45.27	52.38
Si	39.25	25.87
Co	1.73	0.54

4.2.3 Electrochemical characterization and sensor performance

Figure 4.11 shows the cyclic voltammograms obtained for the SiO₂/C electrode modified with CoPc in the absence (a) and presence (b) of 9.1 mg L⁻¹ of oxygen, and the bare SiO₂/C electrode in the presence of oxygen in the same concentration(c) were recorded. As can be seen the material SiO₂/C/CoPc allows a reduction at -0.23 V, a potential closer to zero, suggesting a good electrocatalysis and reduces the influence of the interfering in the measurement signal. The absence of the anodic wave in the voltammograms suggests that this process is controlled by the electron transfer step. To confirm this fact the k_0 was calculated using $|E_p - E_{p/2}|$ for a relationship according to Equation 4.3.¹²⁶

$$(k_0)_{25^\circ\text{C}} = 1.11 D_o^{1/2} (E_p - E_{p/2})^{-1/2} v^{1/2} \quad \text{eq 4.3}$$

where, D_o (cm² s⁻¹) is the diffusion coefficient and v (V s⁻¹) is the scan rate. The $|E_p - E_{p/2}|$ for a scan rate of 10 mV s⁻¹ was 84 mV and the electron transfer constant (k_0) was 1.67 x 10⁻³ cm s⁻¹, characteristics of a quasi-reversible system where the electro transfer is reasonable.

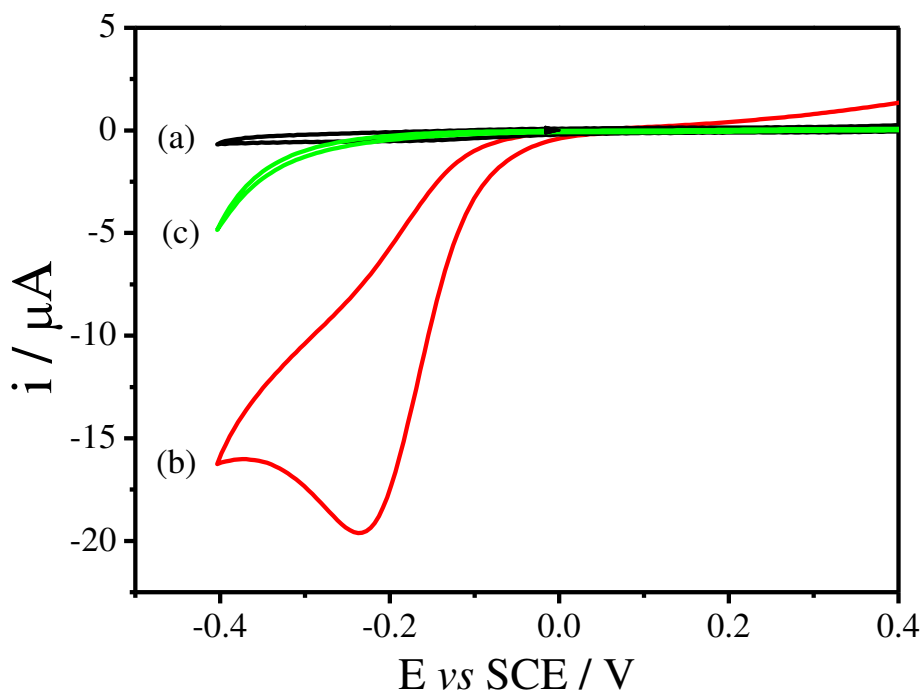


Figure 4.11: Cyclic voltammograms for: $\text{SiO}_2/\text{C}/\text{CoPc}$ electrode in the absence (a) and presence of O_2 (b) and voltammogram of SiO_2/C bare electrode in the presence of O_2 (c) in the concentration of $9.1 \text{ mg L}^{-1} \text{ O}_2$. Experimental conditions: $T = 298 \text{ K}$, scan rate $\nu = 10 \text{ mV s}^{-1}$; $1 \text{ mol L}^{-1} \text{ KCl}$; $\text{pH} = 7$.

The bare SiO_2/C electrode did not show any redox peak. The presence of carbon in the silica matrix is very important to reduce the electrical resistance and increasing the conductivity of the materials and also the incorporate ion of pure fused paraffin in the electrode eliminates the gas from the matrix pores and reducing the capacitive current.

4.2.4 Electrocatalytic reduction of oxygen on CoPc modified SiO₂/C electrode and influence of Phthalocyanine

Figure 4.12 shows the cyclic voltammogram obtained for the oxygen reduction on the SiO₂/C/CoPc *in situ* (solid line), on the SiO₂/C/CoPc classically (dotted line) and SiO₂/C/Co electrode (dashed line). Two important aspects can be verified in this figure, i.e (i) a slightly positive shift of 157 mV for *in situ* immobilized CoPc on SiO₂/C matrix, when compared with classically mixed CoPc with SiO₂/C electrode and (ii) a more pronounced shift of 220 mV for the SiO₂/C/CoPc (*in situ*) electrode, when compared to the SiO₂/C/Co electrode. It is also evident from this figure that phthalocyanine plays an important role in the reduction of oxygen, due to their macrocyclic nature including extended π -systems, phthalocyanines are capable of undergoing fast redox processes, with minimal reorganizational energies and can act as mediators in electron transfer processes involving a great variety of molecules.¹²⁷

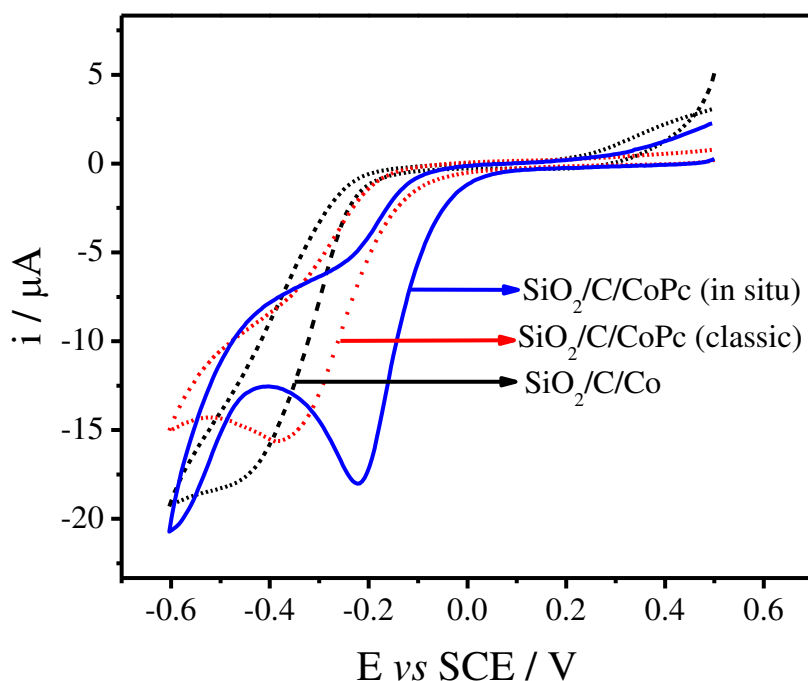


Figure 4.12: Cyclic voltammograms obtained for: $\text{SiO}_2/\text{C}/\text{CoPc}$ -*in situ* electrode (solid line), $\text{SiO}_2/\text{C}/\text{CoPc}$ -classically electrode (dotted line) and $\text{SiO}_2/\text{C}/\text{Co}$ electrode (dashed line), all in the presence of $8.2 \text{ mg L}^{-1} \text{ O}_2$. Experimental conditions: $T = 298 \text{ K}$, $\nu = 10 \text{ mV s}^{-1}$; $1 \text{ mol L}^{-1} \text{ KCl}$, $\text{pH} = 7$.

4.2.5 Mechanistic studies of the oxygen reduction on $\text{SiO}_2/\text{C}/\text{CoPc}$

Additional information about the oxygen reduction on $\text{SiO}_2/\text{C}/\text{CoPc}$ was obtained by analyzing the catalytic currents from the cyclic voltammograms. There are two possible mechanisms for oxygen reduction, one involving two electrons, with formation of H_2O_2 (Equation 4.4) and other involving four electrons, with formation of water (Equation 4.5).



Study of the mechanism of the electrochemical oxygen reduction can be performed by changing the scan rate in the cyclic voltammetry under a constant oxygen concentration (Figure 4.13a). The measurements have showed a linear correlation between current response and the square root of scan rate (Figure 4.13b). Since cobalt phthalocyanine is strongly confined in the pores of the matrix, dissolved oxygen must diffuse into the surface-solution interface. Using these results can be possible to perform a mechanistic study of oxygen reduction reaction.

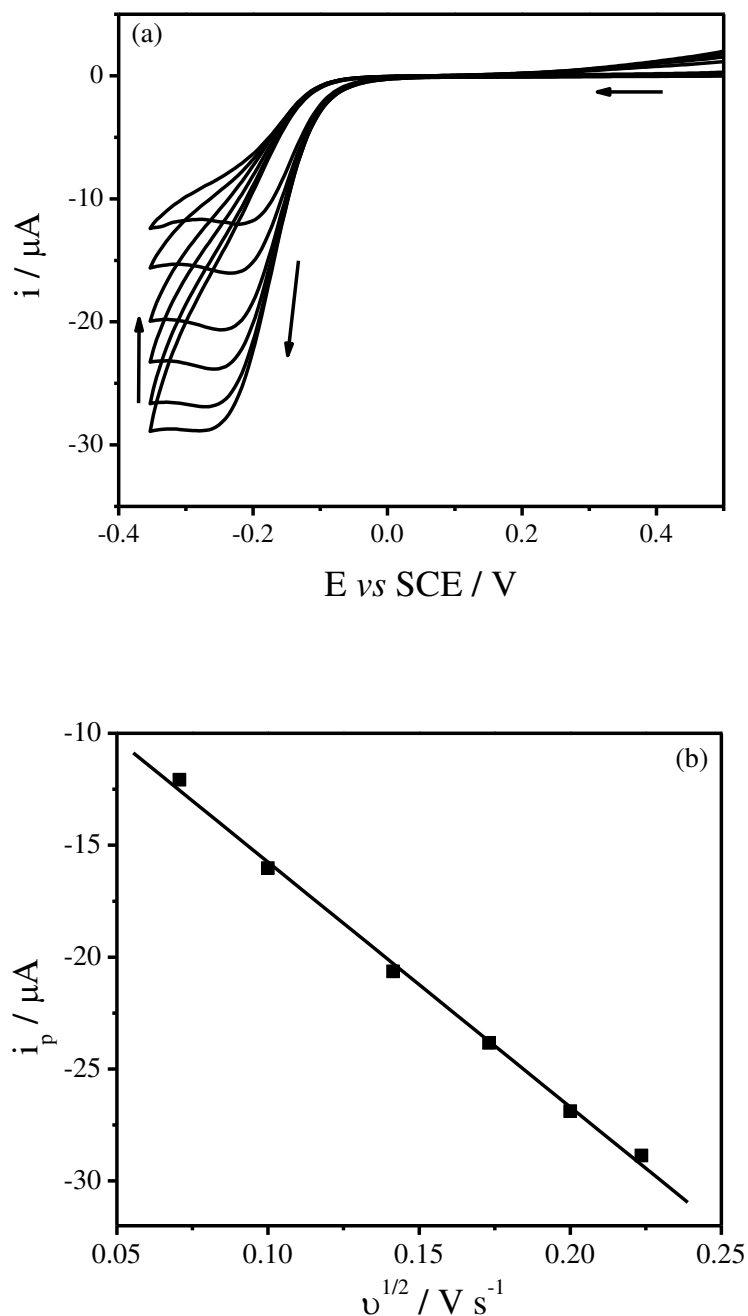


Figure 4.13: (a) Cyclic voltammograms of the SiO₂/C/CoPc electrode at different scan rates (mV s⁻¹): from top to bottom: 5, 10, 20, 50, 75, 100, 150, 200. (b) Plot of cathodic peak current against square root of the scan rate ($v^{1/2}$). Experimental conditions: T = 298 K, [O₂] = 9.0 mg L⁻¹; 1 mol L⁻¹ KCl; pH = 7.

The relationship between cathodic peak current and square root of the scan rate ($v^{1/2}$) can provide important information about the oxygen reduction reaction. In this case, the numbers of electrons (n) involved in the overall reaction can be calculated from the slope of the curve of Fig. 4.13(b), according to the equation for a totally irreversible process controlled by diffusion.¹¹⁸

$$i_p = (2.99 \times 10^5)n[(\alpha)n_a]^{1/2} C_o^* D_o^{1/2} v^{1/2} A \quad \text{eq 4.6}$$

where α is the electron transfer coefficient, n_a represents the number of electrons involved in the rate-determining step, D_o ($\text{cm}^2 \text{s}^{-1}$) is the diffusion coefficient, C_o^* (mol cm^{-3}) is the concentration of electroactive species, A (cm^2) is the electrode surface area, n is the total number of electrons, and v (Vs^{-1}) is the scan rate. The measurements were performed in the concentration of oxygen at 9.0 mg L^{-1} and diffusion coefficient for oxygen in aqueous solution considered was $1.9 \times 10^{-5} \text{ cm}^2 \text{ s}^{-1}$.¹²⁸

The $(\alpha)n_a$ value can be calculated using a relationship between the peak potential E_p and the potential of the half wave peak $E_{p/2}$, which is described in the equation:

$$(\alpha)n_a = \frac{47.7 \text{ mV}}{E_p - E_{p/2}} \quad \text{eq 4.7}$$

The reduction process of the analyte hampered by diffusion in the pores of the material $\text{SiO}_2/\text{C}/\text{CoPc}$, with increasing scan rate 5 to 50 mVs^{-1} , obtaining an average value of $|E_p - E_{p/2}|$ equal to 91.35 mV. The value obtained for $(\alpha)n_a$ was equal to 0.52. By using this value and the slope $109.46 \mu\text{A}/(\text{Vs}^{-1})^{1/2}$ of the curve obtained in Figure 4.13b, the value of n is equal to 2.07. This means that the proposed mechanism have predominantly with participation of 2 electrons, with formation of H_2O_2 . Therefore, a peak must be observed for the peroxide reduction with formation of water. Differential pulse voltammetry was used to demonstrate

two peaks (Figure 4.14), one at -0.17 V potential, related to the oxygen reduction, and another at -0.57 V, assigned to the peroxide reduction.

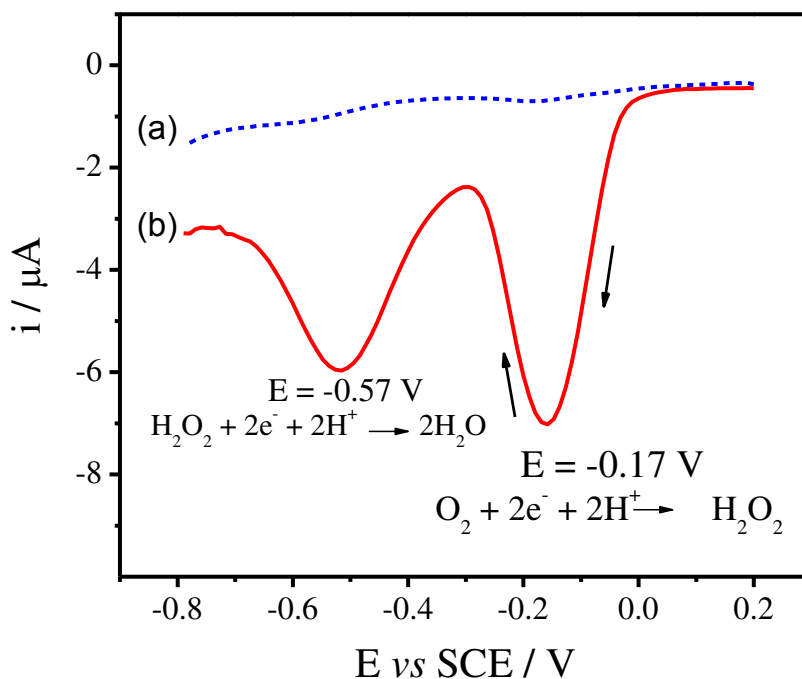
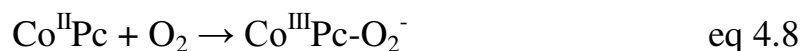


Figure 4.14: Differential pulse voltammetry measurement of SiO₂/C/CoPc electrode in the absence (a) and presence (b) of 9.0 mg L⁻¹ O₂. Experimental conditions: T = 298 K; 1 mol L⁻¹ KCl; pH = 7; v = 10 mV s⁻¹.

For systems with cobalt phthalocyanine, the α value commonly used in the literature¹²⁹ is 0.5 and from Equation 4.7, was possible to calculate the n_a . The value obtained was 0.96, suggesting that only one electron participate in the determining step. With this information, it is possible to propose a mechanism for the oxygen reduction reaction.

The electrochemical behavior in different solution pH was verified in the range between 4 and 8. The peak potential does not show a great variation, this

behavior is characteristic of the system, where metal center of the complex is responsible for the electrocatalytical process. Therefore, to understand a possible mechanism involved in the electrocatalysis of oxygen reduction. The proposed mechanism is described hereafter:¹²⁹



In the pH 4 to 8, the small current changes have been observed (Figure 4.15). There was slight increase in the current at lower pH values. Further measurements were performed at pH equal to 7, since, there was no significant difference in the current as compared to lower pH, while, this is the pH of physiological media. Measurements performed among successive cycles showed a good stability of this material, indicating that the material does not suffers a leaching process.

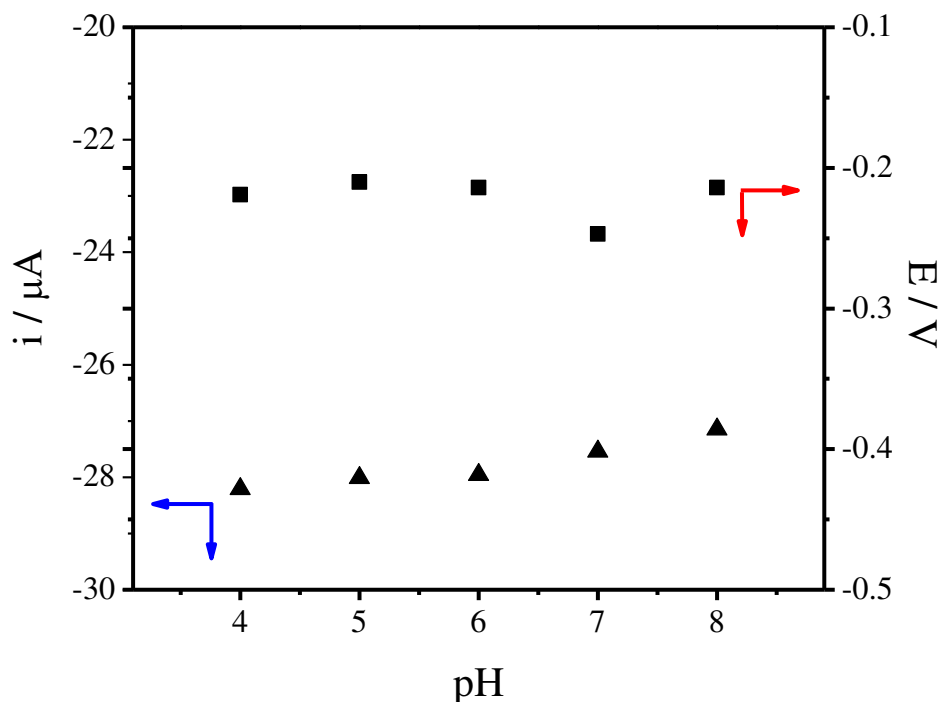


Figure 4.15: Values of cathodic peak current and reduction peak potential at a function of the solution pH obtained for the $\text{SiO}_2/\text{C}/\text{CoPc}$ electrode. $[\text{O}_2] = 9.0 \text{ mg L}^{-1}$; $T = 298 \text{ K}$, and $v = 10 \text{ mV s}^{-1}$.

4.2.6 The sensor characteristics

The sensor characteristics of $\text{SiO}_2/\text{C}/\text{CoPc}$ were verified by amperometry technique. In these measurements, an initial study was performed in order to determine the best potential to be applied in the electrode. The applied potential was chosen based on the measurement of the catalytic current verified at applied potential of -0.23 V versus SCE (data not shown). The amperometric curves were recorded at different concentrations of oxygen in solution (Figure 3.16a). A linear response range resulted from 0.5 to 6.6 mg L^{-1} , which can be expressed according to the equation: $\Delta i (\mu\text{A}) = -0.84 (\pm 0.27) - 2.16 (\pm 0.07) [\text{O}_2] (\text{mg L}^{-1})$, with a correlation coefficient of 0.996 (for $n=9$), was obtained from Figure 3.16b. This

behavior permits the use of this material as sensor to monitor dissolved oxygen. The sensor presented a sensitivity of $2.16 \mu\text{A L mg}^{-1}$ and a limit of detection 0.01 mg L^{-1} , in a dynamic range from 0.5 up to 6.6 mg L^{-1} of oxygen.

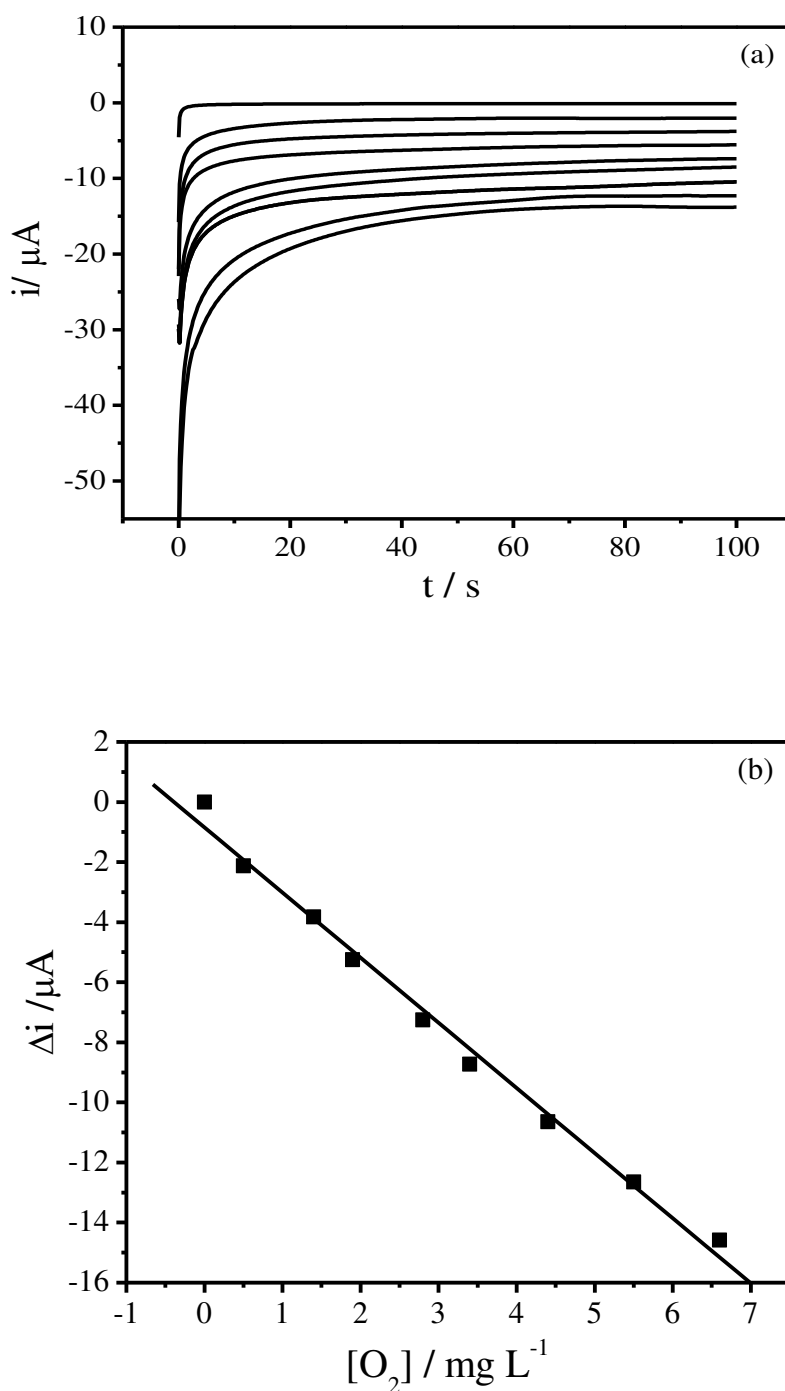


Figure 3.16: (a) Amperometry response of the SiO₂/C/CoPc electrode in different oxygen concentrations (mg L⁻¹): from top to bottom: 0.0, 0.5, 1.4, 1.9, 2.8, 3.4, 4.4, 5.5, 6.6 (b) Plot of cathodic current (Δi_{cp}) vs [O₂] (measured at 50 s). Experimental conditions: T = 298 K, E_{appl} = -0.23 V; 1 mol L⁻¹ KCl; pH 7.

4.2.7 Stability of CoPc on the SiO₂/C electrode

The stability of the SiO₂/C/CoPc electrode was checked by recording successive cyclic voltammograms. After 100 cycles no significant changes in the currents response was observed. Furthermore, when the electrode was stored at room temperature no significant change in the response was observed for more than 24 months, just by polishing with emery paper to renew the surface to obtain the same response. This electrode showed good repeatability for oxygen determination. The relative standard deviation of the cathodic peak for ten determinations of 6.5 mg L⁻¹ O₂ was 1.6 %. Similarly, a series of 5 sensors prepared in the same procedure and tested in the same experimental condition containing 6 mg L⁻¹ of oxygen gave responses with a relative standard deviation of 4.7 % shown in Table 4.3. These experiments indicated that the SiO₂/C/CoPc have good stability (data not shown) and repeatability, probably due to the strong adsorption of CoPc in the SiO₂ matrix.

Table 4.3: Electrode response obtained with different electrode prepared in the same way, containing 6 mg L⁻¹ of oxygen

Electrode	1	2	3	4	5
<i>i</i> / μA	14.66	14.64	15.02	14.59	16.28
RSD %	4.7				

4.2.8 Application to the water sample and interference studies

The developed sensor was applied for the determination of dissolved oxygen level in pond and tap water samples, comparing with the oxygen determined by using a dissolved oxygen meter according to Chen *et al.*¹³⁰ The results of the determinations are listed on Table 4.4. The results obtained with the proposed sensor were consistent with those obtained with the dissolved oxygen meter. In addition, applying a paired student's t-test to compare such methods, it was possible to observe that, at 95% confidence level, there was no statistical difference between the comparative and proposed methods.

Table 4.4: Determination of dissolved oxygen in pond and tap water by the proposed sensor and DO meter (determinations in triplicate)

Dissolved oxygen (mg L ⁻¹)		
Samples	Proposed method	DO meter
Pond water1	4.65 (±0.13)	4.60 (±0.10)
Pond water2	4.74 (±0.15)	4.68 (±0.11)
Tap water1	4.46 (±0.12)	4.40 (±0.14)
Tap water2	4.42(±0.13)	4.37 (±0.11)

$E_{\text{appl}} = -0.23 \text{ V vs SCE}$

The effects of foreign species commonly found in water samples on the determination of dissolved oxygen were investigated and the results are listed in Table 4.5. The sensor response was evaluated in the presence of 150 mg L⁻¹ Na⁺ (NaCl), Mg²⁺ (MgCl₂), Ca²⁺ (CaCl₂), Cu²⁺ (Cu²⁺ (NO₃)₂), NH₄⁺ (NH₄Cl), Fe³⁺ (FeCl₃), NO₃⁻ (KNO₃), SO₄²⁻ (K₂SO₄) and resorcinol, in a solution of 6 mgL⁻¹ O₂. As can be verified, the observed influences are all less than 2% on dissolved oxygen response. These results reveal that the developed sensor can tolerate a high

concentration of foreign species and, therefore, can be stated as selective over the commonly present species in the samples.

Table 4.5. Interference effects on the detection of dissolved oxygen determination with proposed method in KOH/HCl pH 7 and oxygen concentration of 6 mg L⁻¹ and interference species concentration=150 mg L⁻¹

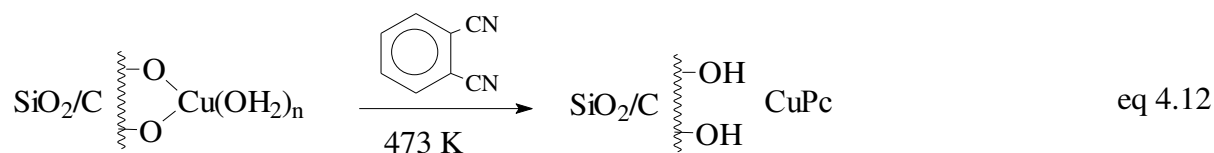
Added Species	Response change (%)
Na ⁺	1.02
Ca ²⁺	1.00
NH ₄ ⁺	0.97
Fe ³⁺	0.97
Mg ²⁺	0.99
NO ₃ ⁻	1.02
SO ₄ ²⁻	1.03
Cu ²⁺	0.97
Resorcinol	0.90

4.3) *SiO₂/C/CuPc as a biomimetic catalyst for dopamine monooxygenase in the development of an amperometric sensor.*

The same SiO₂/C matrices are used as was used in the previous work. In this case the matrix was modified with copper phthalocyanine.

4.3.1 *In situ* generation of CuPc

The *in situ* generation of CuPc can be described by two steps reaction. In the first step, (eq 4.11) Cu(II) is adsorbed on the silica surface by a reaction with formation of a Si–O–Cu bond:



where -OH represents the Brønsted acid groups present on the matrix surface. In the second step the adsorbed Cu(II) served as the template for phthalocyanine complex formation inside the silica pores. The adsorbed Cu(II) on the matrix surface, in the presence of phthalonitrile at 473 K, forms CuPc through the reaction described by eq 4.12.

4.3.2 Electronic spectroscopy in UV-Vis region

The UV-vis diffuse reflectance spectrum of the immobilized CuPc on SiO₂/C material, shows two electronic transition peaks observed at 589 and 689 nm (Figure 4.17) and for standard CuPc at 560 and 689 nm. These two transitions are

assigned as Q bands for Cu(II) under D_{4h} symmetry, slightly distorted in the CuPc confined in the pores of the matrix.¹³¹

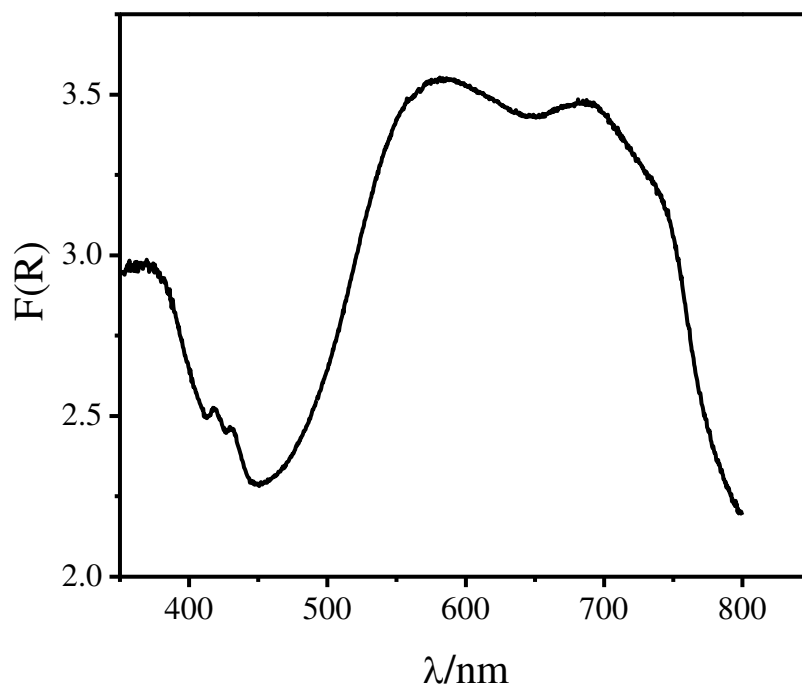


Figure 4.17: Diffuse reflectance spectrum of SiO₂/C/CuPc, expressed in Kubelka–Munk units.

4.3.3 Electrochemical measurements and electrode response

A pressed disk of SiO₂/C/CuPc was used to fabricate the electrode to test the potential usefulness of the catalyst to mimic the dopamine monooxygenase. The quantity of electroactive species was estimated from a cyclic voltammetry technique obtained in 0.08 mol dm⁻³ BRB at pH 6.0 containing 1 mol dm⁻³ KCl, scan rate of 0.005 V s⁻¹, under a nitrogen atmosphere (data not show). The charge, Q, flowing during the oxidation–reduction process of the CuPc was determined by

integrating the area under the cyclic voltammetric curve. The amount of electroactive species estimated was $7.3 \times 10^{-8} \text{ mol cm}^{-2}$.

Figure 4.18 shows the results obtained in the experiments carried out in the presence and absence of hydrogen peroxide. In the absence of H_2O_2 (curve a), no cathodic currents were observed, which could be attributed to the incapability of the $\text{SiO}_2/\text{C}/\text{CuPc}$ to directly oxidize the dopamine. On the other hand, good cathodic current after adding peroxide and dopamine is observed (curve b in Figure 4.18), demonstrating that peroxide plays an important role in the catalytic process.

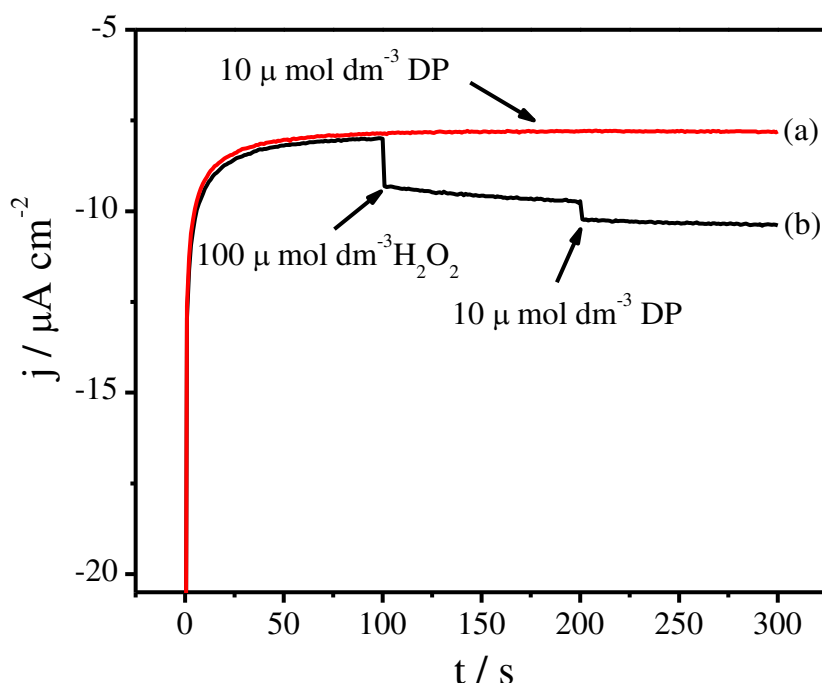


Figure 4.18: Signals obtained with the proposed sensor using $\text{SiO}_2/\text{C}/\text{CuPc}$: (a) in absence and (b) presence of $100 \mu\text{mol dm}^{-3} \text{H}_2\text{O}_2$. Each step corresponds to the increment of $10 \mu\text{mol dm}^{-3}$ dopamine. The inset figure shows the analytical curve. Applied potential -20 mV vs SCE in $0.08 \text{ mol dm}^{-3} \text{BRB}$ at $\text{pH}=6.0$ containing $1 \text{ mol dm}^{-3} \text{KCl}$.

A higher sensitivity was obtained for H_2O_2 concentration of $200 \mu\text{mol dm}^{-3}$, however such higher concentration resulted in poor stability of the electrode. Probably the hydrogen peroxide in high concentration leads to form an inactive form of the catalyst like in enzyme system.⁹¹ Therefore, the use of a minimum amount of hydrogen peroxide in the media is desirable, but it should be sufficient to present high sensitivity. Thus, $100 \mu\text{mol dm}^{-3}$ hydrogen peroxide allows good sensitivity, without affecting the stability. This concentration was established for further experiments.

Based on these results, a possible mechanism for the sensor response was proposed as schematized in Figure 4.19. This mechanism is similar to those proposed for phenolic compound with biomimetic catalysts of dopamine β -monooxygenase.¹³² The most important stage for dopamine quantification is the chemical oxidation of dopamine species by the activated PcCu-OOH on the electrode surface, the oxidized dopamine is electrochemically reduced on the electrode surface recycling the substrate, and consequently resulting in signal amplification. The hydrogen peroxide is necessary to activate the CuPc forming an active form PcCu-OOH to oxidize dopamine, which is electrochemically reduced on the electrode surface. One point that should be emphasized is the role of SiO_2 in this material. Copper is mostly adsorbed on SiO_2 , which is insulator and thus, the electron transfer between CuPc and electrode is not favored, corroborating that the electrons transfer occur predominately between quinone species and carbon domain of the electrode.

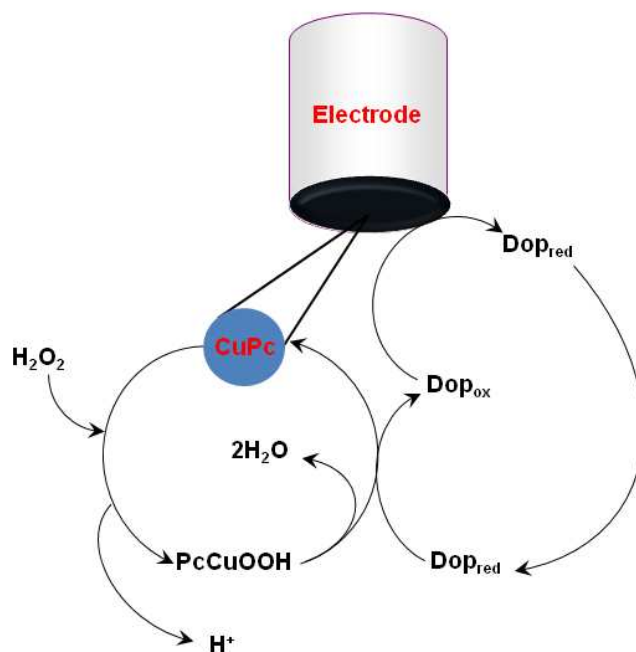


Figure 4.19: Proposed mechanism for the sensor SiO₂/C/CuPc response for dopamine.

4.3.4 Influence of hydrogen peroxide

In the proposed sensor, the prior addition of hydrogen peroxide, before adding dopamine, increased the sensitivity of the electrode. This fact can be explained based on the catalysis mechanism of the dopamine monooxygenase, very well explained in literature¹³³⁻¹³⁵ which involves the generation of copper-hydroperoxy species (Cu^{II}-O-O-H). In the enzyme, the initial chemical event involves two electron and one proton transfer from the copper sites and an active site with acidic group of the protein, respectively, to oxygen to yield a copper-hydroperoxy intermediate. Cleavage of the O-O bond and hydrogen extraction from the substrate forms water, copper-oxo and substrate radical, which

consequently combine to form hydroxylated product. In our case, the hydrogen peroxide addition in the working solution is necessary to form $\text{Cu}^{\text{II}}\text{-O-O-H}$ like in enzyme to be able to oxidize the substrate. On the other hand, the regeneration of the oxidized catecholamines by applying an adequate potential is feasible. On this basis, the mechanism presented in Figure 4.19 was proposed for this biomimetic biosensor. Initially, Cu^{2+} in presence of H_2O_2 forms the $\text{Cu}^{\text{II}}\text{-O-O-H}$ species. This species will oxidize dopamine in the catechol ring to form 1,2-quinone. In this stage, that represents the most important step for dopamine quantification, occurs the electrochemical reduction of the quinone species on the electrode surface, through the application of a suitable potential. This mechanism also explains the high sensitivity of the sensor by the signal amplification due to the cyclic reaction.^{136, 137} Figure 4.20 shows the prior addition of H_2O_2 to the solution before adding dopamine and shows a very good sensitivity of the electrode. It corroborates the proposed mechanism as depicted in Figure 4.19.

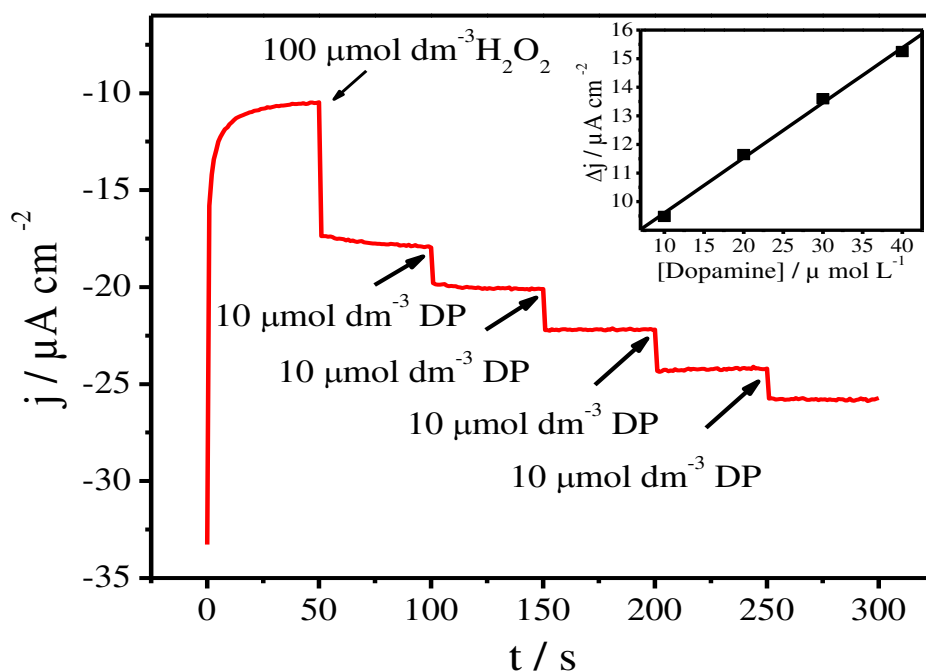


Figure 4.20: Amperometric response for the biomimetic biosensor for dopamine. Each step corresponds to the increment of $10 \mu\text{mol dm}^{-3}$ dopamine and containing $100 \mu\text{mol dm}^{-3}$. The inset figure shows the analytical curve. Applied potential -20 mV vs SCE in 0.08 mol dm^{-3} BRB at $\text{pH}=6.0$ containing 1 mol dm^{-3} KCl.

4.3.5 Influences of the applied potential, buffer and solutions pH

In order to establish the optimized conditions for amperometric measurements, the influence of the applied potential, buffer solution and pH were also investigated and the best sensor responses were obtained at -20 mV vs SCE at $\text{pH}=6$ (Figure 4.21). It can be seen that the current density referring to dopamine reduction increases from $E=-80$ up to maximum at -20 mV and then decrease up to 80mV . This behavior has been described as a competitive mechanism for copper electro-reduction (at about -40 mV and 0 mV versus SCE), which can result in a low number of active sites of oxidized copper species (CuPc_{ox}) promoting a

decrease in the efficiency of dopamine oxidation by the chemical route (as depicted in Figure 4.20). To determine the influence of different buffers on the electrode response for dopamine measurements were carried out in 0.08 mol dm^{-3} buffers (BRB, HCl/KOH and Tris) at pH= 6.0 in the presence of $100 \text{ } \mu\text{mol dm}^{-3}$ H_2O_2 and $10 \text{ } \mu\text{mol dm}^{-3}$ of dopamine, at applied potential of -20 mV vs SCE. The results obtained for current intensity changes, $\Delta j / \mu\text{A cm}^{-2}$, for BRB = 1.76, HCl/KOH = 1.56 and Tris- = 1.42 are indicating that the influence of the buffers used does not significantly affect the electrode response.

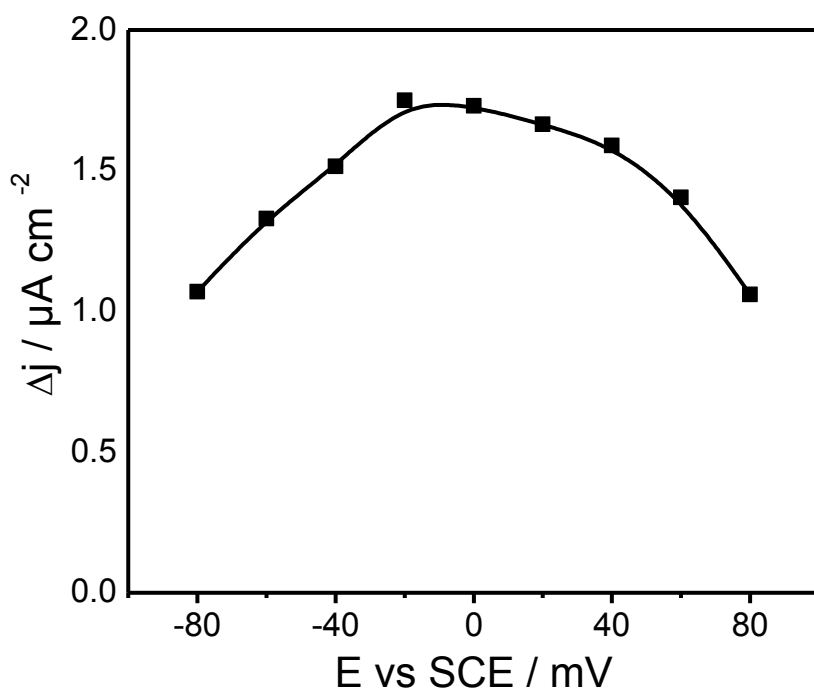


Figure 4.21: Influence of the applied potential on the current density Δj . Measurements carried out in 0.08 mol dm^{-3} BRB at pH=6.0 containing 1 mol dm^{-3} KCl, and $10 \text{ } \mu\text{mol dm}^{-3}$ of dopamine and $100 \text{ } \mu\text{mol dm}^{-3}$ of H_2O_2 .

In the study carried out to determine the influence of the BRB concentration on the sensor response for dopamine was also checked. The results showed that

practically the same responses were obtained in the concentration range from 0.02 up to 0.12 mol dm⁻³. Thus, the best response was obtained at 0.08 mol dm⁻³ and thus selected for further experiments.

The investigation to evaluate the pH effect on the sensor response showed an optimum pH of 6.0 (Figure 4.22) in 0.08 mol dm⁻³.

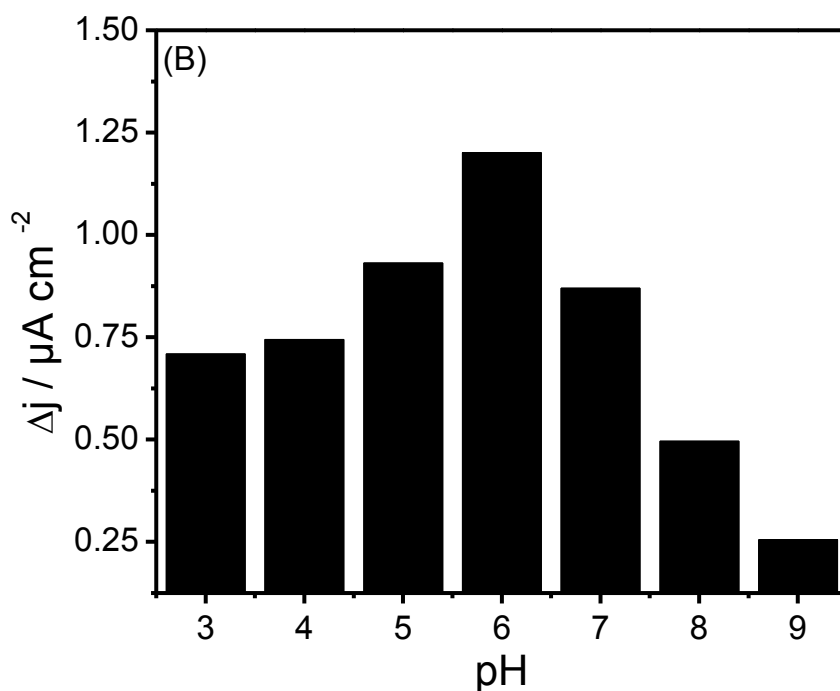


Figure 4.22: Influence of the pH on the current density Δj . Measurements carried out in 0.08 mol dm⁻³ BRB containing 1 mol dm⁻³ KCl, and 10 $\mu\text{mol dm}^{-3}$ of dopamine and 100 $\mu\text{mol dm}^{-3}$ of H₂O₂

4.3.6 Sensor characteristics

Under optimized conditions, the proposed sensor showed a linear response range for dopamine concentration, varying from 10 up to 140 $\mu\text{mol dm}^{-3}$ with a sensitivity of 0.63 nA dm³ μmol^{-1} cm⁻² (Figure 4.23), and expressed by the equation:

$\Delta j / \text{nA cm}^{-2} = 0.141 (\pm 0.491) + 0.628 (\pm 0.006) [\text{Dopamine}] / \mu\text{mol dm}^{-3}$ with a correlation coefficient of 0.999 for $n = 14$.

The limit of detection (3 times standard deviation of the blank divided by the slope of calibration curve), $\text{LOD} = 0.62 \mu\text{mol dm}^{-3}$ was found. In addition, considering the time to reach 100% of the signal, the response time was about 1 s, which is better than the response times of other sensors presented in the literature for phenolic compounds.^{91,138,139}

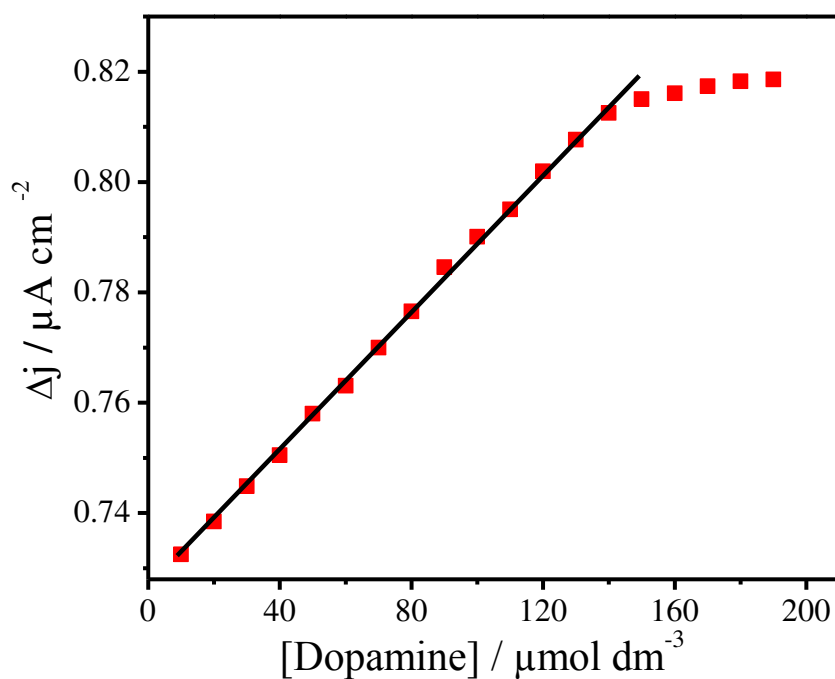


Figure 4.23: A typical profile of the sensor response using the optimized conditions. Applied potential of -20 mV vs SCE, in 0.08 mol dm^{-3} BRB at $\text{pH} = 6.0$ containing 1 mol dm^{-3} KCl, and $100 \mu\text{mol dm}^{-3}$ of H_2O_2

The repeatability in the measurements was evaluated through 10 successive experiments carried out with $10 \mu\text{mol dm}^{-3}$ dopamine solution. The repeatability

was evaluated as the relative standard deviation (RSD) resulting in a value 1.37 %. The life time of the sensor was more than 9 months, stored at room temperature and there is no significant decrease in the sensitivity of the sensor was observed (data not shown).

A comparison of the analytical parameters for dopamine with those previously reported for other biomimetic systems,¹⁴⁰⁻¹⁴⁴ under similar experimental conditions, is presented in Table 3.6. A low detection limit and a high sensitivity are observed, even when compared to biosensors based on peroxidase or tyrosinase enzymes^{145,146} for phenol determinations. Such good analytical responses can be attributed to the efficiency of the reaction between the peroxide and SiO₂/C/CuPc (biomimetic catalyst) and also SiO₂/C/PcCuOOH with dopamine as well as the electrons transfer from quinone to electrode surface.

Table 4.6: Analytical parameters for dopamine detection with biomimetic sensors under optimized amperometric conditions

Biomimetic Sensor	Dynamic Range/ ($\mu\text{mol dm}^{-3}$)	LOD / ($\mu\text{mol dm}^{-3}$)	Sensitivity / ($\text{nA dm}^{-3} \mu\text{mol}^{-1} \text{cm}^2$)	Ref.
$\text{Th}^{\text{IV}}\text{-HCF}^{\text{a}}$	8-2000	4.7	-	[141]
$\text{Fe}^{\text{III}}\text{T4MpyP-His}^{\text{b}}$	0.6-6.0	0.35	0.061	[140]
$[\text{Cu}(\text{bipy})_2]\text{Cl}_2 \cdot 6\text{H}_2\text{O}^{\text{c}}$	35-240	8.0	2.02	[142]
Ag/CCE^{d}	6.6 -120	1.4	26.30	[143]
$\text{RuO}_2/\text{MWNT}^{\text{e}}$	0.6 - 360	0.06	0.084	[144]
$\text{SiO}_2/\text{C}/\text{CuPc}$	10-140	0.60	0.63	This work

^a($\text{Th}^{\text{IV}}\text{-HCF}$): Thorium (IV)-hexacyanoferrate; ^b $\text{Fe}^{\text{III}}\text{T4MpyP-His}$: iron Tetra-(N-methyl-4-pyridyl)porphyrin–histidine; ^c $[\text{Cu}(\text{bipy})_2]\text{Cl}_2$: bis(2,2' bipyridil) copper chloride; ^d Ag/CCE : Silver Ceramic composite electrode; ^e MWNT: multiwalled carbon nanotubes.

4.3.7 Sensor application: interference and determination of dopamine in physiological solution

The sensor response was tested in the presence of $10 \mu\text{mol dm}^{-3}$ dopamine and interfering compounds such as catechol, resorcinol and ascorbic acid. It can be seen in Figure 4.24 that there is no interference with catechol and resorcinol even in the same concentration with dopamine and only ascorbic acid gave a negative

interference from concentrations higher than $4.0 \mu\text{mol dm}^{-3}$. This behavior can be assigned to the reaction between ascorbic acid and hydrogen peroxide, decreasing the formation of the copper hydroperoxy sites.

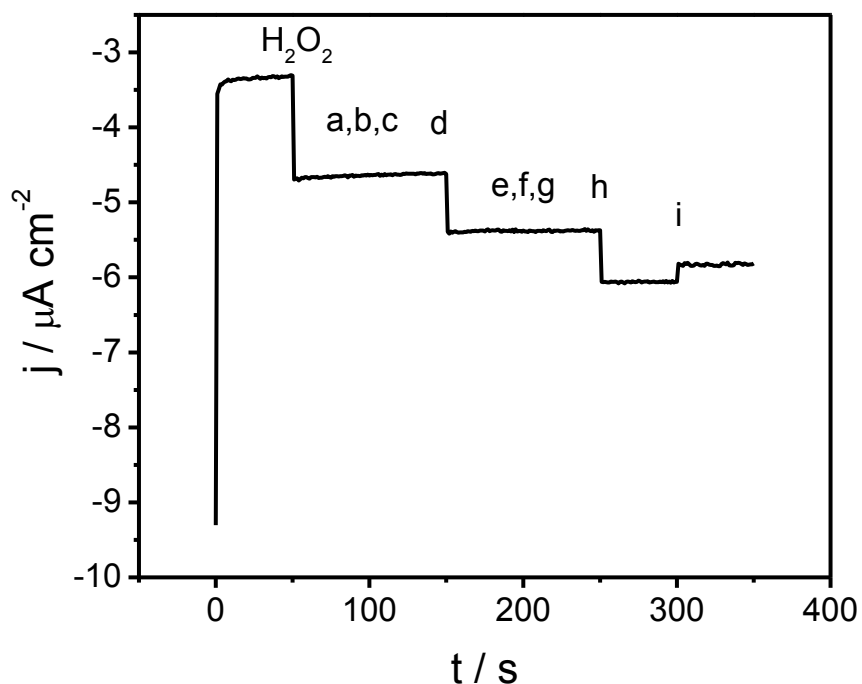


Figure 4.24: Current i vs. time for the addition of catechol (CA) resorcinol (RE) ascorbic acid (AA) and DA into the electrochemical cell in sequence at 75, 150, 175, 250 and 300 s. Concentrations in ($\mu\text{mol dm}^{-3}$) of the analytes in the reaction cell: (a) [CA] = 10, (b) [RE] = 10; (c) [AA] = 2; (d) [DA] = 10 (e) [CA] = 20 (f) [RE] = 20 (g) [AA] = 4 (h) [DA] = 20 and (i) [AA] = 5. Applied potential of -20 mV vs SCE, in 0.08 mol dm^{-3} BRB at pH= 6.0 containing 1 mol dm^{-3} KCl, and $100 \mu\text{mol dm}^{-3}$ H_2O_2 .

In order to evaluate the sensors applicability, dopamine was determined in a sample. A known concentration of dopamine solution was made in the physiological solution (0.9% m/v) and also the physiological solution was used as

supporting electrolyte. The sensor gives a very good response for dopamine determination in this solution as shown in Table 4.7.

Table 4.7: Determination of dopamine in sample

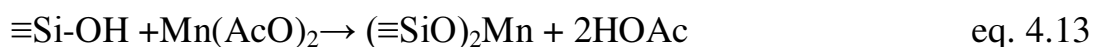
Dopamine concentration in the sample	
Nominal Value / $\mu\text{mol/ dm}^{-3}$	Found by Sensor / $\mu\text{mol/ dm}^{-3}$
20.0	20 \pm 1

4.4) Electrochemical detection of nitrite in meat and water samples using a mesoporous carbon ceramic SiO₂/C electrode modified with Manganese (II) phthalocyanine.

In this work the same SiO₂/C matrix are used as a support material as was used in the other previous work. In this case the matrix was modified with manganese(II) phthalocyanine.

4.4.1 *In situ* synthesis of manganese phthalocyanine (MnPc)

The *in situ* synthesis of MnPc can be described by two reaction steps.²⁰ In the first step, manganese acetate reacts with Bronsted acid –OH groups present on the silica surface (eq. 4.13), making the metal chemically adsorbed on the silica surface by a reaction with the formation of a Si–O–Mn bond. In the second step the adsorbed Mn(II) served as the support for phthalocyanine complex formation inside the silica pores (eq. 4.14).



The solid state diffuse reflectance spectrum of the immobilized MnPc on SiO₂/C material shows two electronic transition peaks observed at 624 and 712 nm (Figure 4.25), and standard MnPc also shows two peaks at the same wavelength. These two transitions are assigned as Q bands for Mn(II) under D_{4h} symmetry.¹⁴⁷ A weak band around in 550 nm corresponds to the charge transfer from metal to ligand or from ligand to metal.¹⁴⁸

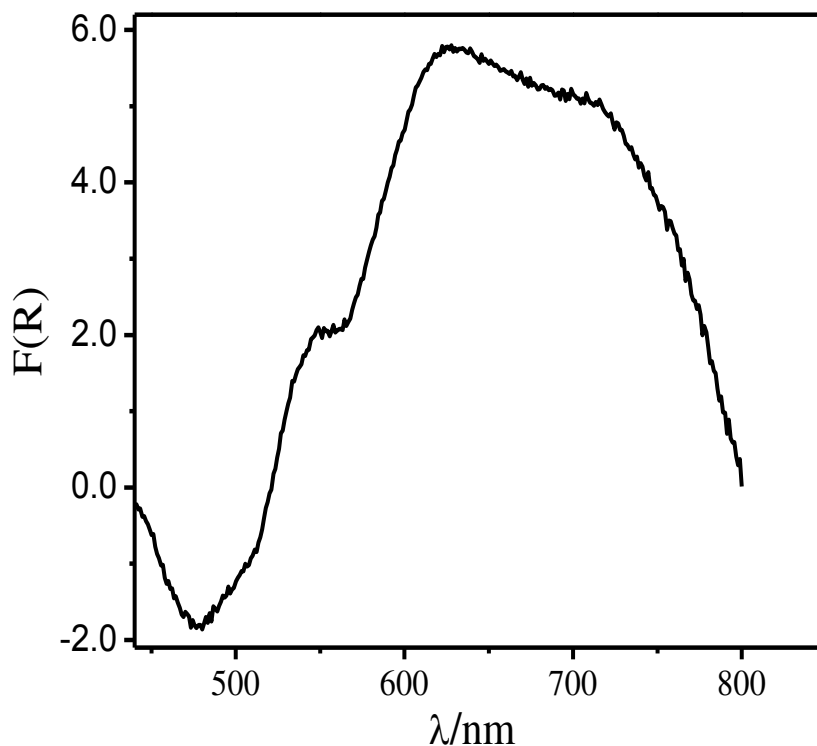


Figure 4.25: UV–Vis diffuse reflectance spectra of $\text{SiO}_2/\text{C}/\text{MnPc}$, expressed in Kubelka–Munk units.

4.4.2 X-rays photoelectron spectroscopy (XPS)

The XPS spectra for Mn and N for the material $\text{SiO}_2/\text{C}/\text{MnPc}$ are shown in Figures 4.26 a and 4.26 b, respectively. In $\text{SiO}_2/\text{C}/\text{MnPc}$, the Mn $2p_{3/2}$ and $2p_{1/2}$ BE peaks are shown in 641.6 and 653.3 eV, respectively.¹⁴⁹ Other peaks, centered at 396.1 and 400 eV with the N 1s BE, assigned to the pyrrolic and meso-nitrogen atoms in MnPc.¹⁵⁰

Table 4.8 shows the peak intensities and the atoms % obtained by XPS for $\text{SiO}_2/\text{C}/\text{MnPc}$. In particular the peak of interest, Mn $2p_{3/2}$ BE, allowed to estimate the amount of 0.5 Mn atom % at the depth probed by the technique.

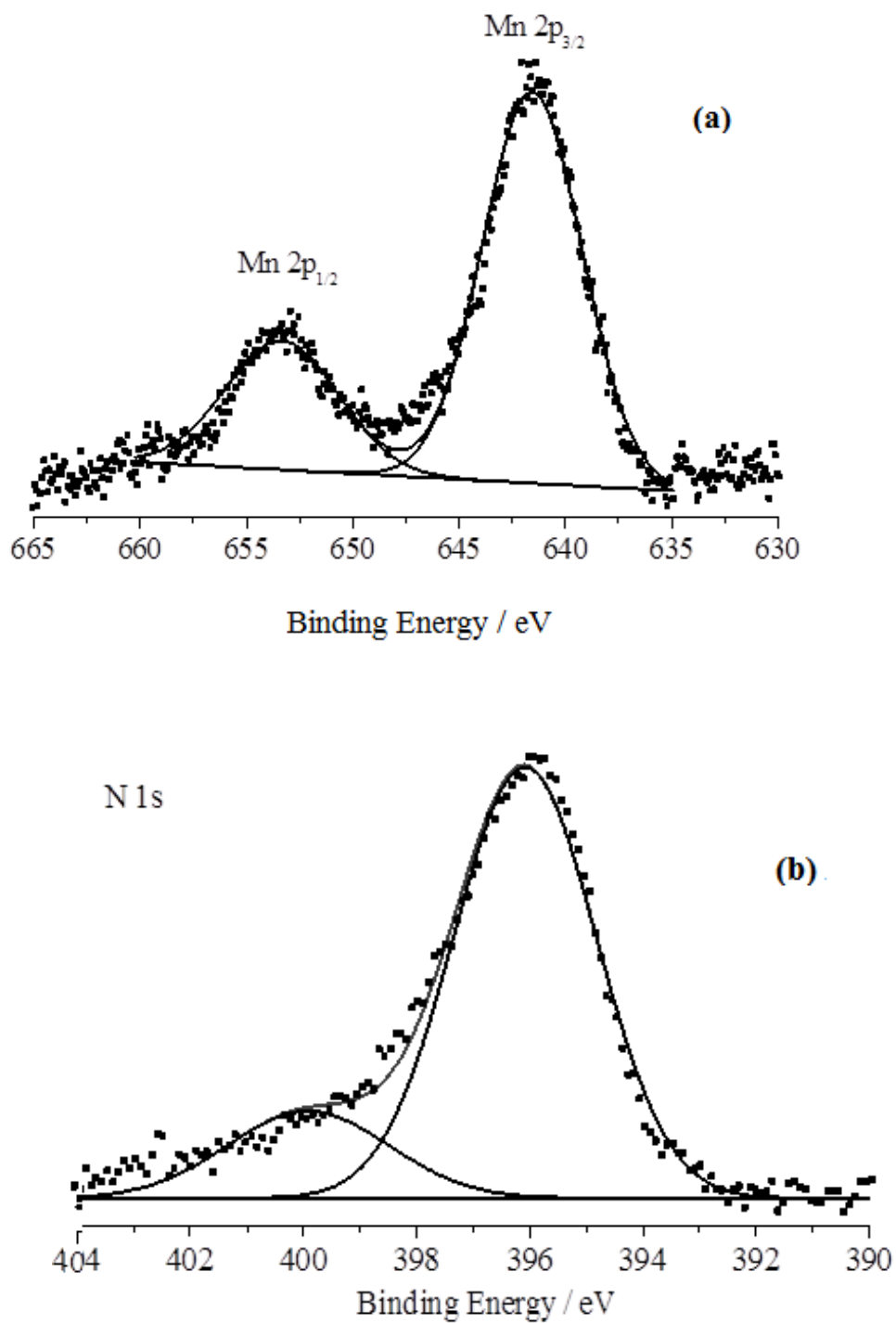


Figure 4.26: XPS spectrum for Manganese (a) and N (b).

Table 4.8. Peak intensities and atoms % for SiO₂/C/MnPc calculated from XPS data

SiO ₂ /C/MnPc	Peak intensity	Atoms %
N1s	3.19	1.4
Si2p	56.0	25.4
O1s	83.45	37.8
C1s	77.12	34.9
Mn2p _{3/2}	0.99	0.5

4.4.3 Electrocatalytic oxidation of nitrite on MnPc modified SiO₂/C electrode and influence of Phthalocyanine

Figure 4.27 shows the cyclic voltammograms for the bare SiO₂/C electrode (a), SiO₂/C/Mn electrode (b) and SiO₂/C/MnPc electrode (c) in presence of 15.74 μmol L⁻¹ nitrite in 0.1 M phosphate buffer solution pH 4. As can be seen from the Figure (c), a well defined oxidation peak of nitrite was obtained on the surface of SiO₂/C/MnPc electrode, when compared with SiO₂/C/Mn (b) a small and fairly defined nitrite oxidation peak and on the bare SiO₂/C electrodes there are no oxidation peak of nitrite. It is also evident from this figure that phthalocyanine plays an important role in the nitrite oxidation due to their macrocyclic nature including extended π-systems. Phthalocyanines are capable of undergoing fast redox processes, with minimal reorganizational energies and can act as catalyst in electron transfer processes involving a great variety of molecules.¹²⁷

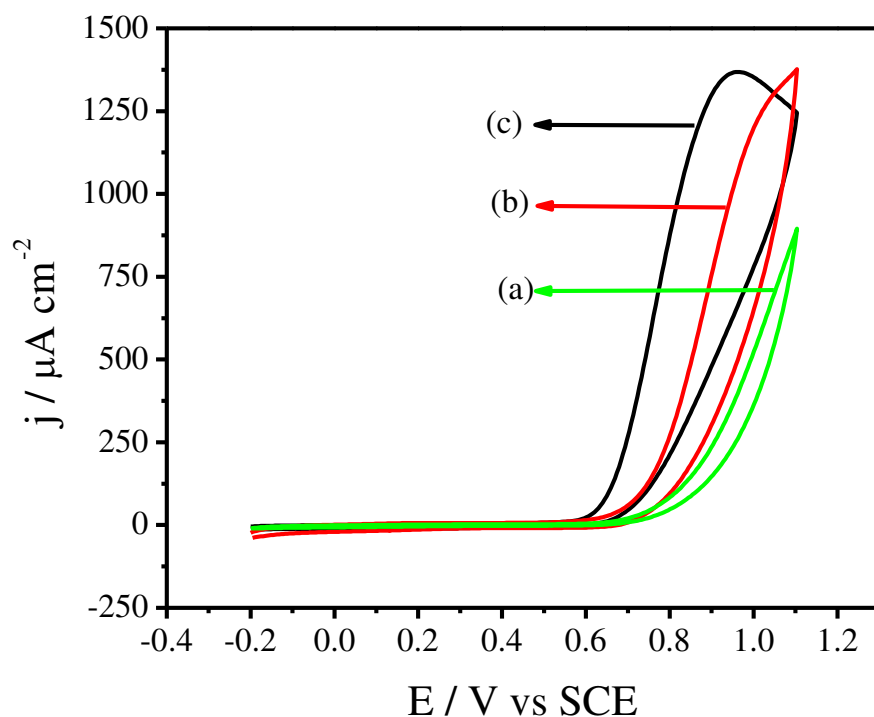


Figure 4.27: Cyclic voltammograms obtained for: bare SiO_2/Ce electrode (a), $\text{SiO}_2/\text{C}/\text{Mn}$ electrode (b) and $\text{SiO}_2/\text{C}/\text{MnPc}$ electrode (c), all in the presence of $15.74 \mu\text{mol L}^{-1}$ nitrite in 1 M KCl solution, 0.1 mol L^{-1} phosphate buffer (pH 4), scan rate: 20 mV s^{-1} .

4.4.4 Influence of the solution pH value

The effect of solution pH on the electrochemical response of nitrite was investigated in the pH range from 2.0 up to 8.0 in 0.1 M phosphate buffer solution. Figure 4.28 shows the effect of pH values on the oxidation peak current of $12.63 \mu\text{mol L}^{-1}$ nitrite. It can be seen that the peak current increases with pH value from 2.0 to 4.0, and then a decrease in the current is observed for pH higher than 4.0. At pH 4.0, the peak current reaches a maximum. Thus, the optimum pH for further studies was set in 4.0. In addition, this study showed that the peak potential for

nitrite oxidation is not affected by the solution pH (data not shown). This feature has been also verified by Pournaghi-Azar et al¹⁵¹ and Zen et al¹⁵² and it can be attributed to a kinetically controlled oxidation process, i.e. a proton independent catalytic step.

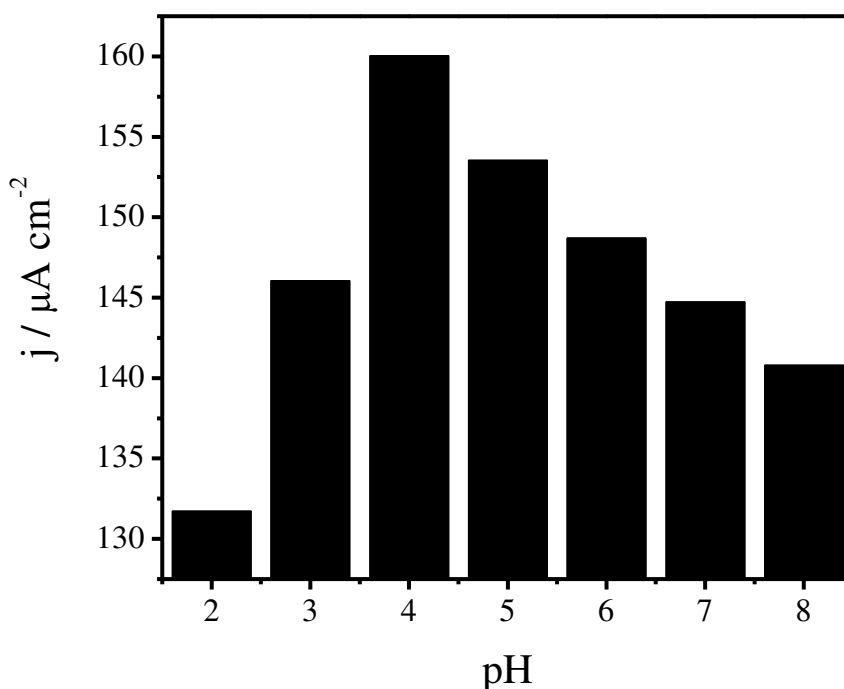


Figure 4.28: Dependence of the oxidation peak current on pH values in 12.63 $\mu\text{mol L}^{-1}$ nitrite in 1 M KCl solution, scan rate: 20 mV s^{-1} .

4.4.5 Analytical characterization

Under optimized conditions, in order to obtain an analytical curve for the sensor, cyclic voltammograms for oxidation of nitrite were carried out at different concentrations in 0.1 mol L^{-1} phosphate buffer solution at pH 4.0 (Figure. 4.29 a). The plot of current intensities against the concentration of nitrite, inset Figure 4.30 b, shows a linear relationship, in the concentration range between 0.79 -15.74

$\mu\text{mol L}^{-1}$ represented by the following equation: $j / \mu\text{A cm}^{-2} = 17.42 (\pm 1.1) + 86.57(\pm 0.2) [\text{nitrite}] (\mu\text{mol L}^{-1})$

with a correlation coefficient of 0.999 (for $n = 12$) and sensitivity of $86.57 \mu\text{A L} \mu\text{mol}^{-1}\text{cm}^{-2}$. Such good sensitivity can be attributed to the efficiency of the electron-transfer between the modified electrode and nitrite due to the catalytic effect and low charge transfer resistance of MnPc. The limit of detection (LOD) of $0.004 \mu\text{mol L}^{-1}$ was determined using a $3\sigma/\text{slope}$ ratio and limit of quantification (LOQ) was $0.013 \mu\text{mol L}^{-1}$ using $10 \sigma/\text{slope}$, where σ is the standard deviation (S.D.) of the mean value for 10 voltammograms of the blank, determined according to the IUPAC recommendations.¹⁵³

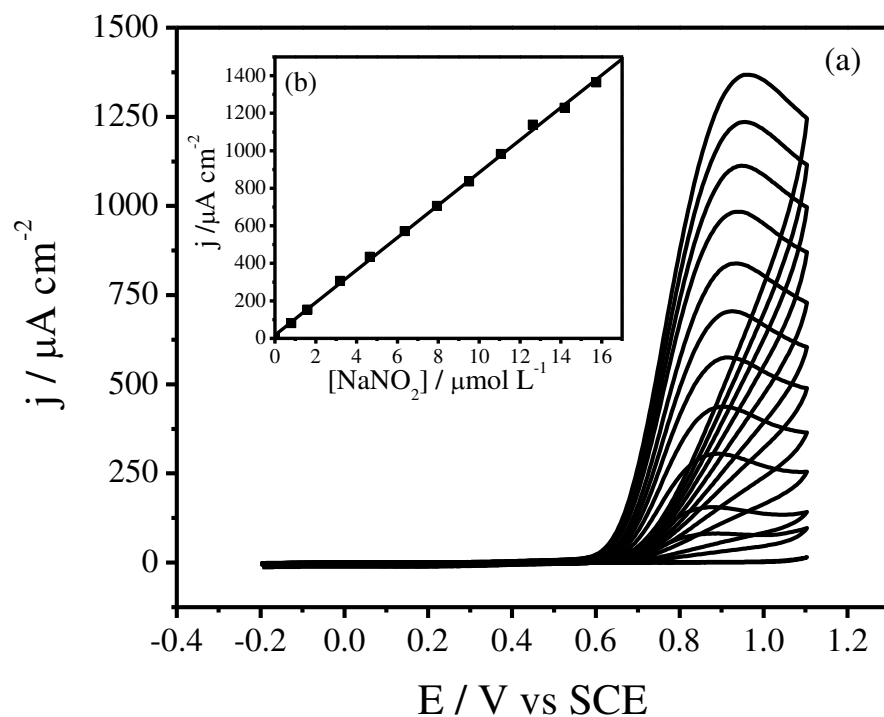


Fig. 4.29: (a) Cyclic voltammograms for SiO₂/C/MnPc electrode in different concentrations: (a) 0 (b) 0.79 (c) 1.59 (d) 3.19 (e) 4.65 (f) 6.36 (g) 7.93 (h) 9.51 (i) 11.07 (j) 12.63 (k) 14.19 and (l) 15.74 μmol L⁻¹ nitrite in 1 M KCl solution, 0.1 mol L⁻¹ phosphate buffer (pH 4), scan rate: 20 mV s⁻¹. Inset figure is a plot of peak current density against nitrite concentration.

4.4.6 Studies on the surface confined redox process behavior of MnPc

The adsorptive or surface confined redox process behavior of MnPc was confirmed by registering cyclic voltammograms at various potential scan rates from 10 up to 180 mV s⁻¹. A plot of the anodic peak current (i_{pa}) against the square root of scan rate ($v^{1/2}$) shows a linear relationship (Figure. 4.30), adjusted by the equation: i_{pa} (μA) = 17.4(±1.2) + 15.1(±0.1) $v^{1/2}$ (mVs⁻¹)^{1/2} and $r = 0.999$. This

linearity indicates that the oxidation process of nitrite is controlled by diffusion process.¹¹⁷ Since MnPc is strongly confined in the pores of the matrix surface, the analyte must diffuse into the surface–solution interface.

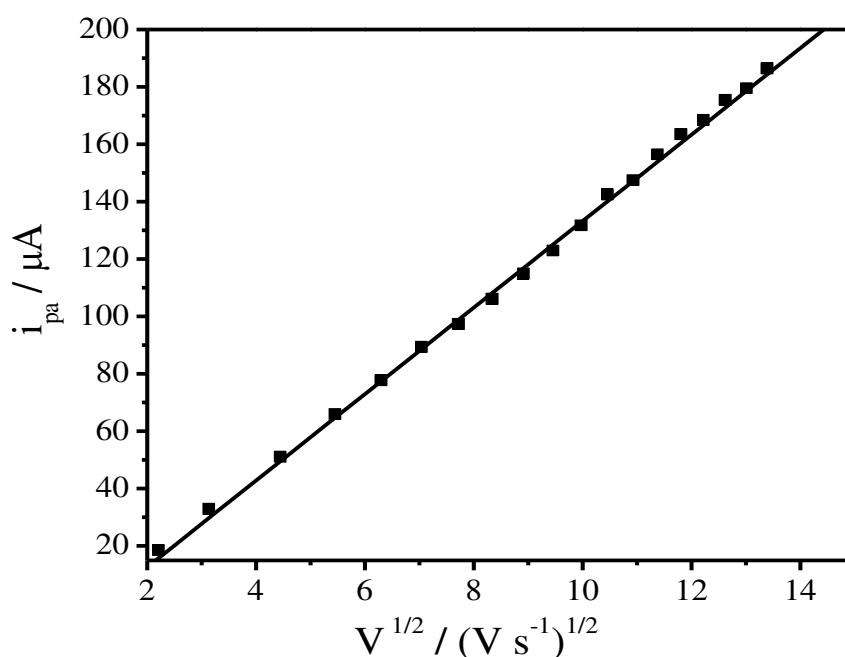


Figure 4.30: Variation of the anodic peak current I_{pa} vs. the square root of the potential scan rate $v^{1/2}$ for the $\text{SiO}_2/\text{C}/\text{MnPc}$ electrode in 0.1 mol L^{-1} phosphate buffer solution (pH 4) containing $12.63 \mu\text{mol L}^{-1}$ nitrite. Scan rate $5\text{--}180 \text{ mVs}^{-1}$.

4.4.7 Stability of MnPc on the SiO_2/C electrode

The stability of the $\text{SiO}_2/\text{C}/\text{MnPc}$ electrode was checked by recording successive cyclic voltammograms. After 100 cycles no significant changes in the currents response was observed (Figure. 4.31). Furthermore, when the electrode

was stored at room temperature no significant change in the response was observed for more than 24 months, just by polishing with emery paper to renew the surface to obtain the same response. This electrode showed good repeatability for nitrite determination. The relative standard deviation of the anodic peak for ten determinations of $12.63 \mu\text{mol L}^{-1}$ nitrite was 1.7 %. Similarly, a series of 5 sensors prepared in the same procedure and tested in the same experimental condition containing $12.63 \mu\text{mol L}^{-1}$ nitrite gave responses with a relative standard deviation of 4.6 %. These experiments indicated that the $\text{SiO}_2/\text{C}/\text{MnPc}$ have good stability (data not shown) and repeatability, probably due to the strong adsorption of MnPc in the SiO_2 matrix.

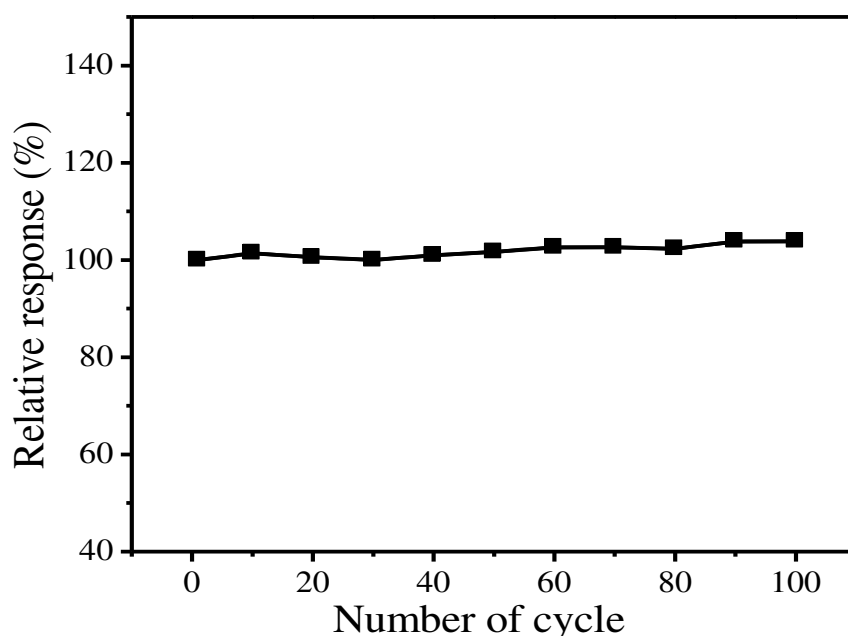


Figure 4.31: Relative response (%) at a function of the number of determinations. Applied scan rate = 20 mVs^{-1} , in 0.1 mol L^{-1} phosphate buffer (pH 4.0), containing $12.63 \mu\text{mol L}^{-1}$ of nitrite.

4.4.8 Interferences

Some chemical species were tested to check their levels of interference for the detection of nitrite on the SiO₂/C/MnPc electrode by adding various ions into a 0.1 mol L⁻¹ phosphate buffer solution (pH 4.0), containing 12.63 μmol L⁻¹ nitrite. The results showed that most of the ions, such as Ca²⁺, Mg²⁺, Al³⁺, NO₃⁻, SO₃²⁻, SO₄²⁻, K⁺, Na⁺, Mg²⁺, Ca²⁺, Zn²⁺, Cd²⁺, NH₄⁺, F⁻, and HSO₄⁻, even in 100-fold excess concentrations did not interfere in the determination. Thus, this study reveals that the developed sensor can tolerate a high concentration of common ions and, therefore can be stated as selective in the presence of the most common ions.

4.4.9 Determination of nitrite in water and sausage meat samples

In order to evaluate the practical utility of the method, nitrite was determined in samples using the standard addition method. Water samples were collected from lake and river, and sausage meat were purchased from local market. After filtration of the water to remove the suspension solid substances, and chemical treatment of sausage meat, the concentration values of nitrite in the samples were determined by the proposed method. The nitrite amount and the recoveries were displayed in Table 4.9, and in all cases, the RSD for each sample was less than 4%. The recoveries for the method were investigated and the values changed from 99.4 to 103.8 %. These experimental data indicate that the determination of nitrite using the SiO₂/C/MnPc electrode was effective and sensitive. The results show that the proposed methods could be efficiently used for the nitrite determination in environmental and food samples.

In addition, applying a paired t-Student test to compare these results, it was possible to observe that, at 95% confidence level, there was no statistical difference. This good agreement indicates the reliability of the present electrochemical sensor for nitrite determination samples.

Based on the experimental data, it was clear that this $\text{SiO}_2/\text{C}/\text{MnPc}$ sensor possess high sensitivity and low limit of detection for sensing nitrite in samples. As shown in Table 4.10, the present sensor shows low limit of detections and high sensitivity when compared to the sensor reported in the literature.¹⁵⁴⁻¹⁶³ This excellent performance may be attributed to the mesoporous nature of the matrix prepared by the sol-gel method and strong adsorption of MnPc in the matrix. In this process, C particles are highly and homogeneously dispersed throughout the bulk matrix phase, improving the connectivity of C particles and then increasing the conductivity of the material.

Table 4.9: Determination of nitrite in water sample and sausage meat samples (n=3)

Samples	Detected (mg kg^{-1})	Added (mg kg^{-1})	Found (mg kg^{-1})	Recovery (%)
Lake water	6.78±(0.01)	7.00	13.80± (0.01)	99.85±(0.02)
River water	47.23 ± (0.03)	7.00	52.38 ±(0.02)	103.53±(0.01)
Sausage 1	14. 13 ± (0.02)	9.00	24.01± (0.01)	103.80 ±(0.01)
Sausage 2	12.02 ± (0.03)	9.00	20.3 ± (0.02)	99.37±(0.03)

Table 4.10: Comparison of different nitrite sensors for the nitrite determination

Electrode	Detection limit (μmol^{-1})	Sensitivity ($\mu\text{A L } \mu\text{mol}^{-1} \text{ cm}^{-2}$)	References
CPE-Mn-complex	0.8	1.27	[154]
CuTSPc/PLL/GCE	0.036	0.83	[155]
PdCu/GCE	0.3	0.056	[156]
Pt/Ch/GCE	0.4	0.0885	[157]
Thionine/ACNTs	1.12	0.0023	[158]
Hb-Au-CPE	0.06	0.071	[159]
p-NiTAPc/GCE	0.9	0.186	[160]
PNB/GCE	0.1	0.0002	[161]
MC/GCE	0.10	0.1172	[162]
SWNTs/ssDNA/ GCE	0.15	0.2160	[163]
SiO ₂ /C/MnPc	0.004	86.57	This work

Conclusions

The development of this work allows us to reach the following conclusions:

- ❖ A SiO₂/C/CoPc pressed disk electrode with solid paraffin filled pores, considerably decreased the electrical resistance. Material containing 50 wt% C was chosen and the electrode prepared with this material showed lower LOD, when compared with other electrodes based on SiO₂ as the basic substrate to provide structural rigidity and chemical stability. The relatively good electrical conductivity presented by SiO₂/50 wt% C/CoPc makes this a material of great potential in preparing a new electrochemical sensor for oxalic acid and other analytes since many other electroactive species that can be easily confined on this matrix surface. Comparing the dramatic increase of detectivity of SiO₂/50 wt% C/CoPc (LOD = 5.8×10^{-7} mol L⁻¹) with that shown by SiO₂/CoPc (CPE) [123] (LOD = 1.0×10^{-3} mol L⁻¹), the comparatively better performance of the new electrode is presumably related to the mesoporous nature of the matrix prepared by the sol-gel method. In this process C particles are highly and homogeneously dispersed throughout the bulk matrix phase, improving the connectivity of C particles and then increasing the conductivity of the material.
- ❖ A SiO₂/C/CoPc pressed disk electrode was used as electrochemical sensor for dissolved oxygen. Pressed disk electrode is a good alternative when compared with other electrodes based on SiO₂ to provide structural rigidity and chemical stability. The proposed sensor presented a good response for dissolved oxygen at applied potential of -0.23 V. Optimization of the experimental condition yielded detection of O₂ much better than those sensors reported in the literature. This sensor showed good repeatability for both the measurement and electrode preparation, evaluated in term of relative standard deviation, allied with a simple and easy preparation. Thus, the present sensor is a feasible alternative to Clark-Type

amperometric sensor, since it possesses the advantages of membrane-free, maintenance free, can be miniaturized and present low detection limit.

❖ The proposed enzymeless biosensor, as a $\text{SiO}_2/\text{C}/\text{CuPc}$, showed a wide response range (10–140 $\mu\text{mol L}^{-1}$), high sensitivity of 0.63 $\text{nA L}^{-1} \mu\text{mol}^{-1} \text{cm}^{-2}$ and with a detection limit of 0.6 $\mu\text{mol L}^{-1}$ of dopamine. This sensor showed a long lifetime of 9 months, great stability and repeatability and a short response time of (1 s) for determination of dopamine. The proposed sensor was better than the most of conventional biosensors (based on enzyme) and other enzymeless biosensors described in the literature. These characteristics can be assigned to the conductivity of the material and the environment of the copper complex in the porous material keeping the great reactivity after activating it with hydrogen peroxide. The proposed sensor is highly selective for dopamine determination; it does not show any interference with other phenolic compounds. Indeed, this sensor was successfully employed for determination of dopamine in sample. In this sense, this work depicts that the development of biomimetic biosensors is a promising subject, since simple stable molecules can be used to catalyze redox reaction of extremely important analytes like dopamine.

❖ The mesoporous carbon ceramics $\text{SiO}_2/50 \text{ wt\% C}$ ($S_{\text{BET}} = 170 \text{ m}^2 \text{ g}^{-1}$), prepared by the sol–gel method was used as a matrix to support manganese phthalocyanine (MnPc), prepared in situ on their surface, to assure homogeneous dispersion of the electrocatalyst complex in the pores of the matrix. Pressed disk electrode made with $\text{SiO}_2/\text{C}/\text{MnPc}$ was used to analyze the oxidation of nitrite by an electrochemical technique. The proposed sensor presented an excellent response for oxidation of nitrite. This sensor showed good repeatability for both the measurement and electrode preparation, evaluated in term of relative standard deviation, allied with a simple and easy preparation. Furthermore, its sensitivity, repeatability and stability are excellent. The proposed sensor is highly selective for

nitrite determination; it does not show any interference with other ions present in the water. Indeed, this sensor was successfully employed for determination of nitrite in sausage meat and water sample.

- ❖ The electrically conductive ceramic carbon material presented in this work proved to be very versatile and promising to the development of new electrodes with a potential application as an electrochemical sensor and biosensor.

References

- [1] B. R. Eggins, *Chemical Sensors and Biosensors*, John Wiley & Sons, West Sussex, England 2002.
- [2] N. J. Ronkainen, H. B. Halsall, W. R. Heineman, *Chem. Soc. Rev.* 39 (2010) 1747.
- [3] A. J. S. Ahammad, J.-J. Lee, M. A. Rahman, *Sensors* 9 (2009) 2289.
- [4] S. J. Updike, B.J. Gilligan, M.C. Shults, R.K. Rhodes, *Diabetes Care* 23 (2000) 208.
- [5] B. Aussedat, V. Thome-Duret, G. Reach, F. Lemmonier, J.-C. Klein, Y. Hu, G.S. Wilson, *Biosens. Bioelectron.* 12 (1997) 1061.
- [6] L. Campanella, F. Pacifici, M.P. Sammartino, M. Tomassetti, *Bioelectrochem. Bioenerg.* 47 (1998) 25.
- [7] K. Kriz, M. Anderlund, D. Kriz, *Biosens. Bioelectron.* 16 (2001) 363.
- [8] W. Yantasee, B. Charnhattakorn, G. E. Fryxell, Y. Lin, C. Timchalk, R. S. Addleman, *Anal. Chim. Acta* 620 (2008) 55.
- [9] R.W. Keay, C.J. McNeil, *Biosens. Bioelectron.* 13 (1998) 963.
- [10] K. Rekha, M.D. Gouda, M.S. Thakur, N.G. Karanth, *Biosens. Bioelectron.* 15 (2000) 499.
- [11] A. Walcarius, *Electroanalysis*, 10 (1998) 1217.
- [12] R. W. Murray, *Acc. Chem. Res.* 13 (1980) 135.
- [13] J. Moiroux, P. J. Elving, *Anal. Chem.* 50 (1978) 1056.
- [14] A. C. Pereira, A. S. Santos, L. T. Kubota, *Quim. Nova* 25 (2002) 1012.
- [15] C.J. Miller, M. Majda, *J. Am. Chem. Soc.* 107 (1985) 1419.
- [16] P.J. Kulesza, L.R. Faulkner, *J. Am. Chem. Soc.* 110 (1988) 4905.
- [17] K.A. Macor, T.G. Spiro, *J. Electroanal. Chem.* 163 (1984) 223.
- [18] A. Bettelheim, R. Reed, N.H. Hendricks, J.P. Collman, R.W. Murray, *J. Electroanal. Chem.* 238 (1987) 259.
- [19] A. Rahim, S. B.A. Barros, L. T. Kubota, Y. Gushikem, *Electrochim. Acta* 56 (2011) 10116.
- [20] A. Rahim, S. B.A. Barros, L. T. Arenas, Y. Gushikem, *Electrochim. Acta* 56 (2011) 1256.
- [21] J.A. Cox, R.K. Jaworski, P.J. Kulesza, *Electroanalysis* 3 (1991) 869.
- [22] J. Joseph, H. Gomathi, G.P. Rao, *J. Electroanal. Chem.* 431 (1997) 231.
- [23] H. Lee, L.J. Kepley, H.-G. Hong, T.E. Mallouk, *J. Am. Chem. Soc.* 110 (1988) 618.
- [24] S. Akhter, H. Lee, H.-G. Hong, T.E. Mallouk, J.M. White, *J. Vac. Sci. Tech. B* 7 (1989) 1608.

- [25] M. Ohtani, O. Ikeda, *J. Electroanal. Chem.* 354 (1995) 311.
- [26] G.A.P. Zaldivar, Y. Gushikem, L.T. Kubota, *J. Electroanal. Chem.* 318 (1991) 247.
- [27] L.T. Kubota, Y. Gushikem, *Electrochim. Acta* 37 (1992) 2477.
- [28] J. Wang, J. Liu, *Anal. Chim. Acta* 284 (1993) 385.
- [29] K.S. Alber, J.A. Cox, *Mikrochim. Acta* 127 (1997) 131.
- [30] O. Lev, Z. Wu, S. Bharathi, V. Glezer, A. Modestov, J. Gun, L. Rabinovich, S. Sampath, *Chem. Mater.* 9 (1997) 2354.
- [31] N. Oyama, F.C. Anson, *J. Electroanal. Chem.* 199 (1986) 467.
- [32] S.M. Macha, A. Fitch, *Mikrochim. Acta* 128 (1998) 1.
- [33] K. Itaya, H.-C. Chang, I. Uchida, *Inorg. Chem.* 26(1987) 624.
- [34] J. Qiu, G. Villemure, *J. Electroanal. Chem.* 428 (1997) 165.
- [35] D.R. Rolison, *Chem. Rev.* 90 (1990) 867.
- [36] D.R. Rolison, R.J. Nowak, T. Welsh, C.G. Murray, *Talanta* 38 (1991) 27.
- [37] F. Bedioui, *Coord. Chem. Rev.* 144 (1995) 39.
- [38] A. Walcarius, *Electroanalysis* 13 (2001) 701.
- [39] I. Svancara, K. Vytras, K. Kalcher, A. Walcarius, J. Wang, *Electroanalysis* 21 (2009) 7.
- [40] E.S. Ribeiro, S.L.P. Dias, Y. Gushikem, L.T. Kubota, *Electrochim. Acta* 49 (2004) 829.
- [41] M.S.P. Francisco, W.S. Cardoso, Y. Gushikem, *J. Electroanal. Chem.* 574 (2005) 291.
- [42] W.S. Cardoso, M.S.P. Francisco, R. Landers, Y. Gushikem, *Electrochim. Acta* 50 (2005) 4378.
- [43] J. Li, S.N. Tana, H. Ge, *Anal. Chim. Acta* 335 (1996) 137.
- [44] M. Ghiaci, B. Rezaei, R.J. Kalbasi, *Talanta* 73 (2007) 37.
- [45] J. Li, L.S. Chia, N.K. Goh, S.N. Tan, *Anal. Chim. Acta* 362 (1998) 203.
- [46] R. Liang, J. Jiang, J. Qiu, *Anal. Sci.* 24 (2008) 1425.
- [47] M.S.P. Francisco, W.S. Cardoso, L.T. Kubota, Y. Gushikem, *J. Electroanal. Chem.* 602 (2007) 29.
- [48] G. Zaitseva, Y. Gushikem, E.S. Ribeiro, S.S. Rosatto, *Electrochim. Acta* 47 (2002) 1469.
- [49] A.S. Santos, L. Gorton, L.T. Kubota, *Electroanalysis* 14 (2002) 805.
- [50] A.C. Pereira, D.V. Macedo, A.S. Santos, L.T. Kubota, *Electroanalysis* 18 (2006) 1208.
- [51] C. Henry, *Anal. Chem.* 70 (1998) 594.
- [52] J.C. Pickup, F. Hussain, N.D. Evans, N. Sachedina, *Biosens. Bioelectron.* 20 (2005) 1897.
- [53] T. Chen, S.C. Barton, G. Binyamin, Z. Gao, Y. Zhang, A. Heller, *J. Am. Chem. Soc.* 123 (2001) 8630.

- [54] M. Tsionky, G. Gun, V. Glezer, O. Lev, *Anal. Chem.* 66 (1994) 1747.
- [55] G. Gun, M. Tsionsky, O. Lev, *Anal. Chim. Acta* 294 (1994) 261.
- [56] L. Rabinovich, O. Lev, *Electroanalysis* 13 (2001) 265.
- [57] A. Walcarius, D. Mandler, J.A. Cox, M. Collinson, O. Lev, *J. Matter. Chem.* 15 (2005) 3663.
- [58] G. Oskam, P.C. Searson, *J. Phys. Chem. B* 102 (1998) 2464.
- [59] L. Rabinovich, J. Fun, O. Lev, D. Aurbach, B. Markovsky, M.D. Levi, *Adv. Mater.* 10 (1998) 577.
- [60] C. M. Maroneze, L. T. Arenas, R. C.S. Luz, E. V. Benvenutti, R. Landers, Y. Gushikem, *Electrochim. Acta* 53 (2008) 4167.
- [61] E. Marafon, L. T. Kubota, Y. Gushikem, *J. Solid State Electrochem.* 13 (2009) 377.
- [62] A. Salimi, H. Mamkhezri, R. Hallaj, *Talanta* 70 (2006) 826.
- [63] L. T. Arenas, P. C. M. Villis, J. Arguello, R. Landers, E. V. Benvenutti, Y. Gushikem, *Talanta* 83 (2010) 241.
- [64] Y. Lin, X. Cui, X. Ye, *Electrochem. Commun.* 7 (2005) 267-274.
- [65] S. Tsujimura, K. Kano, T. Ikeda, *J. Electroanal. Chem.* 576 (2005) 113-120.
- [66] I. Koc, M. Camur, M. Bulut, A. R. Ozkaya, *Catal. Lett.* 131 (2009) 370.
- [67] J.A.P. Chaves, M.F.A. Araujo, J.J.G. Varela Junior, A.A. Tanaka, *Ecl. Quim.* 28 (2003) 9.
- [68] Y. Murakami, K. Tanaka, Y. Takechi, S. Takahashi, Y. Nakano, T. Matsumoto, W. Sugimoto, Y. Takasu, *J. Sol-Gel Sci. Technol.* 29 (2004) 19.
- [69] L. L. Hench, J. K. West, *Chem. Rev.* 90 (1990) 33
- [70] C. J. Brinker, G.W. Scherer, *Sol-Gel Science. The Physics and Chemistry of Sol-Gel Processing*, Academic Press, San Diego, 1990.
- [71] K.M. Radish, K.M. Smith, R. Guilard, *The Porphyrin Handbook*, Academic Press, San Diego. Vol. 19, ed., 2003.
- [72] D.N. Reinhoudt, *Comprehensive supra-molecular chemistry*, Pergamon, London. Vol. 10, ed., 1996.
- [73] I. Rosenthal, *Photochem. Photobiol.* 6 (1991) 859.
- [74] C.C. Leznoff, A.B.P. Lever, *Phthalocyanines: Properties and applications*, VCH Publishers, New York. Vol.4, ed., 1996.
- [75] S. Griveau, J. Pavez, J. Zagal, F. Bedioui, *J. Electroanal. Chem.* 497 (2001) 75.
- [76] C.A. Caro, J.H. Zagal, F. Bedioui, *J. Electrochem. Soc.* 150 (2003) E95.
- [77] K. Kasuga, K. Mori, T. Sugimori, M. Handa, *Bull. Chem. Soc. Jpn.* 73 (2000) 939.
- [78] J.D. Spikes, *Photochem. Photobiol. B* 6 (1990) 259.
- [79] R. Hagen, T. Bieringer, *Adv. Mater.* 13 (2001) 1805.

- [80] C.C. Leznoff, A.B.P. Lever, *Phthalocyanines: Properties and applications*, VCH Publishers, New York. Vol. 3, ed., 1993.
- [81] D. Wöhrle, G. Schnurpfeil, G. Knothe, *Dyes and Pigments*, 18 (1992) 69.
- [82] A. Lützen, S.D. Starnes, D.M. Rudkevich, J. Rebeck Jr, *Tet. Lett.* 41(2000) 3777.
- [83] F. Yilmaz, D. Atilla, V. Ahsen, *Polyhedron*, 23 (2004) 1931.
- [84] T. C. Canevari, J. Arguello, M.S.P. Francisco, Y. Gushikem, *J. Electroanal. Chem.* 609 (2007) 61.
- [85] K. R. Rajesh, C. S. Menon, *Mater. Letters*, 51 (2001) 266.
- [86] R. Taube, *Pure Appl. Chem.* 38 (1974) 427.
- [87] A. B. P. Lever, J. P. Wilshire, S. K. Quan, *Inor. Chem.* 20 (1980) 761.
- [88] R. Kraus, M. Grobosch, M. Knupfer, *Chem. Phys. Lett.* 469 (2009) 121.
- [89] S. Gupta, T. N. Misra, *Sens. Actuat. B*, 41 (1997) 199.
- [90] T. C. Canevari, R. C. S. Luz, Y. Gushikem, *Electroanalysis* 20 (2008) 765.
- [91] W. J. R. Santos, A. L. Sousa, M. D.P. T. Sotomayor, F. S. Damos, S. M. C. N. Tanaka, L. T. Kubota, A. A. Tanaka, *J. Braz. Chem. Soc.* 20 (2009) 1180.
- [92] J. Oni, P. Westbroek, T. Nyokong, *Electroanalysis* 17 (2002) 1165.
- [93] L.S.S. Santosa, R. Landers, Y. Gushikem, *Talanta* 85 (2011) 1213.
- [94] A. Rahim, L. S.S. Santos, S.B.A. Barros, L.T. Kubota, Y. Gushikem, *Sens. Actuat. B* 177(2013) 231.
- [95] T. A. Ivandini, T. N. Rao, A. Fujishima, Y. Einaga, *Anal. Chem.* 78 (2006) 3467.
- [96] A. A. Ensafi, S. Abassi, B. Rezaei, *Spectrochim. Acta A*, 57(2001)1833.
- [97] C. Fu, L. Wang, Y. Fang, *Talanta* 50 (1999) 953.
- [98] J.W. Mo, B. Ogorevc, *Anal. Chem.* 73 (2001) 1196.
- [99] C. A. C. Sequeira, D. M. F. Santos, W. Baptista, *J. Braz. Chem. Soc.* 17(2006) 910.
- [100] R. C. S. Luz, F. S. Damos, A. A. Tanaka, L. T. Kubota, *Sens. Actuat. B*, 114 (2006) 1019.
- [101] P. T. Kissinger, W. R. Heineman, *Laboratory Techniques in Electroanalytical Chemistry*. 2^a ed, Marcel Dekker, New York, 1996.
- [102] J. Hendrikse, W. Olthuis, P. Bergveld, *Sens. Actuat. B* 59 (1999) 35.
- [103] A. M. O. Brett, C. M. A. Brett, *Eletroquímica: Princípios, métodos e aplicações*. Coimbra: Livraria Almeida, 1993. 471.
- [104] G.-R. Xu, G. Xu, M.-L. Xu, Z. Zhang, Y. Tian, H. N. Choi, W.-Y. Lee, *Bull. Korean Chem. Soc.* 33 (2012) 415.
- [105] J. Davis, R. G. Compton, *Anal. Chim. Acta* 404(2000) 241.
- [106] S. Brunauer, P.H. Emmett, E. Teller, *J. Am. Chem. Soc.* 60 (1938) 309.
- [107] E.P. Barret, L.G. Joyner, P.P. Halenda, *J. Am. Chem. Soc.* 73 (1951) 373.
- [108] E.M. Giroto, I.A. Santos, *Quim. Nova* 25 (2002) 639.

- [109] J.F Moulder, W.F. Stickle, B.P. Sobol, K.D. Bomben, X-ray Handbook of Photoelectron Spectroscopy, Perkin-Elmer Corporation/Physical Electronics Division (1992).
- [110] W. J.R. Santos, P. R. Lima, A. A. Tanaka, S.M.C.N. Tanaka, L. T. Kubota, Food Chemistry 113 (2009) 1206.
- [111] S.J. Gregg, K.S.W. Sing, Adsorption, Surface Area and Porosity, 2nd ed., Academic Press, London, 1982.
- [112] K.S.W. Sing, D.H. Everett, R.A.W. Haul, L. Moscou, R.A. Pierotti, J. Rouquerol, T. Siemieniewska, Pure Appl. Chem. 57 (1985) 603.
- [113] S. Ray, S. Vasudevan, Inorg. Chem. 42 (2003) 1711.
- [114] D. Wöhrle, U. Hündorf, G. Schulz-Ekloff, E. Ignatzek, Z. Naturforsch 41b (1986) 179.
- [115] J. Wang, P.V. A. Pamidi, C. Parrado, D.S. Park, J. Pingarron, Electroanalysis 9 (1997) 908.
- [116] A.M.S. Lucho, E.C. Oliveira, H.O. Pastore, Y. Gushikem, J. Electroanal. Chem. 573 (2004) 55.
- [117] A.J. Bard, L.R. Faulkner, Electrochemical Methods: Fundamentals and Applications, 2nd Ed, Wiley, New York, 2001.
- [118] Y. Zheng , C. Yang , W. Pu, J. Zhang , Food Chemistry 114 (2009) 1523.
- [119] S.Yamazaki, N. Fujiwara, K.Yasuda, Electrochim. Acta 55 (2010) 753.
- [120] B. Sljukic, R. Baron, R. G. Compton, Electroanalysis 19 (2007) 918.
- [121] F.Manea, C. Radovan, I. Corb, A. Pop, G. Burtica, P. Malchev, S. Picken, J. Schoonman, Sensors 7(2007) 615.
- [122] T. A. Ivandini, T. N. Rao, A. Fujishima, Y. Einaga, Anal. Chem. 78(2006) 3467.
- [123] M.Toledo, A.M.S. Lucho, Y. Gushikem, J. Mater. Sci. 39 (2004) 6851.
- [124] J. Arguello, H.A. Magosso, R.R. Ramos, T.C. Canevari, R. Landers, V.L. Pimentel, Y. Gushikem, Electrochim. Acta 54 (2009) 1948.
- [125] R.N. Goldberg, N. Kishore, R.M. Lennen, J. Phys. Chem. 31 (2002) 231.
- [126] G. Velasco, Electroanalysis 9 (1997) 80.
- [127] J. H. Zagal, S. Griveau, J. F. Silva, T. Nyokong, F. Bedioui, Coord. Chem. Rev. 254 (2010) 2755.
- [128] R.C.S. Luz, F.S. Damos, A.A. Tanaka, L.T. Kubota, Sens. Actuators B 114 (2006) 1019.
- [129] J. Zagal, P. Bindra, E. Yeager, J. Electrochem. Soc. 127 (1980) 1506.
- [130] Y.P. Chen, S.Y. Liu, H.Q. Yu, Anal. Chim. Acta 598 (2007) 249.
- [131] E. Armengol, A. Corma, V. Fornes, H. Garcia, J. Primo, Appl. Catal. A: General 181 (1999) 305.
- [132] M. D. P.T. Sotomayor, A. A. Tanaka, L. T. Kubota, Anal. Chim. Acta 455 (2002) 215.

- [133] J.P. Klinman, *Chem. Rev.* 96 (1996) 2541.
- [134] M. Fontecave, J.L. Pierre, *Coord. Chem. Rev.* 170 (1998) 125.
- [135] N.K. Williams, J.P. Klinman, *J. Mol. Catal. B Enzym.* 8 (2000) 95.
- [136] F. Lisdat, U. Wollenberger, A. Makower, H. Hörtnagl, D. Pfeiffer, F.W. Scheller, *Biosens. Bioelectron.* 12 (1997) 1199.
- [137] C. Nistor, J. Emnéus, L. Gorton, A. Ciucu, *Anal. Chim. Acta* 387 (1999) 309.
- [138] S. S. Rosatto, L. T. Kubota, G.N. Oliveira, *Anal. Chim. Acta* 390 (1999) 65.
- [139] S. Cosnier, J.J. Fombon, P. Labbe, D. Limosin, *Sens. Actuators B* 59(1999) 134.
- [140] F.S. Damos, M. D. P.T. Sotomayor, L.T. Kubota, S. M. C. N. Tanaka, A. A. Tanaka, *Analyst* 128 (2003) 255.
- [141] K. Farhadi, F. Kheiria, M. Golzanb, *J. Braz. Chem. Soc.* 19 (2008) 1405.
- [142] M. D.P.T. Sotomayor, A. A. Tanaka, L.T. Kubota, *Electroanalysis* 15 (2003) 787.
- [143] D. R. Shankaran, N. Uehara, T. Kato, *Anal. Chim. Acta* 478 (2003) 321.
- [144] L.C. Jiang, W.D. Zhang, *Electroanalysis* 21 (2009) 1811.
- [145] S. S. Rosatto, L. T. Kubota, G.N. Oliveira, *Anal. Chim. Acta* 390 (1999) 65.
- [146] B. Wang, S. Dong, *J. Electroanal. Chem.* 487 (2000) 45.
- [147] N. Sehlotho, T. Nyokong, *J. Electroanal. Chem.* 595 (2006) 161.
- [148] A. B. P. Lever, S. R. Pickens, P. C. Minor, S. Licoccia, B. S. Ramaswamy, K. Magnell, *J. Am. Chem. Soc.* 103 (1981) 6800.
- [149] Z-L. Yang, H-Z. Chen, L. Cao, H-Y. Li, M. Wang, *Mater. Sci. Eng. B* 106 (2004) 73.
- [150] J. Ahlund, K. Nilson, J. Kjeldgaard, S. Berner, N. Martensson, C. Puglia, B. Brena, M. Nyberg, Y. Luo., *J. Chemical Physics* 125 (2006) 34709.
- [151] M. H. Pournaghi-Azar, H. Dastango, *J. Electroanal. Chem.*, 567 (2004) 211.
- [152] J. M. Zen, A. S. Kumar, H. W. Chen, *Electroanalysis* 13 (2001) 1171.
- [153] Analytical methods committee, Recommendations for the definition, estimation and use of the detection limit. *Analyst*, 1987, 112, 199.
- [154] M.A. Kamyabi, Z. Asgari, H. H. Monfared, *J Solid State Electrochem* 14 (2010) 1547.
- [155] A.L. Sousa, W.J.R. Santos, R.C.S. Luz, F.S. Damos, L.T. Kubota, A.A. Tanaka, S. M. C. N. Tanaka, *Talanta* 75 (2008) 333.
- [156] X.H. Zhu, G.F. Kang, X.Q. Lin. *Microchim Acta* 159 (2007) 141.
- [157] P. Wang, F. Li, Y.X. H. Li, L. Wang, *Electrochem Commun* 10 (2008) 195.
- [158] K. Zhao, H.Y. Song, S.Q. Zhuang, L.M. Dai, P.G. He, Y.Z. Fang, *Electrochem Commun* 9 (2007) 65.
- [159] S.Q. Liu, H.X. Ju, *Analyst* 128 (2003) 1420.
- [160] Z.H. Wen, T.F. Kang, *Talanta* 62 (2004) 351.

- [161] X.W. Chen, F. Wang, Z.L. Chen, *Anal Chim. Acta.*623 (2008) 213.
- [162] L.Y. Jiang, R.X. Wang, X.M. Li, L.P. Jiang, G.H. Lu, *Electrochem. Commun.* 7 (2005) 597.
- [163] H. Xian, P. Wang, Y. Zhou, Q. Lu, S. Wu, Y. Li, L. Wang, *Microchim. Acta* 171 (2010) 63.